APL Photonics

On-chip optical comb sources

Cite as: APL Photonics **7**, 100901 (2022); https://doi.org/10.1063/5.0105164
Submitted: 22 June 2022 • Accepted: 13 September 2022 • Published Online: 11 October 2022

Artur Hermans, Kasper Van Gasse and Bart Kuyken

COLLECTIONS

F This paper was selected as Featured

View Online Export Citation CrossMark

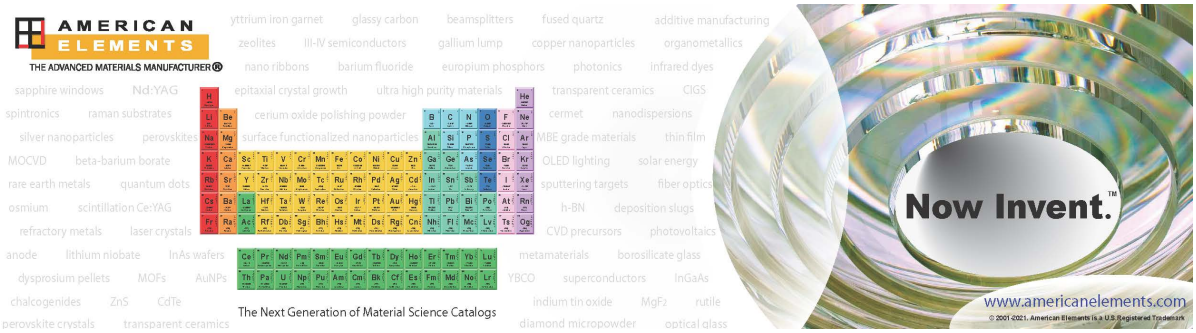

© 2022 Author(s).

On-chip optical comb sources

Cite as: APL Photon. 7, 100901 (2022); doi: 10.1063/5.0105164
Submitted: 22 June 2022 • Accepted: 13 September 2022 •
Published Online: 11 October 2022

View Online Export Citation CrossMark

Artur Hermans,[1,2,3,a)] Kasper Van Gasse,[1,2,4] and Bart Kuyken[1,2]

AFFILIATIONS

[1] Photonics Research Group, Department of Information Technology, Ghent University - imec, Technologiepark-Zwijnaarde 126, 9052 Ghent, Belgium
[2] Center for Nano- and Biophotonics (NB-Photonics), Ghent University, Technologiepark-Zwijnaarde 126, 9052 Ghent, Belgium
[3] Research Laboratory of Electronics, Massachusetts Institute of Technology, 50 Vassar Street, Cambridge, Massachusetts 02139, USA
[4] E. L. Ginzton Laboratory, Stanford University, Stanford, California 94305, USA

[a)] **Author to whom correspondence should be addressed:** artur.hermans@ugent.be

ABSTRACT

On-chip integration of optical comb sources is crucial in enabling their widespread use. Integrated photonic devices that can be mass-manufactured in semiconductor processing facilities offer a solution for the realization of miniaturized, robust, low-cost, and energy-efficient comb sources. Here, we review the state of the art in on-chip comb sources, their applications, and anticipated developments.

© 2022 Author(s). All article content, except where otherwise noted, is licensed under a Creative Commons Attribution (CC BY) license (http://creativecommons.org/licenses/by/4.0/). https://doi.org/10.1063/5.0105164

I. INTRODUCTION

The application space of optical comb sources has expanded rapidly over the past decades.[1] Prominent applications include optical frequency metrology,[2] optical atomic clocks,[3] light detection and ranging (LiDAR),[4] telecommunication,[5] and spectroscopic sensing.[6] Many of the early demonstrations relied on solid-state (often Ti:sapphire) or fiber-based mode-locked lasers as the comb source, combined with discrete optical components. To enable widespread use of optical comb technology, outside of a laboratory environment, compact, robust, inexpensive, and power-efficient comb sources are needed. Integrated photonic devices fabricated with well-developed semiconductor processing technology can fulfill this need. The development of integrated comb sources is a very active area of research[7–12] with many groundbreaking demonstrations in recent years, both on the device and system level.

Here, we give an overview of state-of-the-art on-chip optical comb sources, their applications, and anticipated developments. We start with a discussion of basic comb properties and comb generation mechanisms (Sec. II). This is followed by a review of state-of-the-art on-chip comb sources, where we dedicate a section to monolithic III-V semiconductor comb sources (Sec. III), hybridly (Sec. IV), and heterogeneously integrated comb sources (Sec. V). Finally, we discuss the applications of on-chip comb sources (Sec. VI) and have a look at what lies ahead (Sec. VII). For the review of on-chip comb sources (Secs. III–V), we restrict ourselves to fully integrated comb sources, i.e., comb sources for which all components are integrated on-chip, except for the electrical power supply, possible alternating current (AC) sources, and temperature control modules. The most well-developed electrically pumped on-chip light sources are arguably those made out of direct bandgap III-V semiconductors. All of the demonstrated fully integrated comb sources discussed here contain III-V semiconductor material to convert electrical energy into optical energy. Through hybrid and heterogeneous integration techniques,[13] III-V semiconductors can be combined with other material platforms, such as silicon nitride, silicon, or lithium niobate photonic integrated circuits (PICs). As we will see later, hybrid and heterogeneous integration of III-V semiconductors with other material platforms can lead to significant performance improvements for on-chip comb sources, primarily in terms of noise.

II. COMB PROPERTIES AND GENERATION MECHANISMS

Before we discuss comb generation mechanisms, we briefly go over some of the basic, general properties of comb sources. We define an optical comb source as a source generating an optical spectrum that consists of a set of phase-locked lines with a constant frequency spacing f_r, also known as the repetition rate or frequency.

The frequencies of these lines can be expressed as $\nu_n = f_0 + nf_r$, with f_0 the carrier–envelope offset frequency ($f_0 < f_r$) and n a whole number.[19,20] The temporal profile of the electric field corresponding to this comb depends on both the amplitude and phase spectrum. For example, if the comb lines are all in phase, short pulses are generated (with pulse repetition rate f_r), while a splay–phase relationship results in the generation of a frequency modulated wave (with repetition frequency f_r) with a quasi-constant intensity.[21] In general, the generated waveform is modulated both in amplitude and frequency. In literature, one often makes the distinction between amplitude modulated (AM) and frequency modulated (FM) comb sources,[21,22] where the former refers to a source that generates a sequence of short pulses, while the latter emits a waveform with a quasi-constant intensity. The distinction between AM and FM comb sources is well illustrated in Ref. 21. As many comb sources have a dominant AM or FM character, we will attempt to categorize them accordingly.

Other basic comb properties that we will refer to are the center emission wavelength λ_c or frequency ν_c, the optical bandwidth $\Delta\lambda$ or $\Delta\nu$, the pulse duration τ_p (only for AM combs), the average optical output power P_{avg}, the radio frequency (RF) linewidth δf_r, and optical linewidth $\delta\nu$. Unless mentioned otherwise, we will use

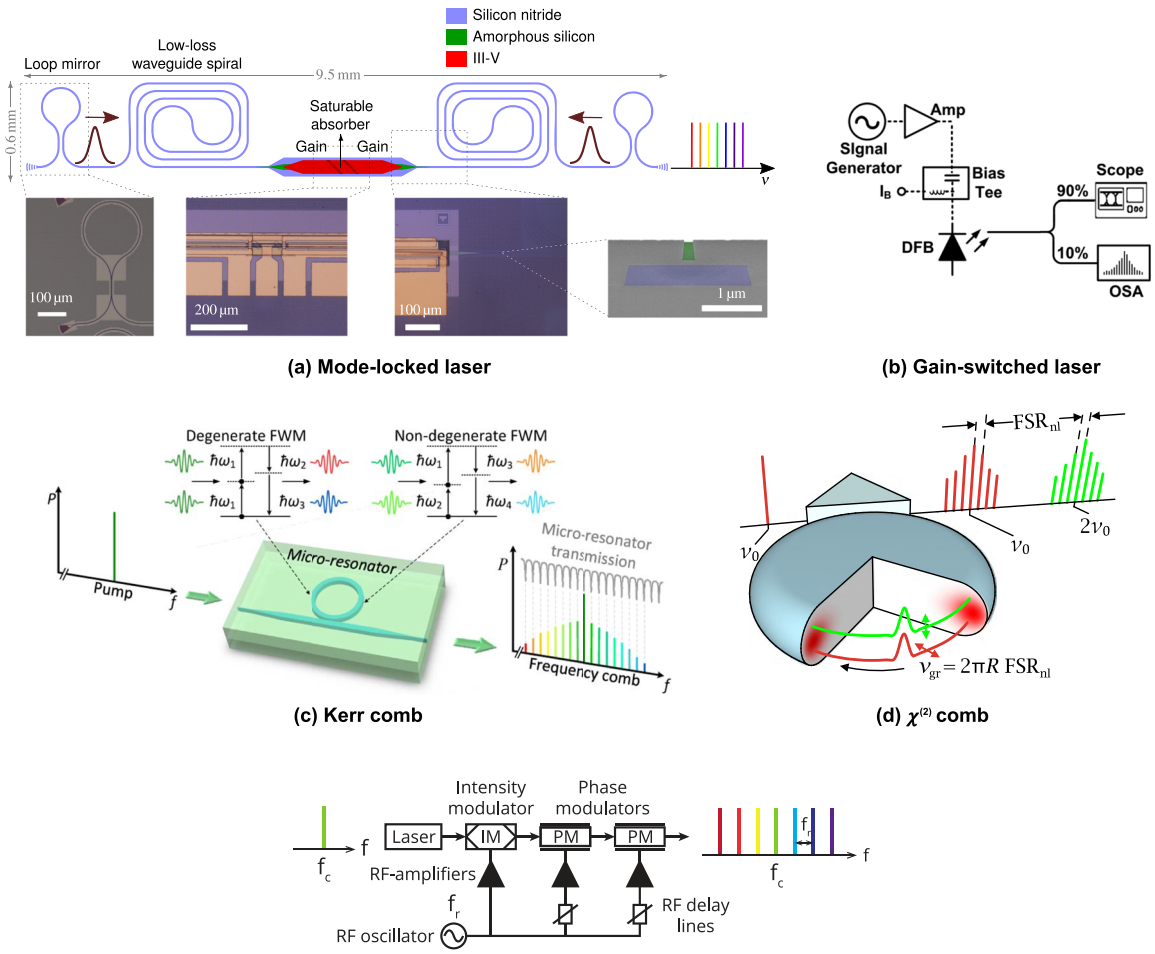

FIG. 1. Examples of different comb generation mechanisms. (a) A heterogeneous III-V-on-silicon-nitride colliding-pulse mode-locked laser.[14] The device consists of a passive silicon nitride waveguide cavity with loop mirrors on either end. The active III-V section in the middle of the cavity provides the gain and saturable absorption for mode-locking. An intermediate amorphous silicon waveguide layer is used to achieve low-loss coupling from the active to passive section. Insets: optical and electron microscope images of various parts of the laser. (b) Schematic of the setup to generate a comb through gain-switching of a distributed feedback (DFB) laser diode.[15] OSA: optical spectrum analyzer. (c) A Kerr comb generated by pumping a high-Q ring resonator with a single-frequency laser.[16] FWM: four-wave mixing. (d) Schematic of $\chi^{(2)}$ comb generation in a microresonator (with radius R) pumped by a single-frequency laser.[17] A comb is generated at the pump and second-harmonic frequency with a repetition rate equaling the nonlinear free spectral range (FSR$_{nl}$). (e) A common setup to generate wide, flat electro-optic combs: a single-frequency laser signal is sent through a cascade of intensity and phase modulators.[18] (a) Reproduced from Hermans *et al.*, APL Photonics **6**, 096102 (2021), with the permission of AIP Publishing. (b) Reproduced with permission from Anandarajah *et al.*, IEEE J. Sel. Top. Quantum Electron. **21**, 1801609 (2015). Copyright 2015, IEEE. (c) Reproduced with permission from Pu *et al.*, Optica **3**, 823 (2016). Copyright 2016, Optical Society of America. (d) Reproduced with permission from Szabados *et al.*, Phys. Rev. Lett. **124**, 203902 (2020). Copyright 2020, American Physical Society. (e) Reproduced with permission from Lundberg *et al.*, Appl. Sci. **8**, 718 (2018). Copyright 2018, MDPI.

© Author(s) 2022

the full width at half maximum (FWHM) values for the optical bandwidth, pulse duration, RF, and optical linewidth. The average optical output power refers to the total output power of the comb source (not of a single line). We chose here to list the average optical power, not the peak power, because the average power is what is measured in most cases. If the pulse duration, repetition rate, and average power are known, the peak power can be estimated. Yet without knowledge of the exact pulse shape, this is only an estimate. The RF linewidth or beat note linewidth refers to the width of the peak at f_r in the spectrum of the measured intensity (measured with a fast

TABLE I. List of comb generator categories, the associated pump types, and pros and cons for each category.

Category	Pump	Pros and cons
Mode-locked lasers		
Active mode-locking	Electrical[a] (DC and AC)	(+) Repetition rate stabilized to external oscillator (−) AC source needed (−) Relatively long pulses
Passive mode-locking	Electrical[a] (DC)	(+) No AC source needed (+) Short pulses can be generated (−) Repetition rate not stabilized
Hybrid mode-locking	Electrical[a] (DC and AC)	(+) Repetition rate stabilized to external oscillator (+) Short pulses can be generated (−) AC source needed
Gain-switched lasers	Electrical[a] (DC and AC)	(+) Repetition rate stabilized to external oscillator (+) Large repetition rate tunability (−) AC source needed (−) Limited optical bandwidth and long pulses
$\chi^{(3)}$ or Kerr combs		
Supercontinuum generation	Optical (comb)	(+) Octave-spanning combs can be generated (−) Need optical pump with high pulse energies and short pulse durations
Kerr microresonator comb	Optical (single-frequency)	(+) Low-noise comb states (+) Octave-spanning combs can be generated (−) but requires high-power optical pump (−) Control complexity
$\chi^{(2)}$ combs		
Comb wavelength translation	Optical (comb)	(+) Combs can be generated in otherwise hard to access wavelength ranges (−) Need a pump comb source (−) Many materials commonly used in PICs have a vanishing $\chi^{(2)}$ nonlinearity
$\chi^{(2)}$ microresonator comb	Optical (single-frequency)	(+) Potentially higher pump-to-comb conversion efficiency and lower threshold power compared to Kerr combs (−) Many materials commonly used in PICs have a vanishing $\chi^{(2)}$ nonlinearity (−) Optical pump needed
Electro-optic combs		
Non-resonant	Optical (single-frequency) and electrical (DC and AC)	(+) Repetition rate stabilized to external oscillator (+) Large repetition rate tunability (−) Optical pump and high-power AC source needed
Resonant	Optical (single-frequency) and electrical (AC)	(+) Repetition rate stabilized to external oscillator (−) Optical pump and AC source needed

[a]These lasers can also be optically pumped, but we only consider electrically pumped lasers based on III-V semiconductor gain media here.

© Author(s) 2022

photodetector). The optical linewidth refers to the width of a single comb line. The RF and optical linewidth are a measure of the RF and optical phase noise, respectively. There are several linewidth characterization methods.[23–25] In some cases, both the instantaneous (or intrinsic) and integrated linewidth (influenced by technical noise such as temperature and pump current fluctuations) are extracted. If both are determined, the linewidth quoted here is the instantaneous linewidth; otherwise, we quote whichever linewidth is measured in the associated reference, and we encourage the reader to consult that reference for details. Note that the optical linewidth can vary with the mode number n.[26–28] If, in a certain reference, the optical linewidth is measured for multiple mode numbers, we quote the minimum linewidth here.

Next, we will cover how combs can be generated. The comb generator categories discussed here are mode-locked lasers, gain-switched lasers, $\chi^{(3)}$ or Kerr combs, $\chi^{(2)}$ combs, and electro-optic combs. Figure 1 shows examples of comb sources belonging to each of these categories. Table I lists the comb generator categories, the associated pump types, and pros and cons for each comb generation approach. The history of on-chip optical comb sources is illustrated in Fig. 2.

A. Mode-locked lasers

In their simplest form, mode-locked lasers are made up of a cavity with a gain medium and a mode-locking element inside.[53] This mode-locking element can be the gain medium itself. The mode-locking element forces the laser to emit an optical spectrum consisting of lines with a constant frequency spacing, i.e., a comb. This is different from the spectrum of a multimode laser (with a single transverse mode), which consists of multiple non-equidistant lines that are not phase-locked. Due to dispersion, the longitudinal cavity modes are not naturally equidistant. While a mode-locking element will try to enforce emission at a constant fre-

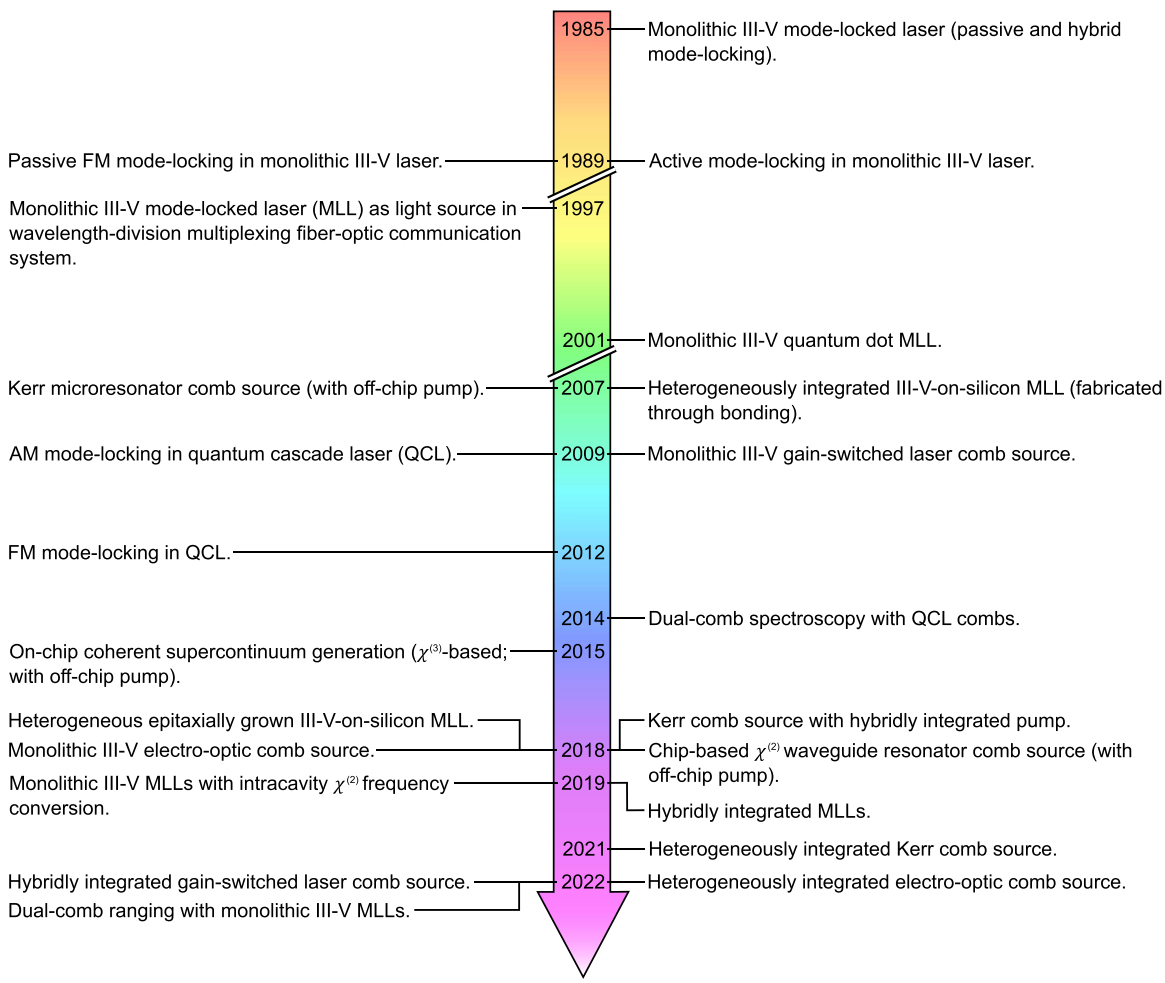

FIG. 2. History of on-chip optical comb sources. 1985: Ref. 29; 1989: Refs. 30 and 31; 1997: Ref. 5; 2001: Ref. 32; 2007: Refs. 33 and 34; 2009: Refs. 35 and 36; 2012: Ref. 37; 2014: Ref. 38; 2015: Refs. 39 and 40; 2018: Refs. 41–44; 2019: Refs. 45–48; 2021: Ref. 49; and 2022: Refs. 50–52.

© Author(s) 2022

quency spacing, this will become increasingly hard the more the cavity modes deviate from equidistant spacing. This ultimately limits the comb's optical bandwidth, along with other mechanisms such as the gain bandwidth, the bandwidth of the cavity mirrors, and the speed of the mode-locking element. The repetition rate f_r of a mode-locked laser corresponds to the inverse of the cavity round trip time (≈cavity mode spacing), for fundamental mode-locking, or a multiple of it, for harmonic mode-locking. Mode-locked lasers can emit both AM and FM combs.[21,22,30,54,55] The term "mode-locking" is sometimes used exclusively for AM, pulsed mode-locking, but here we will use it to refer to both AM and FM mode-locking.

Mode-locking mechanisms can be categorized into passive, active, and hybrid mode-locking. In an actively mode-locked laser, mode-locking is achieved by periodically modulating the round-trip gain, loss, or phase shift. This is done using an AC pump signal, an intracavity intensity or phase modulator. One typically uses a drive signal with a frequency that equals the inverse of the cavity round-trip time (for fundamental mode-locking) or an integer multiple of it (for harmonic mode-locking). Within the category of actively mode-locked lasers, the terms "AM" and "FM mode-locked lasers" are sometimes used as well, but to refer to the use of an intracavity intensity or phase modulator as a mode-locking element, respectively.[56] Yet, these FM-type actively mode-locked lasers can produce a pulsed output. We will refrain from using this terminology here.

In a passively mode-locked laser, no external AC signals are applied for mode-locking. Instead, one generally uses a saturable absorber. This is a component for which the absorption is reduced at high light intensities, which promotes the formation of short pulses in the cavity. Free-space and fiber-based mode-locked lasers often use semiconductor saturable absorber mirrors (SESAMs), which combine a mirror and saturable absorber material in a single component.[57] Saturable absorbers based on Kerr lensing combined with an aperture are frequently used for ultrashort pulse generation in free-space lasers (referred to as Kerr lens mode-locking).[53] In integrated mode-locked lasers based on III-V semiconductors, one typically constructs a saturable absorber by not pumping a short part of the gain section or even applying a reverse bias, to reduce the absorber's recovery time.[58] In addition, integrated saturable absorbers based on the Kerr effect in an interferometer have been explored[59] but have so far not been demonstrated in on-chip III-V-based mode-locked lasers. Even without saturable absorber, passive mode-locking has been observed in on-chip lasers, relying on four-wave mixing for mode-locking.[30,60] Passive mode-locking without saturable absorber is sometimes referred to as self-mode-locking,[60–62] although in the past this term has been used in other contexts as well.[63–65] In addition, Kerr nonlinear microresonators can serve as mode-locking elements.[66] Passive mode-locking has the advantage that it does not require an external AC signal generator and allows for shorter pulses. For high repetition frequencies (on-chip passively mode-locked lasers with terahertz repetition rates have been demonstrated[67,68]), compact and low-cost AC signal generators are not readily available.

In hybrid mode-locking, an external AC signal at the repetition frequency f_r is applied to a passively mode-locked laser, commonly to the saturable absorber or gain section. This can be useful if one wants to stabilize the repetition rate or synchronize it with an external clock, while still having the short pulses and wide optical bandwidths than can be achieved in a passively mode-locked laser with a fast mode-locking element.

There have been a lot of demonstrations of on-chip mode-locked lasers, with emission frequencies ranging from visible to terahertz frequencies. Monolithic III-V mode-locked lasers, as well as hybridly and heterogeneously integrated mode-locked lasers, have been realized (see Secs. III–V).

B. Gain-switched lasers

Gain-switching is a method of generating pulses by modulating the pump power of a laser, so as to switch between a state below and above the lasing threshold.[69] In contrast to mode-locking, the modulation frequency does not correspond to the inverse of the cavity round-trip time or a multiple of it. Although large timing jitter and loss of coherence between subsequent pulses may wash out any discernible lines in the optical spectrum, it has been shown that under appropriate operating conditions, gain-switched single-mode semiconductor lasers can generate combs.[36] Modulation frequencies close to the relaxation oscillation frequency have been found to be optimal.[15] However, significantly lower repetition rates can also be achieved utilizing optical injection to avoid loss of coherence during the long off periods between pulses.[70] As the repetition rate is not directly linked to the cavity round-trip time, it can be tuned continuously over a large range.[71] Yet, the comb bandwidths of gain-switched lasers are relatively small.

Several monolithic III-V gain-switched comb sources have been demonstrated (see Sec. III) as well as a hybrid gain-switched comb source (see Sec. IV).

C. $\chi^{(3)}$ or Kerr combs

Four-wave mixing processes enabled by the $\chi^{(3)}$ or Kerr nonlinearity of materials can be used for comb generation. Two schemes are commonly utilized: supercontinuum generation and Kerr comb generation.[7]

In supercontinuum generation, short pulses with high peak powers are spectrally broadened by sending them through a nonlinear medium. Generating a broadband coherent comb through supercontinuum generation requires careful control of the experimental parameters and usually leans on the use of an AM comb source generating short pulses with high peak powers that are sent through a dispersion-engineered nonlinear waveguide. On-chip coherent supercontinuum generation with integrated comb sources has not yet been demonstrated, but there have been a lot of demonstrations of coherent supercontinuum generation in on-chip waveguides with an off-chip pump.[40,72–77] The generation of on-chip octave-spanning coherent supercontinua typically starts from pump pulses with a pulse duration on the order of 100 fs and pulse energies of several pJ to over 100 pJ, depending on the strength of the nonlinearity and the waveguide loss, i.e., its effective length. While these numbers are getting within reach of on-chip mode-locked lasers, it is an outstanding challenge to integrate all the required materials and devices.

© Author(s) 2022

In Kerr comb generation, a high-quality-factor (high-Q) cavity with a nonlinear medium inside is pumped with a continuous-wave (CW), single-frequency laser.[78] The pumped Kerr nonlinear medium provides parametric gain that can result in parametric oscillation if the threshold is surpassed. This process bears similarities with a laser, but here the gain is provided by a parametric nonlinear process. Cascaded four-wave mixing in a resonator can lead to the formation of a comb with equidistant spectral lines. Similar to mode-locked lasers, the cavity modes are not naturally equidistant, which leads to a finite comb bandwidth. Kerr comb generation in chip-based microresonators has been around since the 2000s.[33] Kerr comb generators have long relied on off-chip, high-power, narrow-linewidth, tunable pump lasers, and complex tuning mechanisms. Only recently, have Kerr comb sources with integrated CW pump lasers been realized[42] and has turnkey operation been demonstrated.[79,80] Multiple hybrid Kerr comb sources have been reported and also a heterogeneously integrated Kerr comb source has been demonstrated (see Secs. IV and V). The generation of low-noise, coherent Kerr combs requires careful control of the experimental conditions. Most demonstrations focus on the generation of temporal dissipative Kerr solitons in the anomalous group velocity dispersion regime.[81] These solitons correspond to highly coherent combs in the frequency domain. Generally, the solitons are superimposed on a CW background with only a small percentage of the pump power being converted into comb power.[7] The conversion efficiency decreases with decreasing repetition rate, as the overlap between the solitons and the background pump radiation decreases.[7,82,83] Generating combs in the normal group velocity dispersion regime[7,84] or making use of coupled resonators can increase the conversion efficiency.[85,86] Several integrated Kerr comb sources operating in the normal group velocity dispersion regime have already been demonstrated (see also Sec. IV).[80,84] Wide, octave-spanning soliton combs have been demonstrated in on-chip microresonators,[87,88] but these demonstrations still relied on high-power, off-chip pump lasers (> 100 mW pump power to access 1 THz-repetition-rate single-soliton states).

Recently, a $\chi^{(3)}$-based comb generation scheme has been reported, which can be considered a combination between conventional supercontinuum generation and Kerr comb generation, as a microresonator is pumped with a pulsed input.[89–91] This scheme boosts the efficiency of Kerr soliton combs and enables supercontinuum generation with lower peak powers compared to conventional non-resonant supercontinuum generation. Yet, so far only off-chip pump sources have been used.

D. $\chi^{(2)}$ combs

While the $\chi^{(3)}$-based comb sources generate a comb around the pump wavelength, $\chi^{(2)}$ or three-wave mixing processes can enable the generation of combs at wavelengths that are far away from the pump wavelength(s). $\chi^{(2)}$-based comb sources can be divided into two major categories. First, $\chi^{(2)}$ nonlinear processes can be used to translate combs (e.g., Kerr combs, mode-locked laser combs) to another wavelength range, e.g., by sum or difference frequency generation[45,46,98–103] or pumping an optical parametric oscillator (OPO) with a comb source.[104] The up- or down-conversion can happen in the same cavity or medium as the base comb generation or in a separate device. Second, combs can be generated directly by cascaded $\chi^{(2)}$ processes in a cavity with a $\chi^{(2)}$ nonlinear medium pumped by a CW laser, akin to Kerr comb generation.[105–107] This approach has the potential to lead to higher pump-to-comb conversion efficiencies and lower threshold powers compared to the Kerr-based approach. In addition, supercontinuum generation based on cascaded $\chi^{(2)}$ processes has been demonstrated.[108,109]

$\chi^{(2)}$-based comb sources have received less attention compared to their $\chi^{(3)}$-based counterparts. Many of the materials often used in $\chi^{(3)}$-based comb sources and integrated photonics have a vanishing $\chi^{(2)}$ nonlinearity due to their centrosymmetric nature (e.g., amorphous silicon nitride and silicon dioxide, crystalline silicon).[110] Yet, silicon nitride thin films have been shown to have a non-zero $\chi^{(2)}$ nonlinearity as-deposited, with the magnitude depending on the deposition conditions.[111,112] A $\chi^{(2)}$ nonlinearity can also be induced optically via the photogalvanic effect,[113–115] by permanently applying an electric field,[116,117] via thermal poling,[118] strain,[119] or symmetry breaking at material interfaces.[120–122] In recent years, multiple integrated photonics platforms based on $\chi^{(2)}$ materials (e.g., $LiNbO_3$,[123] AlN,[124] SiC,[125] (Al)GaAs,[126] and (In)GaP[72,103]) have been developed, with several demonstrations of $\chi^{(2)}$-based comb generation (often combined with $\chi^{(3)}$ effects).[100,101,103,107,109]

Yet, so far the only reports of fully integrated comb sources relying on three-wave mixing are monolithic III-V mode-locked lasers with intracavity sum or difference frequency generation (see also Sec. III).[45,46]

E. Electro-optic combs

A final comb category we are briefly discussing here are the electro-optic comb sources.[11,28] An electro-optic comb is generated by sending a CW laser through one or more electro-optic modulators. These modulators can modulate the phase, amplitude, and/or polarization of the incident beam. As modulation leads to the generation of sidebands at (multiples of) the modulation frequency, one can understand that modulators can be used for comb generation. Various physical effects can be used to modulate the refractive index, such as the Pockels effect (only in $\chi^{(2)}$ materials), the Kerr effect, the plasma dispersion effect, and the quantum-confined Stark effect. To generate wide combs, one often cascades multiple phase modulators followed by an intensity modulator to flatten the spectrum.[28] Another approach is to use resonant electro-optic comb sources, where a phase modulator is placed in a cavity and driven at a frequency that corresponds to an integer times the free spectral range.[28] The repetition frequency of non-resonant combs can easily be tuned over a large range and low repetition frequencies can be achieved without the need for long cavities.

Many chip-based electro-optic comb sources (e.g., based on III-V semiconductors, silicon, or lithium niobate) have been realized, but most use an off-chip laser.[11] Still, there have been several demonstrations of fully integrated electro-optic comb sources, monolithic III-V,[43,127,128] as well as hybrid and heterogeneous III-V-$LiNbO_3$ comb sources[51,129] (see Secs. III–V).

III. MONOLITHIC III-V SEMICONDUCTOR COMB SOURCES

In this section, we review the state-of-the-art monolithic III-V semiconductor comb sources [see Figs. 3(a) and 3(b) for examples].

© Author(s) 2022

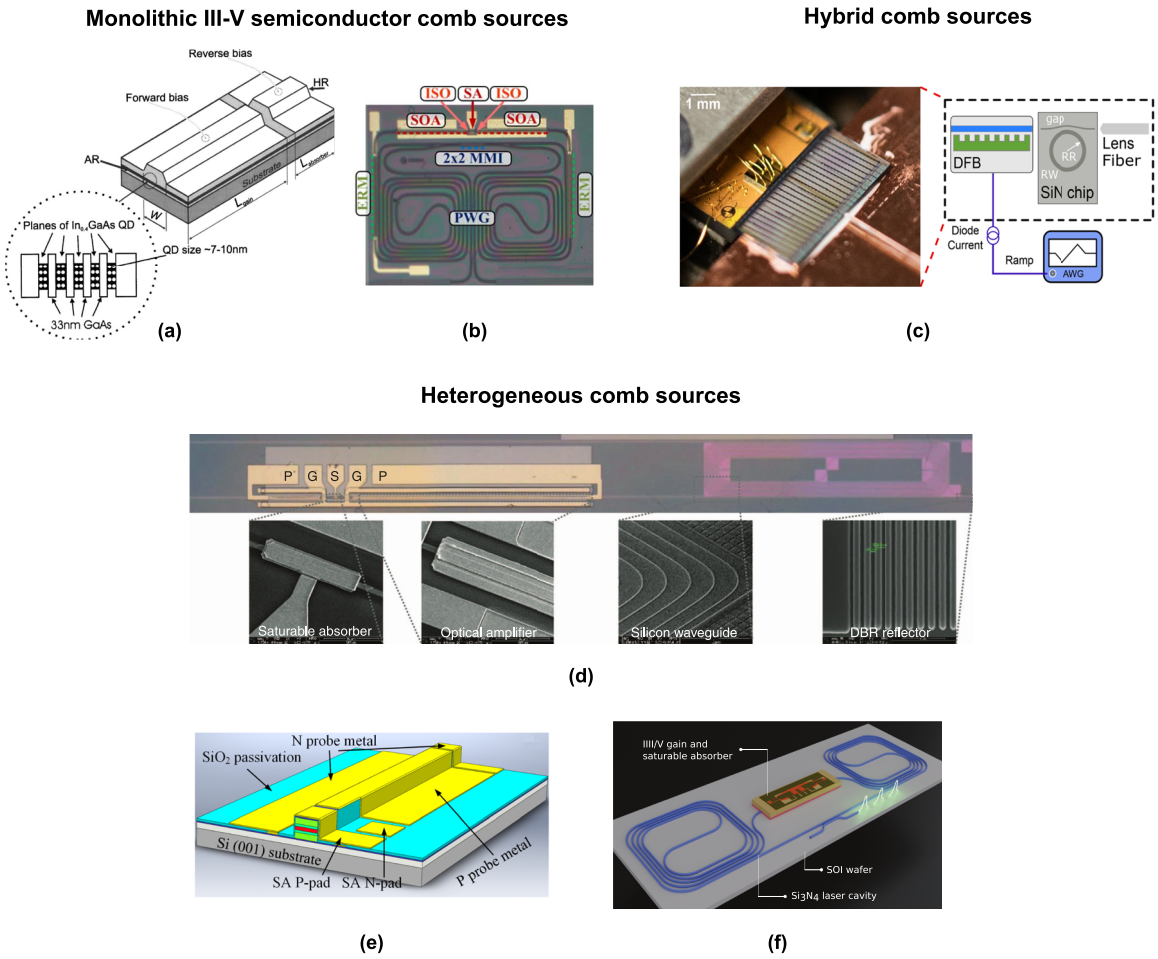

FIG. 3. Examples of monolithic III-V comb sources, hybridly and heterogeneously integrated comb sources. (a) Simplified schematic of a two-section Fabry–Pérot quantum dot (QD) mode-locked laser, grown on a GaAs substrate, with ridge width $W = 5\ \mu$m, gain section length $L_{gain} = 1.8$ mm, and saturable absorber length $L_{absorber} = 0.30$ mm.[92] (b) Microscope image of a mode-locked extended-cavity quantum well ring laser (2.3 mm by 1.75 mm) realized in passive–active InP photonic integrated circuit technology.[93] SOA: semiconductor optical amplifier; SA: saturable absorber; ISO: electrical isolation; ERM: electro-refractive modulator; MMI: multimode interference coupler; and PWG: passive waveguides. (c) A chip-scale distributed feedback (DFB) laser butt-coupled to a silicon nitride (SiN) chip containing a microresonator where Kerr solitons are generated and coupled off-chip with a lensed fiber.[94] AWG: arbitrary waveform generator; RR: ring radius; and RW: resonator waveguide width. (d) Microscope image of a heterogeneous III-V-on-silicon mode-locked laser with a 1 GHz repetition rate, fabricated by bonding.[95] Insets: Scanning electron microscope images of various parts of the laser. DBR: distributed Bragg reflector. (e) Schematic diagram of a Fabry–Pérot quantum dot mode-locked laser grown on silicon.[96] SA: saturable absorber. (f) Artistic rendering of a heterogeneous extended-cavity ring mode-locked laser with two long SiN spirals and a transfer printed III-V amplifier with saturable absorber.[97] (a) Reproduced from Rafailov *et al.*, Appl. Phys. Lett. **87**, 081107 (2005), with the permission of AIP Publishing. (b) Reproduced with permission from Latkowski *et al.*, Opt. Lett. **40**, 77 (2015). Copyright 2014, Optical Society of America. (c) Reproduced from Briles *et al.*, APL Photonics **6**, 026102 (2021), with the permission of AIP Publishing. (d) Reproduced with permission from Wang *et al.*, Light: Sci. Appl. **6**, e16260 (2017). Copyright 2017, Springer Nature Limited. (e) Reproduced with permission from Liu *et al.*, Optica **6**, 128 (2019). Copyright 2019, Optical Society of America. (f) Reproduced with permission from Cuyvers *et al.*, Laser Photonics Rev. **15**, 2000485 (2021). Copyright 2017, John Wiley & Sons, Inc.

The term "monolithic" means that only a single substrate is used in the fabrication of these comb sources. All the required materials are grown or deposited directly (as thin films) on this single III-V substrate. Compared to the hybridly and heterogeneously integrated comb sources discussed later [see Figs. 3(c)–3(f) for examples], the monolithic III-V semiconductor comb sources have a much longer history with many more demonstrations and center emission frequencies spanning the visible to the terahertz spectrum.

A. Visible spectrum (400–750 nm)

There have been very few demonstrations of monolithic III-V semiconductor comb sources emitting in the visible wavelength range compared to the other wavelength ranges discussed here. Passively mode-locked two-section Fabry–Pérot quantum well diode lasers emitting around 420[130] and 752 nm[131] have been reported. The violet-blue mode-locked lasers have InGaN quantum wells grown on GaN substrates and emit pulses as short as 3 ps with

© Author(s) 2022

peak powers up to 320 mW and a repetition rate in the range of 40–93 GHz, when operated under pulsed driving conditions. The red mode-locked lasers have AlGaAs quantum wells grown on GaAs substrates and emit pulses as short as 3.5 ps at a repetition rate of 19.37 GHz with an average optical power of 5.9 mW and an optical bandwidth of 0.62 nm. The limited amount of comb demonstrations in the visible wavelength range may be due to the application perspectives (e.g., optical atomic clocks,[132] astronomical spectrograph calibration,[133] and biological imaging;[134] see also Table II) being perceived less compelling or highly demanding in terms of comb performance. In addition, gallium nitride material technology has some peculiar features making mode-locking challenging.[130]

Table III lists the specifications for state-of-the-art monolithic III-V comb sources in the visible wavelength range.

B. Near-infrared (750 nm to 2 μm)

There is a large body of research focusing on near-infrared monolithic III-V mode-locked (interband) diode lasers, primarily at wavelengths of ~850 nm, ~1.3, and ~1.6 μm.[30,54,160–167] These are the main wavelengths used in fiber-optic communications, which has been one of the key drivers behind the development of diode lasers and integrated optics.[168] For wavelengths of ~1.6 μm, common gain media are InGaAsP and AlGaInAs quantum wells,[163,164,166,169,170] and InAs quantum dots or dashes (i.e., elongated quantum dots),[60,153,171–173] all grown on InP substrates. 1.3 μm lasers typically rely on InGaAsP or AlGaInAs quantum wells grown on InP substrates[160,174] or InAs quantum dots on GaAs substrates.[32,175,176] For wavelengths of ~850 nm, GaAs quantum wells grown on GaAs substrates are commonly used.[136,163,177]

While research on near-infrared monolithic III-V comb sources has focused primarily on conventional AM comb sources based on passive, active, or hybrid mode-locking schemes, there have been multiple reports of FM comb sources as well,[30] both for quantum well[22,151,159,178–180] and quantum dot/dash devices.[21,143,152,158,181] FM mode-locking has mostly been observed in single-section Fabry–Pérot devices without saturable absorber, although it has also been reported in devices with saturable absorber.[21,143,173] In Ref. 21, it is shown that AM and FM combs can be generated in the same device by switching the absorber voltage between −3.8 and 0 V. The use of single-section Fabry–Pérot devices without saturable absorber does not necessarily lead to FM comb operation; it may also result in AM comb formation with short optical pulses.[60,61,146,171,182] FM comb sources based on Fabry–Pérot lasers with an intracavity phase modulator have been demonstrated as well.[179]

For near-infrared monolithic III-V quantum well mode-locked lasers, optical bandwidths up to 14 nm have been observed,[144] pulse durations as short as 0.3 ps,[67,68,149] average powers up to 489 mW (associated pulse energies of 62 pJ),[137] RF linewidths down to 1 kHz in a free-running single-section device[159] and <2 Hz in hybridly mode-locked lasers,[93,150] and optical linewidths below 10 kHz (for a free-running single-section FM comb source).[159] Repetition rates as low as 880 MHz have been demonstrated.[150] Even a 55 MHz repetition rate has been realized by combining a 3.55 GHz III-V mode-locked laser with an on-chip Mach–Zehnder modulator that acts as a pulse selector.[148] Very high repetition rates, exceeding 1 THz, have also been reported in harmonically mode-locked lasers.[67,68] In Ref. 67, the authors observed mode-locking at a 1.54 THz repetition rate in a passively mode-locked laser with a fundamental repetition rate of 39 GHz. One of the mirrors is a 120 μm long distributed Bragg reflector that has peaks in its reflection spectrum spaced by 0.4 THz, causing the laser to operate at repetition rates of integer multiples of 0.4 THz (the repetition rate depends on the gain current).

Many of the above-mentioned monolithic III-V quantum well comb sources are not just all-active Fabry–Pérot devices with cleaved facets as mirrors, but true photonic integrated circuits (PICs) with multiple on-chip components (both passive and active; e.g., mirrors, splitters/combiners, optical amplifiers, saturable absorbers) connected by waveguides, fabricated on InP substrates [see Fig. 3(b) for an example]. The InP photonic integration platform is one of the main commercial PIC platforms. Typical (passive) waveguide propagation losses are 2 dB/cm or less.[183] InP PIC technology allows for the implemenation of more advanced laser architectures. Extended-cavity mode-locked lasers with low repetition rates and narrow linewidths have been realized by combining active sections with long passive waveguide cavities.[150,184] Intracavity gain-flattening filters have been used to generate wider, more uniform comb spectra.[185] On-chip Mach–Zehnder modulators have been

TABLE II. Possible applications of on-chip optical comb sources in different wavelength ranges.

Wavelength range	Typical applications
Visible	Optical atomic clocks,[132,278] astronomical spectrograph calibration,[133,279] and biological imaging[134,280,281]
Near-IR	Telecommunication,[5,36,96,153,198,282–295] LiDAR,[52,296–298] information processing,[295,299,300] optical atomic clocks,[132,278] astronomical spectrograph calibration,[279,301] biological imaging,[134,280,281] and spectroscopy[180,265,302–304]
Mid-IR	Spectroscopy of gases and biomolecules[8,38,206,228,231,305–308]
Far-IR and THz	Spectroscopy of gases and biomolecules[8,218,308–310]

© Author(s) 2022

TABLE III. Overview of state-of-the-art monolithic III-V semiconductor comb sources emitting in the visible and near-infrared wavelength range. MLL: mode-locked laser, GS: gain-switched laser, and EO: electro-optic comb.

λ_c (μm)	ν_c (THz)	f_r (GHz)	$\Delta\nu$ (THz)	AM/FM	τ_p (ps)	P_{avg} (mW)	δf_r (kHz)	$\delta\nu$ (MHz)	Type	References
0.42	7.10×10^2	40.3	0.75[a]	AM	7	~100	···	···	MLL	130
0.752	399	19.37	0.33	AM	3.5	5.9	···	···	MLL	131
0.766	391	19.42	0.4	AM	5.7	11.3	···	···	MLL	135
0.836	359	126	1.0	AM	0.43	17.41	···	···	MLL	136
0.977	307	7.92	0.3	AM	16	489	···	···	MLL	137
1.26	238	21	2.6	AM	0.39	~20	···	···	MLL	92
1.26	238	5	~1.3	AM	5.1	~30	···	···	MLL	138
1.26	238	10	···	AM	2.2	287.7	···	···	MLL	139
1.29	233	238	···	AM	1.3	3.1	···	···	MLL	140
1.29	233	10	0.27	AM	6	~1	0.2	···	MLL	141
1.53	196	15	0.5	AM	5–8	~0.03	<400	~600	MLL	142
1.53	196	4.6	~0.9	FM	···	~0.8	~57	···	MLL	143
1.54	195	21.5	1.8	AM	~0.35	<1	450	···	MLL	144
1.54	195	34.5	1.5	AM	0.8	46	<10	0.850	MLL	145
1.54	195	92	1.5	AM	0.312	8.6	<20	···	MLL	60
1.54	195	50	2.3	AM	0.295	~40	···	···	MLL	146
1.54	194	4.29	0.72	AM	10	250	···	···	MLL	147
1.55	194	6.25	0.06	···	···	···	0.01	1.5	GS	71
1.55	193	0.055[b]	0.29	AM	15.4	~1	···	···	MLL	148
1.55	193	50	~0.9	AM	0.27	<0.15	···	···	MLL	149
1.55	193	0.9	···	AM	~500[c]	···	71[d]	···	MLL	150
1.55	193	21.7	~0.6	FM	···	~1	116	~1	MLL	151
1.55	193	48	1.9	FM	···	40	~60	~10	MLL	152
1.55	193	34.2	~2	···	···	···	1.7	0.62	MLL	153
1.55	193	1	0.04	···	···	···	···	~11	EO	128
1.56	193	1.54×10^3	···	AM	0.26	16	···	···	MLL	67
1.56	193	10	0.70	AM	1.06	<1	2	···	MLL	154
1.56	193	346	1.0	AM	0.56	4	···	···	MLL	155
1.56	192	100	1	FM	···	19	<200	~10	MLL	22
1.56	192	5	~0.02	···	···	···	···	0.350	GS	156
1.57	191	1.28×10^3	1.1	AM	0.30	15.37	···	···	MLL	68
1.58	190	2.5	0.4	AM	9.8	0.080	6.13[e]	···	MLL	93
1.58	190	1	0.6	AM	36	~0.04	~100	~70	MLL	157
1.59	189	4.4	···	FM	···	<350	0.300	···	MLL	158
1.59	189	10	1.1	FM	···	<420	~0.8	···	MLL	158
1.68	178	19.4	···	FM	···	8	1	<0.01	MLL	159
1.81	166	9.7	~1.3	···	···	3.20×10^{-7}	···	···	$\chi^{(2)}$	45

[a]Bandwidth of the main mode cluster. There is a second, weak mode cluster that is only partially locked to the main cluster.
[b]Realized by combining a 3.55 GHz III-V mode-locked laser with an on-chip Mach–Zehnder modulator.
[c]For passive mode-locking. For hybrid mode-locking, the pulse duration goes down to 200 ps.
[d]For passive mode-locking. For hybrid mode-locking, the RF linewidth is reduced to <1 Hz.
[e]For passive mode-locking. For hybrid mode-locking, the RF linewidth is reduced to <2 Hz.

used as pulse selectors.[148] Integrated optical pulse shapers can be constructed, e.g., to compress the pulses emitted by a mode-locked laser.[186,187]

While monolithic quantum well mode-locked lasers have been around for over three decades,[161] the first monolithic III-V quantum dot mode-locked laser was only demonstrated in 2001.[32] The large majority of quantum dot mode-locked lasers are all-active Fabry–Pérot devices [see Fig. 3(a) for an example], yet a device with an integrated passive section has also been reported recently.[188] The use of quantum dots instead of wells is expected to improve the performance of mode-locked lasers. Quantum dot devices have low absorption saturation energy, high gain saturation energy, short absorption recovery times, wide inhomogeneously broadened gain spectra, small linewidth enhancement factors, high gain, high temperature and feedback resilience, and high tolerance to growth defects.[165,175,176,189–195]

© Author(s) 2022

Near-infrared monolithic III-V quantum dot and dash mode-locked lasers with repetition rates ranging from 4.6[143,173] to 346 GHz[155] have already been realized. Optical bandwidths up to 17.9 nm have been reported,[146] pulse durations as short as 295 fs,[146] free-running RF linewidths down to 200 Hz,[141] and free-running optical linewidths down to 620 kHz.[153] AM comb sources (passively mode-locked two-section Fabry–Pérot devices) emitting average optical powers up to 288 mW (corresponding to pulse energies of 28.7 pJ)[139] and FM comb sources (single-section Fabry–Pérot devices) emitting average powers as high as 417 mW have been demonstrated.[158]

Apart from mode-locked lasers, also gain-switched monolithic III-V laser comb sources have been reported in the 1.5 to 1.6 μm wavelength range. Comb generation based on gain-switching has been observed in the discrete mode[36,196] and distributed feedback (DFB) lasers.[15] Optical injection locking of gain-switched lasers has been demonstrated as well, with the master (CW) and slave (gain-switched) lasers integrated on the same chip.[71,156,197–200] Optical injection locking has been shown to reduce the phase noise and increase the comb bandwidth.[71,156,197,200] In contrast to mode-locked lasers, the repetition rate of a gain-switched laser can easily be tuned over a wide range by adjusting the frequency of the applied RF signal. Yet, the optical bandwidth and pulse duration are limited. Repetition rates from 4[197] to 18 GHz[15] have been demonstrated, with bandwidths up to 0.8 nm[15] and pulse durations down to 15 ps.[15] Average optical powers up to 2 mW[36] and RF and optical linewidths down to 10 Hz (corresponding to the resolution bandwidth of the electrical spectrum analyzer)[71] and ~350 kHz[156] have been reported, respectively.

Monolithic III-V electro-optic comb cources have been demonstrated as well.[43,127,128] The comb sources consist of a ~1.55 μm distributed Bragg reflector (DBR) laser followed by a cascade of optical modulators and a semiconductor optical amplifier (SOA), all integrated on an InP PIC. Electro-optic comb sources allow for easy tuning of the repetition rate (within the modulators' electro-optic bandwidth). In Refs. 43, 127, and 128, the authors demonstrate repetition rates ranging from 1 to 10 GHz, with corresponding optical bandwidths of 0.4 and 0.6 nm. A linewidth down to 11 MHz is reported for the DBR laser.[128]

Yet another approach to generate near-infrared combs with a monolithic III-V device is to make use of intracavity sum frequency generation in mid-infrared comb sources. This has been demonstrated in interband cascade lasers (ICLs), but with very low powers in the near-infrared spectral range.[45] In Ref. 45, an ICL emitting 10 mW of average optical power at 3.6 μm and sub-nanowatts of power at 1.8 μm is reported (with a ~14 nm optical bandwidth).

A list of specifications for state-of-the-art monolithic III-V comb sources in the near-infrared wavelength range is given in Table III.

C. Mid-infrared (2 to 20 μm)

Monolithic III-V semiconductor comb sources based on conventional interband diode lasers,[202] interband cascade lasers (ICLs),[10] and quantum cascade lasers (QCLs)[37] have been demonstrated in the mid-infrared wavelength range.

There have been multiple demonstrations of Fabry–Pérot quantum well diode lasers grown on GaSb substrates emitting combs in the 2.0 to 2.2 μm range.[201–204,226] Both two-section passively AM mode-locked lasers[201,204,226] and single-section FM mode-locked lasers[202] have been reported. The passively AM mode-locked GaSb-based lasers have repetition rates ranging from 9.6 to 18.5 GHz, pulse durations down to ~2.4 ps,[204] average optical output powers up to ~5 mW,[201] and RF linewidths down to 8.4 kHz.[204] The 19 GHz-repetition-rate FM comb source outputs 50 mW of optical power, has an RF linewidth down to ~1.5 kHz, and a ~700 kHz optical comb linewidth (determined from a free-running RF dual-comb spectrum).[202]

In recent years, several interband cascade laser (ICL) comb sources have been developed, both type-I[205,227] and type-II quantum well cascade lasers.[45,206,207,228–231] The reported type-I quantum well cascade lasers are passively AM mode-locked two-section Fabry–Pérot devices on GaSb substrates emitting at wavelengths between 2.7 and 3.3 μm.[205,227] AM mode-locking has been observed in these devices when applying a reverse bias to the absorber section with ~10 ps pulses at a repetition rate of 13.2 GHz, an average power exceeding 1 mW, an optical bandwidth of about 20 nm, and an RF linewidth of 180 kHz.[205] The demonstrated type-II quantum well cascade comb lasers are processed on GaSb substrates and emit in the 3.2 to 3.9 μm wavelength range.[45,206,207,228–231] Both two-section[45,206,207,229–231] and single-section[228] Fabry–Pérot devices have been reported. The two-section devices consist of a long gain section and a short section that is typically optimized for a low parasitic capacitance for efficient RF extraction and injection. The short section's DC bias can be tuned to alter the locking properties (by changing the dispersion and gain).[230] To date, passive AM mode-locking has not been observed in type-II ICL comb sources. Instead these devices tend to generate FM combs. Yet, AM operation has been demonstrated in an actively mode-locked two-section device where 32 dBm of RF power is injected in the short section.[207] This actively mode-locked device emits 3.2 ps pulses at a repetition rate of 10.2 GHz and a wavelength of 3.9 μm with an average power of 2.7 mW. For the other type-II ICL combs, average powers up to ~8 mW[45,206] and RF linewidths down to 350 Hz have been reported.[206]

Research on mid-infrared comb generation in quantum cascade lasers (QCLs) has been ongoing for over a decade.[35,37] Common materials used in mid-infrared (mid-IR) QCL comb sources are InGaAs quantum wells and AlInAs barriers grown on InP substrates.[35,37,210,232–235] Both AM[35,212,213,236] and FM[37,215] mode-locked comb operation have been demonstrated, with wavelengths ranging from 4.5[208] to 9 μm[215] and repetition rates ranging from 7[209] to 400 GHz (for a harmonic comb state).[208] AM comb formation in Fabry–Pérot QCLs has been challenging to achieve due to the short gain recovery time (on the order of picoseconds) compared to the cavity round-trip time (typically on the order of 100 ps).[35] Nevertheless, actively AM mode-locked mid-IR Fabry–Pérot QCLs have been realized,[35,213] in which a short section of the QCLs is injected with an RF signal at the repetition rate. In Ref. 35, the authors designed a QCL structure with a longer upper state lifetime compared to convential QCL designs. At a temperature of 77 K, this QCL emits ~3 ps pulses at a wavelength of 6 μm and a repetition rate of 17.9 GHz with an RF linewidth of ~3 kHz and a pulse energy close to 0.5 pJ (average power of ~9 mW). In Ref. 213, the authors designed a QCL structure with a larger modulation depth compared to traditional designs to achieve stable AM mode-locking.

© Author(s) 2022

At a temperature of 288 K (15 °C), this 12 GHz-repetition-rate QCL emits 6.5 ps pulses at an average output power of 20 mW and ~12 ps pulses at an average power of 62 mW, all at a wavelength of 8 μm. For other Fabry–Pérot QCL combs, average powers up to 1 W have been reported,[210,214] RF linewidths below 10 Hz,[37] and optical linewidths as low as (292 ± 79) Hz.[211] Apart from conventional Fabry–Pérot QCLs, also electrically pumped ring cavity QCL combs have been demonstrated recently.[212,234,236] In Fabry–Pérot QCLs, spatial hole burning is responsible for their multimode operation, a requirement for comb formation. However, in ring cavities, spatial hole burning is expected to be negligible. Instead, their multimode operation is thought to be caused by a phenomenon known as phase turbulence.[234] Bright dissipative Kerr solitons of ~3 ps duration have been observed in a ring QCL on top of a dispersive wave background for a total output power of ~0.6 mW and at a wavelength of 7.6 μm.[212] None of the demonstrated ring QCLs used a bus waveguide to extract the generated light from the ring. Instead the authors collected the light radiated tangentially to the ring. It is expected that more power can be extracted by including a bus waveguide. Yet, care must be taken to avoid perturbations that cause backscattering.[212]

Table IV lists some specifications for state-of-the-art monolithic III-V comb sources in the mid-infrared spectral range.

D. Far-infrared and terahertz (20 μm to 1 mm)

Also in the far-infrared and terahertz spectral range, QCLs offer a solution for chip-based comb generation.[237] These QCLs typically contain GaAs quantum wells and AlGaAs barriers grown on GaAs substrates,[222,223,237,238] although also InP-based terahertz QCL combs have been realized that rely on down-converting a mid-infrared comb through difference frequency generation.[46] Many Fabry–Pérot QCL combs have been demonstrated in recent years, both AM and FM combs,[221,224,225,238–244] with repetition rates rang-

TABLE IV. Overview of state-of-the-art monolithic III-V semiconductor comb sources emitting in the mid-infrared to terahertz spectral range. MLL: mode-locked laser.

λ_c (μm)	ν_c (THz)	f_r (GHz)	$\Delta\nu$ (THz)	AM/FM	τ_p (ps)	P_{avg} (mW)	δf_r (kHz)	$\delta\nu$ (MHz)	Type	References
2.0	1.50×10^2	18.5	0.26	AM	···	~1.5	30	···	MLL	201
2.1	1.50×10^2	19	···	FM	···	50	1.5	0.7	MLL	202
2.1	1.40×10^2	20.6	···	···	···	~0.6	10	···	MLL	203
2.2	1.40×10^2	9.6	0.70	AM	~5	~3	8.4	···	MLL	204
3.2	93	13.2	0.57	AM	~10	~1	180	···	MLL	205
3.6	83	9.7	···	···	···	~8	0.350	···	MLL	206
3.9	78	10.2	~0.44	AM	3.2	2.7	···	···	MLL	207
4.5	67	400	···	···	···	···	···	···	MLL	208
4.7	64	7	···	···	···	60	0.3	0.5[a]	MLL	209
5.0	60	9.2	···	···	···	~750	<0.5	···	MLL	210
6.3	48	17.9	~0.2	AM	~3	~9	~3	···	MLL	35
7.0	43	7.5	···	FM	···	~20	0.0088	<1.3	MLL	37
7.1	42	7.5	···	FM	···	25	···	0.0003	MLL	211
7.6	39	23.9	~0.2	AM/FM[b]	3	~0.6	···	···	MLL	212
7.9	38	12.3	~0.07	AM	6.5	20	···	···	MLL	213
8.2	37	9.8	···	···	···	1050	~0.3	···	MLL	214
8.9	34	11.1	···	FM	···	~200	3	···	MLL	215
71	4.2	4.7	···	···	···	~1.5	3.6	<100	MLL	216
71	4.2	6.6	~0.08	···	···	~0.7	···	···	MLL	217
71	4.2	6.2	···	···	···	~1	<0.500	···	MLL	218
79	3.8	15.5	···	c	···	~5	···	···	MLL	219
81	3.7	6.8	···	AM/FM[d]	···	~5	98[e]	1.8	MLL	220 and 221
97	3.1	19.5	···	···	···	~0.06	18	~2.3	MLL	222
1.10×10^2	2.8	245	···	···	···	~0.003	···	···	$\chi^{(2)}$	46
1.10×10^2	2.7	13.3	~0.2	···	···	~0.03	980	···	MLL	223
1.20×10^2	2.6	12.9	0.15	AM	4	···	···	···	MLL	224
1.20×10^2	2.5	13.3	~0.05	AM	~10	~17	···	~0.1[f]	MLL	225

[a]After phase-locking a single comb tooth to a reference laser, the linewidth can be reduced to 1–23 kHz.
[b]There are two mode groups in the spectrum. One mode group corresponds to a frequency-modulated wave, while the other corresponds to an amplitude-modulated wave. The authors filter out the FM wave with a bandpass filter.
[c]Simulations indicate high-contrast amplitude modulation.
[d]There are two lobes in the optical spectrum. One lobe corresponds to an AM comb with ~ 20 ps pulses, while the other lobe has an FM comb character.
[e]<2 Hz when the repetition rate is stabilized.
[f]<1 Hz when the repetition and carrier frequency are both locked.

© Author(s) 2022

ing from 4.7[216] to 245 GHz[46] (harmonic comb state), emission frequencies from 1.6[223] to 4.3 THz,[218] and average powers up to ~17 mW.[225] A free-running RF linewidth < 500 Hz[218] and a stabilized beat note linewidth of 2 Hz[220] have been achieved. Optical linewidths on the order of 100 kHz have been reported for an RF injection-locked terahertz QCL comb, which decreased below 1 Hz when the offset frequency is also locked (to a harmonic of the repetition rate of a fiber-based femtosecond laser).[225] Similar to mid-infrared QCLs, the short gain recovery times make AM operation with short optical pulses challenging in far-infrared and terahertz QCLs.[245,246] While passive AM mode-locking has not yet been achieved,[247] there have been multiple reports of actively AM mode-locked terahertz QCLs,[224,225,239–242] with pulse durations down to 4 ps.[224] Apart from Fabry–Pérot QCL comb sources, also ring-type terahertz QCL combs have been realized with emission frequencies between 3.2 and 4.1 THz, a fundamental repetition rate of 15.5 GHz, and average output powers of several milliwatts.[219] A disadvantage of working with far-infrared and terahertz QCL comb sources is that they generally require cryogenic temperatures for their operation, as opposed to the majority of on-chip comb sources in the visible to mid-infrared wavelength range. Yet, also room-temperature chip-based terahertz combs have been demonstrated relying on difference frequency generation in mid-infrared QCL comb sources.[46] The reported devices operate in a harmonic comb state with mode spacings of 157 or 257 GHz and limited output powers of several microwatts.

A list of specifications for state-of-the-art monolithic III-V comb sources in the far-infrared and terahertz spectral range is given in Table IV.

IV. HYBRID COMB SOURCES

Hybrid comb sources have only started being explored very recently. Research efforts have focused mostly on sources emitting at telecom wavelengths (1.5–1.6 μm), but a 2 μm wavelength device has also been reported.[255] Hybrid integration is a process in which multiple fully processed chips are assembled into a single package.[13] The majority of demonstrated hybrid comb devices consist of an active III-V chip butt-coupled to a passive silicon nitride (SiN) PIC [sometimes with integrated heaters; see Fig. 3(c) for an example], although silicon (Si)[48,255] and lithium niobate ($LiNbO_3$)[129] PICs have been used as well. III-V chips that have been used in hybrid comb sources are simple Fabry–Pérot lasers (emitting at multiple longitudinal modes),[94,252,256] single-frequency distributed feedback (DFB) lasers,[50,79,80,84,94,129,250,252,254] reflective semiconductor optical amplifiers (RSOAs, i.e., SOA chips where one facet has a highly reflective coating),[42,47,249,251] single-section quantum dash mode-locked lasers,[48] GaSb-based mode-locked lasers,[255] and InP PICs (with active and passive components).[248,253]

One major category of hybrid devices that has been explored are the hybrid Kerr comb sources. Kerr comb generators have long relied on off-chip, high-power, narrow-linewidth, tunable pump lasers, and complex tuning mechanisms for soliton generation. Hybrid integration of active III-V chips with high-Q SiN microresonators has finally enabled electrically pumped, chip-based Kerr comb sources.[42,79,80,94,250,254,256] Backscattering in the high-Q ring resonators leads to a dramatic linewidth reduction in the chip-based pump lasers through self-injection-locking. The self-injection-locking mechanism has even allowed turnkey comb generation.[79,80] Most hybrid Kerr comb demonstrations focus on microresonators operating in the anomalous group velocity dispersion (GVD) regime, enabling the formation of well-studied bright, temporal dissipative Kerr solitons (corresponding to highly coherent combs in the frequency domain). Yet also in the normal GVD regime, hybrid Kerr comb sources have been reported.[80,84] Repetition rates ranging from 5 GHz[80] to 2.04 THz (17-soliton crystal state)[254] have been demonstrated. Comb powers up to 17 mW (excluding the pump),[252] temporal solitons with sub-picosecond widths,[250] and optical linewidths below 10 Hz have been observed.[80] RF linewidths have not been reported to our knowledge, but single-sideband phase noise measurements at the repetition frequency (5.4 GHz) have shown a phase noise of −114 dBc/Hz at an offset frequency of 10 kHz and −140 dBc/Hz at 100 kHz.[80] Pump-to-comb sideband conversion efficiencies of 40% have been measured for bright solitons (anomalous GVD regime) with a 1 THz line spacing.[252] For platicon pulses (normal GVD regime) with a 26.2 GHz repetition rate, pump-to-platicon conversion efficiencies of 30% have been estimated.[84] This is a significant improvement compared to the 0.4% pump-to-soliton efficiency previously reported for bright solitons with a 20 GHz repetition rate.[257]

Another class of hybrid devices that has been investigated are hybrid InP–SiN mode-locked lasers. The InP chips provide the gain and mode-locking element, while the low-loss SiN PICs serve as extended cavities that increase the cavity photon lifetime and hence decrease the optical and RF linewidths.[266,267] By doing so, low-noise, low-repetition-rate, chip-scale mode-locked lasers can be made. Both devices with[248,253] and without saturable absorber[47,249,251] have been studied. Repetition rates ranging from 360 MHz[251] to 15.5 GHz,[253] optical bandwidths up to 25 nm,[248] pulse durations down to 3.1 ps,[253] average optical output powers up to 9 mW,[249] RF linewidths down to 31 Hz,[253] and optical linewidths down to 34 kHz have been observed.[47]

A hybrid gain-switched comb source has also been reported, consisting of a DFB laser butt-coupled with a SiN high-Q microring reflector.[50] The self-injection-locking mechanism induced by the microring reflector enhances the comb's coherence, flatness, and carrier-to-noise ratio (CNR). Compared to a solitary DFB laser, the optical linewidth of the hybrid device decreases from 7.34 MHz to 615 kHz, the RF linewidth decreases from 100 to 50 Hz, the CNR increases from 27 to 40 dB, and the number of lines in the 3 dB optical bandwidth increases from 5 to 8 (for a line spacing of 6.5 GHz). The line spacing can be tuned from 5.55 to 8.7 GHz.

Si PICs have been used to provide optical feedback to III-V mode-locked lasers and thereby reduce their phase noise.[48,255] In Ref. 48, the RF linewidth of a 1.5 μm wavelength quantum dash mode-locked lasers is reduced from 15.01 kHz without feedback circuit to 2.77 kHz with feedback. In Ref. 255, the minimum RF linewidth of a 2 μm wavelength passively mode-locked GaSb-based mode-locked lasers is reduced from ~9.1 kHz to ~900 Hz by introducing the Si feedback circuit.

A hybrid III-V-$LiNbO_3$ electro-optic comb source has been reported.[129] The authors butt-couple a DFB laser with a $LiNbO_3$ PIC containing a non-resonant electro-optic amplitude modulator followed by a phase modulator. The cascaded modulators convert the single-frequency pump laser light into a comb. This approach gives great flexibility in repetition rate and operating wavelength and

© Author(s) 2022

TABLE V. Overview of state-of-the-art hybrid comb sources. MLL: mode-locked laser, GS: gain-switched laser, and EO: electro-optic comb.

λ_c (μm)	ν_c (THz)	f_r (GHz)	$\Delta\nu$ (THz)	AM/FM	τ_p (ps)	P_{avg} (mW)	δf_r (kHz)	$\delta\nu$ (MHz)	Type	Integration	References
1.53	195	5.5	···	···	···	2	18	0.034	MLL	Butt-coupling	47
1.54	195	2	3.2	···	···	1.7	110	···	MLL	Butt-coupling	248
1.54	194	2.2	···	AM/FM	···	9	···	···	MLL	Butt-coupling	249
1.54	194	30	···	···	···	···	···	···	EO	Butt-coupling	129
1.55	194	30.6	0.58	AM[a]	<1	1[b]	···	0.001	Kerr	Butt-coupling	250
1.55	193	0.360	0.06	···	···	1	···	···	MLL	Butt-coupling	251
1.55	193	1×10^3	···	AM	···	17[c]	···	~0.008	Kerr	Butt-coupling	252
1.55	193	6.5	0.05	···	···	···	0.050	0.615	GS	Butt-coupling	50
1.56	193	5.4	···	[d]	···	···	···	···	Kerr	Butt-coupling	80
1.56	193	43.2	···	···	···	···	···	$<1 \times 10^{-5}$	Kerr	Butt-coupling	80
1.57	191	15.5	0.18	AM	3.1	~0.3	···	···	MLL	Butt-coupling	253
1.57	191	2.18	0.5	AM	6.31	~0.3	0.031	···	MLL	Butt-coupling	253
1.58	190	2.04×10^3	···	AM	···	···	···	0.001	Kerr	Butt-coupling	254
1.96	153	13.3	0.4	···	···	···	0.9	···	MLL	Butt-coupling	255

[a]Solitons on a CW background.
[b]Soliton power.
[c]Comb power excluding pump line; with pump line the power is 20 mW.
[d]Simulations indicate the formation of flat-top pulses.

results in comb power that scales linearly with pump power, along with a flat spectrum. The authors show that the hybrid device can generate a comb with a 30 GHz line spacing and a 10 dB optical bandwidth of ~12 nm. After pulse compression in a single-mode fiber, a pulse duration of 522 fs is measured. The pulse compression stage can also be integrated on the PIC. An on-chip pump-to-comb conversion efficiency of 25% is reported.

Table V gives an overview of the specifications of state-of-the-art hybrid comb sources.

V. HETEROGENEOUS COMB SOURCES

Heterogeneously integrated comb sources have been investigated for over a decade.[34] Demonstrated devices emit at wavelengths

TABLE VI. Overview of state-of-the-art heterogeneous comb sources. MLL: mode-locked laser and EO: electro-optic comb.

λ_c (μm)	ν_c (THz)	f_r (GHz)	$\Delta\nu$ (THz)	AM/FM	τ_p (ps)	P_{avg} (mW)	δf_r (kHz)	$\delta\nu$ (MHz)	Type	Integration	References
1.27	236	20	1.1	AM	~10	~12	2.7	~10.6	MLL	Epitaxy	96
1.30	231	15	2.1	···	···	···	···	···	MLL	Bonding	258
1.31	229	19	···	AM	~5	~14	···	···	MLL	Bonding	259
1.31	229	19	···	AM	~1.9	~4	6	···	MLL	Bonding	259
1.31	229	9.4	0.79	AM	3.2	0.64	0.400	···	MLL	Epitaxy	260
1.31	228	9.1	0.62	AM	1.3	<1	80	···	MLL	Epitaxy	261
1.32	228	102	1	···	···	···	···	···	MLL	Bonding	262
1.32	228	31	···	AM	0.490	~40	100	30	MLL	Epitaxy	41
1.55	193	100	1.5	AM[a]	···	···	···	3×10^{-4}	Kerr	Bonding	49
1.57	190	19	···	···	···	···	···	···	EO	Transfer printing	51
1.58	190	0.93	0.01	AM	~200	~0.1	···	<7	MLL	Bonding	263
1.58	190	20	0.43	AM	0.890	···	···	···	MLL	Bonding	264
1.58	190	20	0.36	AM	0.900	1.83	1.6	···	MLL	Bonding	166
1.58	190	0.755	0.2	AM	7.5	~0.1	0.001	<0.2	MLL	Transfer printing	97
1.60	187	1	1	AM	···	0.3	0.002	···	MLL	Bonding	265
1.60	187	1	1	AM	~7	~0.3	~0.3	<0.4	MLL	Bonding	95
1.61	186	3	0.2	AM	~8	~6	0.4	<1	MLL	Transfer printing	14

[a]Solitons on a CW background.

© Author(s) 2022

of ~1.3 μm[41,268,269] or ~1.6 μm,[14,34,97] and they rely on III-V quantum dot[41,269] or well[14,34,97,268] material for gain and/or mode-locking. Heterogeneous integration is a process in which multiple material technologies (e.g., III-V semiconductors and Si photonics) are combined on a single chip.[13] Several heterogeneous integration approaches have been explored for the fabrication of on-chip comb sources, including bonding,[34,269] epitaxial growth,[41] and transfer printing.[14,97] Heterogeneous integration is generally considered to be more conducive to low-cost mass manufacturing compared to hybrid integration.

One major class of heterogeneous comb sources are the mode-locked lasers realized by bonding of III-V material with Si waveguide circuits [see Fig. 3(d) for an example].[166,167] After bonding, the active III-V material is processed into SOAs and saturable absorbers. Both bonding of quantum well material (for lasing wavelengths of ~1.3[268] and ~1.6 μm[34]) and quantum dot material (for a ~1.3 μm lasing wavelength[270]) have been reported. The Si PICs serve as extended low-loss cavities, thereby enabling low-noise, low-repetition-rate mode-locked lasers. To achieve low-loss transitions from the passive to the active sections, tapered waveguides are typically used.[271,272] The Si PIC platform also allows for the integration of additional components, both inside and outside the laser cavity. Feedback circuits outside the laser cavity have been utilized for on-chip laser stabilization.[259,268] Intracavity filters have been used to realize low-noise mode-locked lasers with a relatively high repetition rate.[273] Narrower linewidths are typically achieved by increasing the cavity length, but this comes with a decrease in repetition rate. If the application demands a high repetition rate but narrow linewidths, one can use a long cavity combined with an intracavity filter (e.g., a ring resonator) that only passes the frequencies with the desired spacing. Repetition rates from 930 MHz[263] to 102 GHz[262,274] have been reported for bonded III-V-on-Si mode-locked lasers, with optical bandwidths up to 12 nm.[258] Pulse durations as short as 890 fs,[264] average optical output powers up to ~14 mW (on-chip),[259] free-running RF linewidths down to 2 Hz,[265] and optical linewidths below 400 kHz have been observed.[95] Passive,[34,275] active,[263] and hybrid[34,275] mode-locking have been demonstrated.

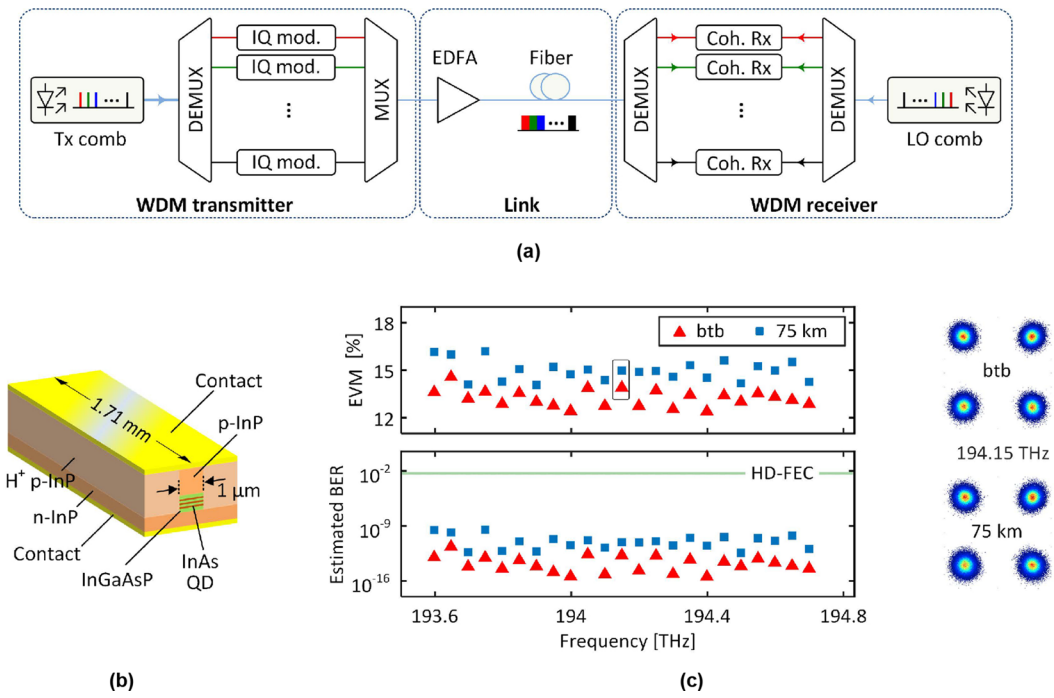

FIG. 4. Example of on-chip optical comb sources used for fiber-optic communication in a wavelength-division multiplexing (WDM) transmitter and receiver.[292] (a) Schematic of a coherent wavelength-division multiplexing (WDM) link using combs as light sources in the transmitter (Tx) and receiver (Rx). The comb lines are demultiplexed (DEMUX) in the transmitter and sent through separate in-phase/quadrature modulators (IQ mod.), after which they are multiplexed (MUX) again to form the WDM sigal. The WDM signal is sent through a fiber link with an erbium-doped fiber amplifier (EDFA). The WDM signal is demultiplexed at the receiver side and sent to separate coherent receivers (Coh. Rx) together with demultiplexed local oscillator (LO) comb lines. (b) Schematic of the quantum dash mode-locked lasers used in the demonstration of the WDM link. The active region consists of three InAs quantum dash layers separated by InGaAsP barriers. Cleaved chip facets form a Fabry–Pérot laser cavity with a length of 1.71 mm, leading to a free spectral range (FSR) of 25 GHz. Top and bottom gold layers provide electrical contacts to the active region via p-doped and n-doped InP layers. (c) Performance of the link using quantum dash mode-locked lasers in the transmitter and receiver. Upper left plot: measured error-vector magnitude (EVM) as a function of the carrier frequency of the channels for both back-to-back (btb) transmission and transmission through 75 km of standard single mode fiber. Lower left plot: bit error rate (BER) estimated from EVM. Right plot: example constellation diagrams for the signal carried by the comb line at 194.15 THz. Reproduced with permission from Kemal *et al.*, Opt. Express **27**, 31164 (2019). Copyright 2019, Optical Society of America.

© Author(s) 2022

Another type of heterogeneous comb sources are the III-V quantum dot lasers grown on Si substrates [see Fig. 3(e) for an example].[41] Reported devices are all-active Fabry–Pérot lasers emitting at a wavelength of ~1.3 μm. Single-[41,276] and two-section[96,260,261,277] mode-locked lasers have been demonstrated. Repetition rates ranging from 9[261] to 31 GHz,[41] optical bandwidths up to 6.1 nm,[96] pulse durations down to 490 fs,[41] average output powers up to 40 mW,[41] RF linewidths as low as 400 Hz,[260] and optical linewidths down to 10.6 MHz have been reported.[96]

Very recently, the first heterogeneous III-V-on-SiN mode-locked lasers have been demonstrated [see Fig. 3(f) for an example].[14,97] These were fabricated by transfer printing III-V thin-film devices (SOAs and saturable absorbers) on SiN PICs. Light is coupled from the active device sections to the passive SiN waveguides through an intermediate Si waveguide layer, enabling a high coupling efficiency. Low-loss SiN extended cavities allow for low-repetition-rate lasers with narrow linewidths. Moreover, two-photon absorption in SiN is negligible at telecom wavelengths, in contrast to Si. This is particularly important for AM comb sources, as their pulsed nature comes with relatively high light intensities. The demonstrated III-V-on-SiN mode-locked lasers have pulse repetition rates of 755 MHz[97] and 3 GHz[14] and emit at a wavelength of 1.6 μm. Optical bandwidths up to 2 nm,[14] pulse durations down to 7.5 ps,[97] and on-chip pulse energies up to ~2 pJ (corresponding average power of ~6 mW) were reported,[14] with free-running RF and optical linewidths down to 1 Hz and <200 kHz, respectively.[97]

The first heterogeneously integrated soliton Kerr comb source was also demonstrated recently.[49] This device consists of a heterogeneously integrated InP/Si DFB laser coupled with a SiN high-Q ring resonator (with a Si thermo-optic phase tuner in between). It was fabricated by sequential bonding of a Si-on-insulator wafer and III-V quantum well material with a patterned SiN PIC. Tapered waveguides are used for low-loss transitions from the DFB laser to the thermo-optic phase tuner to the SiN ring resonator. Depending on the laser current, the authors observe a single-soliton state (100 GHz repetition rate), a two-, three-, or four-soliton crystal state. In the self-injection-locked single-soliton state, they measure a fundamental linewidth of ~25 Hz for the pump laser (at a wavelength of 1.55 μm) and around 200 to 300 Hz for the first pair of neighboring comb lines.

Finally, a heterogeneous III-V-on-$LiNbO_3$ electro-optic comb source has been reported.[51] The device consists of a $LiNbO_3$ ring resonator, for resonant electro-optic comb generation, and an on-chip DFB pump laser. The DFB laser was fabricated by sequential

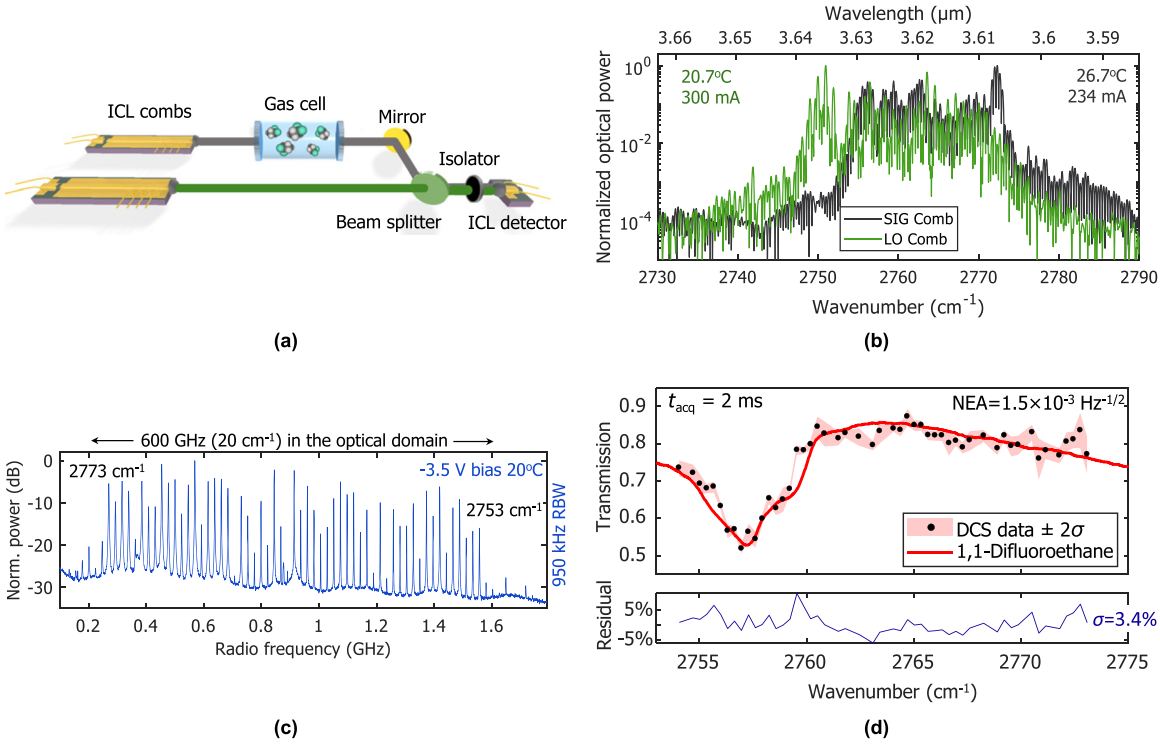

FIG. 5. Example of dual-comb spectroscopy (DCS) using on-chip comb sources.[231] (a) Schematic of a dual-comb spectroscopy setup using mid-IR ICL combs as sources. (b) Optical spectra of the two comb sources (SIG: signal; LO: local oscillator) used in the experiment. The sources have repetition rates of ~ 9.7 GHz (4 mm device length), and the difference in repetition rate between both devices is 23 MHz. (c) Free-running dual-comb RF spectrum obtained by interfering the two combs on an interband cascade photodetector. This RF spectrum is the result of averaging 500 spectra, each spectrum acquired in 4 μs. (d) Experimental (black dots) and simulated transmission spectrum (red line) of 1,1-difluoroethane at atmospheric pressure. The standard deviation of the residual between the data and the model is 3.4%, corresponding to a noise-equivalent absorption (NEA) of 1.5×10^{-3} $Hz^{-1/2}$. Reproduced from Sterczewski *et al.*, Appl. Phys. Lett. **116**, 141102 (2020), with the permission of AIP Publishing.

© Author(s) 2022

transfer printing of a Si grating and a III-V amplifier. The device produces over 25 comb lines around a wavelength of 1.57 μm at a 19 GHz spacing.

The specifications of state-of-the-art heterogeneous comb sources are summarized in Table VI.

VI. APPLICATIONS

On-chip, electrically pumped comb sources have been used for optical communication,[5,36,96,153,198,282–294] spectroscopy,[38,180,206,218,228,231,265,303,305–307,310,311] and LiDAR.[52,296] The majority of these optical communication demonstrations uses combs as a source for wavelength-division multiplexing (WDM) technology in fiber-optic communication systems. Comb sources are a promising alternative to arrays of actively controlled single-frequency laser diodes.[312] Not only is the comb approach expected to reduce footprint, cost, and power consumption, the phase coherence between the comb lines also enables mitigation of nonlinear impairments in fibers[313] and joint phase processing of multiple channels.[314] However, the reliability requirements on a comb source will be more stringent compared to a single laser in an array. Mostly monolithic III-V comb sources have been used, but also heterogeneous combs have been reported as WDM sources.[96] The line spacings typically lie in the 10–100 GHz range, in line with the recommendations of the International Telecommunication Union (ITU).[315] On-chip combs have not only been used as a source in WDM systems but also as a local oscillator for coherent detection schemes (see Fig. 4).[292] Most demonstrations still use multiple discrete components for light generation, modulation, amplification, detection, and (de)multiplexing. Yet, there have been significant efforts to move toward more integrated solutions using Si PICs for modulation, detection, and/or (de)multiplexing, in some cases also with integrated driver and receiver electronics.[286,288,290,291]

The comb-based spectroscopic technique that has gained the most interest is dual-comb spectroscopy.[8,316,317] This has also been the technique of choice for the spectroscopy demonstrations with fully integrated comb sources. In dual-comb spectroscopy, two comb sources with a different repetition rate are interfered on a fast photodetector (see Fig. 5). Provided there is a sufficient degree of mutual coherence, the spectrum of the photocurrent will be a comb in the RF domain, with the spacing given by the difference in repetition rate between the comb sources. When one or both of the combs are sent through a sample before reaching the detector, the absorption spectrum of that sample can be recovered from the RF spectrum (and also the phase response if only one of the combs interrogates the sample).[316] Dual-comb spectroscopy is attractive because broadband spectra can be measured in a very short time with high resolution (determined by the repetition rate) using standard electronics and a photodetector. Spectroscopic sensing is of particular interest in the mid-infrared to terahertz spectral range, where many substances have strong vibrational and rotational transitions. Multiple ICL and QCL dual-comb spectroscopy experiments have been reported in this spectral range.[38,206,218,228,231,305–307,310,311] While the repetition rates of monolithic ICL and QCL combs are often too large to resolve the absorption lines in gas-phase spectroscopy (at standard temperature and pressure, many gases have absorption line widths of several GHz[303,318–321]), they are sufficiently small for samples in the condensed phase.[317] To circumvent the resolution issue, the comb teeth can also be swept, e.g., by tuning temperature or current,[8,38,228] though accurate and fast control of the comb lines while also preserving the comb's coherence can be challenging. A high repetition rate does allow for very short acquisition times.[8]

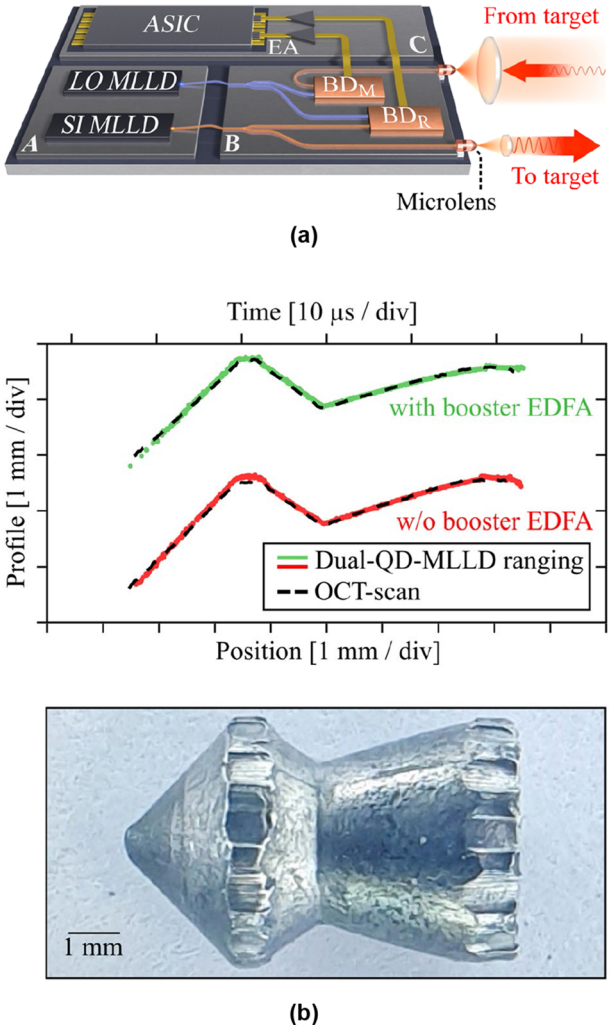

FIG. 6. Example of dual-comb ranging using on-chip comb sources.[52] (a) Vision of a fully integrated dual-comb ranging system. A pair of mode-locked laser diodes (MLLDs) on an InP substrate (A) is combined with a silicon photonic transmitter/receiver circuit (B) and processing electronics (C) in a single package. In their proof-of-concept demonstration, the authors used separate quantum dash MLLDs and discrete optical components, not the single package shown here. LO: local oscillator; SI: signal; ASIC: application-specific integrated circuit; EA: electrical amplifier; BD_M: measurement balanced detector; and BD_R: reference balanced detector. (b) Surface profile measurements of an air-gun projectile (shown in bottom image) flying at a speed of ~150 m/s, acquired with a dual-comb ranging system based on quantum dash mode-locked laser diodes. For reference, the result of an optical coherence tomography (OCT) measurement performed on the static projectile is also shown. Reproduced with permission from P. Trocha *et al.*, Sci. Rep. **12**, 1076 (2022).

© Author(s) 2022

QCL dual-comb spectroscopy of a condensed phase biological sample with sub-microsecond time resolution has been reported.[307] In the near-infrared wavelength range, dual-comb spectroscopy with III-V single-section quantum well diode lasers[180] and heterogeneous III-V-on-Si mode-locked lasers has been demonstrated.[265,303,304] With their 1 GHz repetition rate, the III-V-on-Si mode-locked lasers can resolve the absorption lines of carbon monoxide at 1.6 μm.

Akin to dual-comb spectroscopy, dual-comb ranging is a technique for high-precision, high-speed distance measurements relying on the multi-heterodyne detection of a signal and local oscillator comb with slightly different repetition rates (see Fig. 6).[4] While this scheme has been successfully demonstrated with fiber-based mode-locked lasers,[4,322] electro-optic comb sources,[323] and chip-based Kerr comb sources with off-chip pump lasers,[324,325] it is only recently that dual-comb ranging with on-chip, electrically pumped comb sources has been reported.[52] In Ref. 52, the authors use monolithic III-V single-section quantum dash mode-locked lasers emitting at 1.5 μm with a repetition rate of 50 GHz. They demonstrate measurement rates up to 500 MHz with a precision of 1.7 μm, and a precision of 23 nm for a 10 kHz measurement rate. Moreover, they show reliable ranging with optical return powers of only −40 dBm, corresponding to a total loss of 49 dB in the free-space measurement path. Distance metrology with a 2.5 GHz-repetition-rate InP-based mode-locked ring laser emitting at 1.6 μm has also been reported.[296] The authors determined the distance of a mirror in the arm of a Michelson interferometer by measuring the output spectrum of the interferometer. Another ranging technique that has been demonstrated with chip-based Kerr comb sources is massively parallel frequency-modulated continuous-wave (FMCW) LiDAR.[297,298] In conventional FMCW LiDAR, a frequency-swept CW laser is sent through a beamsplitter after which part of the light goes straight to a photodetector (the local oscillator) and part of the light is reflected of a target and subsequently interfered with the local oscillator on the detector. The target distance and velocity can be extracted from the measurement of the beat note frequency vs time. Using a frequency-swept CW laser as a pump for a Kerr comb source, the frequency sweep can be transferred to all the comb lines, and therefore each line can be used as source for FWCW LiDAR. The comb lines can be spatially dispersed with a diffractive element for massively parallel FMCW LiDAR. So far, this technique has only been demonstrated using off-chip narrow-linewidth tunable pump lasers.

While on-chip, electrically pumped comb sources have only been used in a relatively limited array of applications, chip-based Kerr comb sources with off-chip pump lasers have also been used in optical frequency synthesizers,[326] optical atomic clocks,[278] RF photonic oscillators and signal processors,[257,295] and photonic hardware accelerators,[299,300] for astronomical spectrograph calibration,[279,301] optical coherence tomography (OCT),[281] and other imaging techniques.[280]

VII. DISCUSSION AND OUTLOOK

Figure 7 gives an overview of the repetition rates and center wavelengths of state-of-the-art on-chip comb sources. Many on-chip comb sources have emission wavelengths in the telecom wavelength range. There is a clear gap in the 10 to 70 μm wavelength range, a region of interest for spectroscopic sensing,[308,309] and data points in the visible wavelength range are sparse. QCLs cover a large part of the mid-infrared and terahertz spectral range, but lasing in the 10 to 70 μm wavelength range is challenging due to light coupling strongly with lattice vibrations. Yet, there have already been demonstrations of QCLs emitting in this wavelength range.[327] In the visible wavelength range, we expect to see more demonstrations of on-chip comb sources in the near future given the application potential of this spectral region (e.g., for optical atomic clocks,[132,278] astronomical spectrograph calibration,[133] and biological imaging[134]) and the maturing III-V and PIC technologies (primarily SiN and $LiNbO_3$ PICs).[328–330] Anomalous GVD is hard to achieve in the visible wavelength range but is typically used for Kerr comb generation at near-infrared wavelengths. Recent investigations of fully integrated self-injection-locked Kerr comb sources operating in the normal GVD regime at a wavelength of 1.6 μm[80,84] may be helpful in this context.

Outside of the telecom wavelength range—where the majority of demonstrated on-chip comb sources are monolithic III-V Fabry–Pérot devices—repetition rates do not go much below ~10 GHz. In the mid-infrared to terahertz spectral range, it would be particularly useful to have low-repetition-rate, narrow-linewidth sources for high-resolution gas-phase spectroscopy. To fabricate these low-repetition-rate, narrow-linewidth sources, integration of QCLs with low-loss silicon or germanium waveguide circuits is an interesting approach and another area where we expect to see developments in the future.[331–334]

Figure 8(a) shows the RF linewidth vs repetition rate for state-of-the-art monolithic III-V, hybrid, and heterogeneous passively mode-locked lasers emitting at 1.6 μm (we only look at a single wavelength to avoid complicating the comparison; we choose 1.6 μm as many different types of comb sources have been demonstrated at this wavelength). We include only sources for which the repetition rate is not stabilized to an external RF oscillator for a fair comparison. No Kerr comb sources are included as no RF linewidths have been reported for on-chip Kerr comb sources to our knowledge. Figure 8(a) illustrates that the RF linewidth tends to decrease with decreasing repetition rates (i.e., increasing cavity length), as expected.[166,266,273] In addition, for similar repetition rates, the RF linewidth tends to be lower for the hybridly and heterogeneously integrated lasers, where the III-V material is integrated with low-loss PICs. The lowest RF linewidth has been achieved for a 755 MHz-repetition-rate III-V-on-SiN mode-locked laser with a SiN waveguide loss of 5 dB/m.[97] SiN waveguide losses below 0.1 dB/m have been reported for low-confinement waveguides[335] and losses as low as 1 dB/m for wafer-scale fabricated thick, high-confinement waveguides,[336] so even lower RF linewidths can be expected in future devices.[266]

The majority of applications benefit from having highly stable, low-noise combs. True metrological applications (e.g., optical frequency metrology and synthesis, optical atomic clocks, and astronomical spectrograph calibration) generally require measuring and stabilizing the carrier–envelope offset frequency f_0 and the repetition rate f_r. The repetition rate can be measured with a sufficiently fast photodetector (which can be problematic for repetition rates of 100s of GHz). The carrier–envelope offset frequency is more challenging to measure. The simplest method is to use an f-2f interferometer, but this requires an octave-spanning comb.[337,338]

© Author(s) 2022

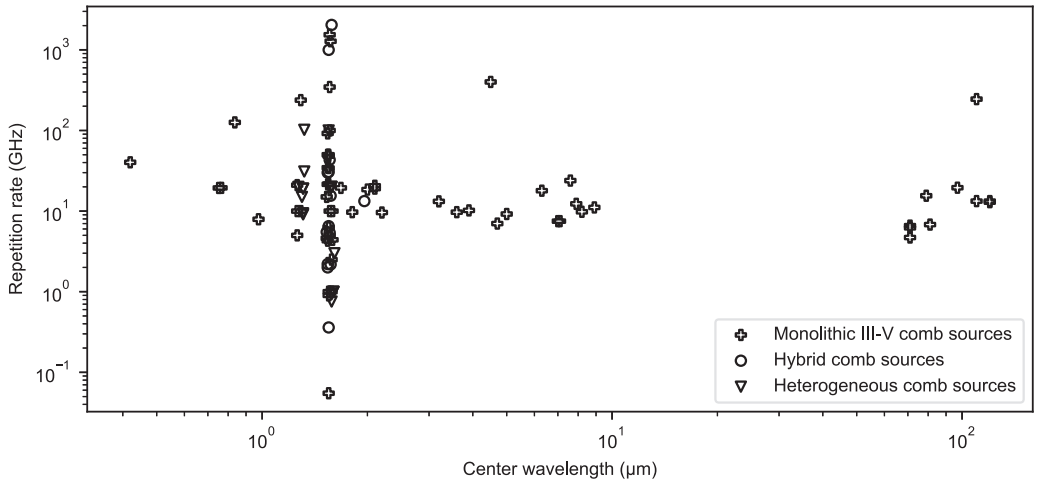

FIG. 7. Repetition rate vs center wavelength for on-chip comb sources. The data plotted in this figure correspond to all the comb sources listed in Table III–Table VI.

Fortunately you do not need a FWHM of an octave; the power in the comb lines separated by an octave can be much below the power at the center of the comb.[338] A frequency comb can be fully stabilized by locking f_0 and f_r to the microwave output of a caesium atomic clock or another frequency standard. For most chip-based comb sources, varying the operating conditions affects both f_0 and f_r, and it is challenging to tune f_0 and f_r independently. In semiconductor mode-locked lasers, one can, for instance, vary the pump current, saturable absorber bias, intracavity phase shifter current, and temperature to tune f_0 and f_r.[339,340] For certain bias points, f_0 and f_r may be tuned quasi-independently. In Kerr microresonator combs, full stabilization has been achieved by using the pump laser frequency to control f_r and the pump power to control f_0.[341] The amount of crosstalk between f_r and f_0 control was observed to depend on the coupling conditions. Realizing octave-spanning combs with on-chip, electrically pumped sources is still very challenging,[94,342] though octave-spanning spectra have been reported for terahertz QCLs.[223] Octave-spanning soliton combs in SiN microresonators have been demonstrated with off-chip pump lasers, but > 100 mW of pump power was required to access 1 THz-repetition-rate single-soliton states.[87,88] Substantially lower, electronically detectable repetition rates are desired for many applications. Decreasing repetition rates come with an increase in required pump power.[87,257] Carrier–envelope offset frequency detection has been realized via simultaneous on-chip octave-spanning coherent supercontinuum generation and second-harmonic generation in SiN[343] and $LiNbO_3$ waveguides.[75] Yet, these demonstrations relied on ~ 200 fs input pulses with energies of 10s to >100 pJ provided by off-chip sources. Using highly nonlinear III-V materials, such as InGaP[72] and AlGaAs,[77] octave-spanning supercontinua have been generated from pJ-level pulses with ~ 100 fs durations. Via resonant supercontinuum generation in a SiN microresonator, broadband combs (up to ~2/3 of an octave) with a 28 GHz repetition rate have been generated from pJ-level input pulses with >1 ps durations supplied by an off-chip source.[90] These numbers are attainable with on-chip mode-locked lasers. (Resonant) supercontinuum generation combined with on-chip pump sources may eventually lead to octave-spanning on-chip comb sources with an electronically detectable repetition rate.

Figure 8(b) shows the optical bandwidth vs repetition rate for state-of-the-art on-chip, electrically pumped comb sources. For the lower repetition rates, we observe more data points with smaller bandwidths compared to the higher repetition rates, suggesting that it is more challenging to get large bandwidths for smaller repetition rates. We also note that the demonstrated gain-switched laser combs have limited bandwidths compared to, for instance, mode-locked lasers and Kerr combs. The bandwidth demonstrated for monolithic III-V electro-optic combs is relatively small, but we expect the bandwidth of on-chip electro-optic comb sources to increase significantly with the advent of low-loss, high-bandwidth, low-voltage, thin-film $LiNbO_3$ modulators.[129]

Apart from narrow linewidths and large bandwidths, high optical output powers are often desired for comb sources. Higher optical output powers and pulse energies have been demonstrated for monolithic III-V comb sources compared to hybrid and heterogeneous comb sources [see Fig. 8(c)]. III-V waveguides can be designed for high-power operation, for example, by using tapered amplifiers[139] or slab-coupled waveguide amplifiers.[137,147] Hybrid integration of such high-power III-V devices with low-loss PICs[344] may enable high-power, narrow-linewidth hybrid comb sources, and octave-spanning hybrid Kerr comb sources. These high-power III-V waveguide designs may be more challenging to implement for heterogeneously integrated devices relying on evanescent coupling between a III-V waveguide and an underlying Si waveguide. In addition, the presence of the oxide cladding in between the Si waveguide and substrate is detrimental for high-power operation because of the oxide's poor thermal conductivity. Transfer printing the III-V device directly on the Si substrate and edge coupling to the silicon (nitride) waveguide can alleviate these issues in heterogeneously integrated comb sources.[345,346]

© Author(s) 2022

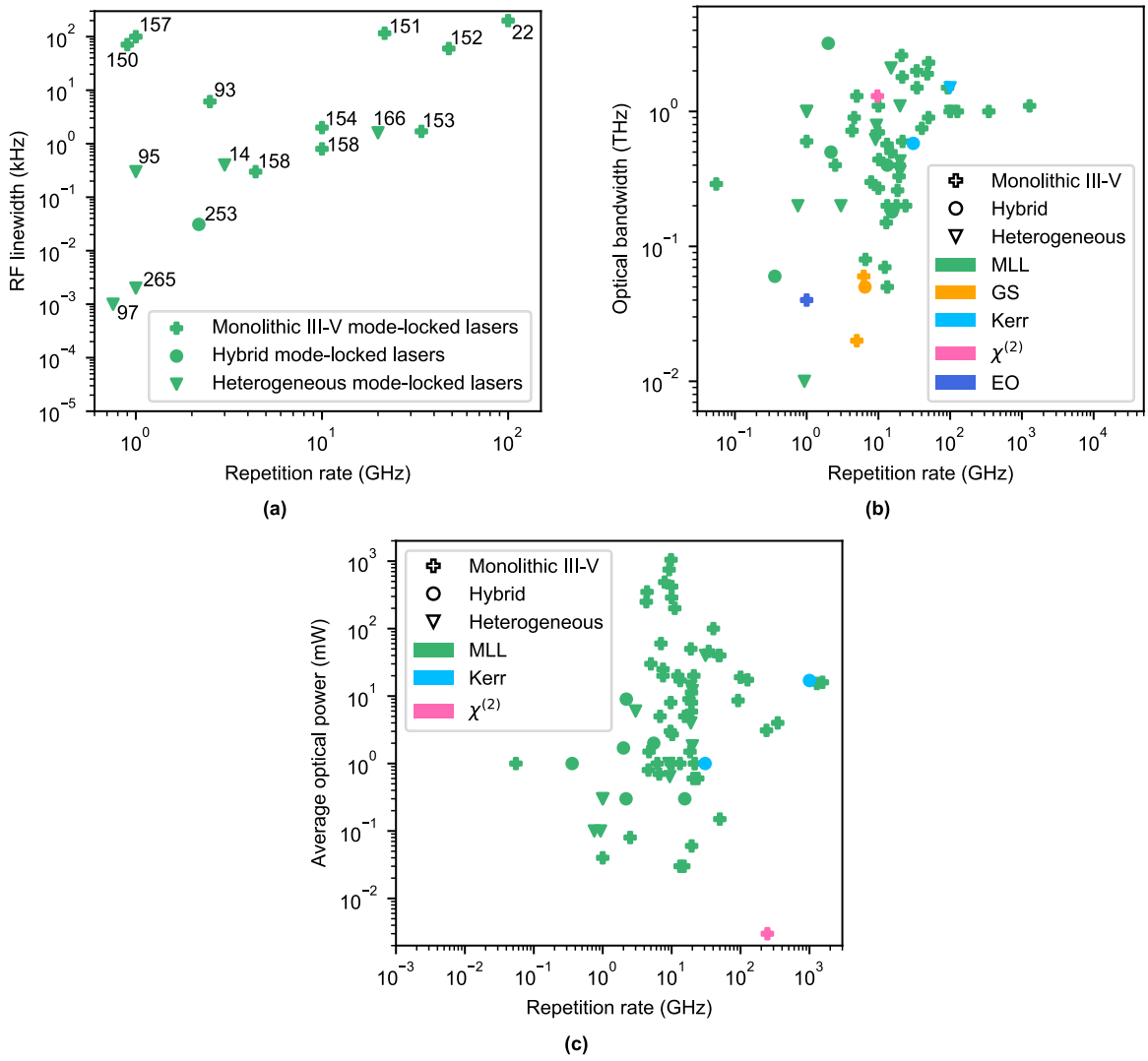

FIG. 8. (a) RF linewidth vs repetition rate for on-chip passively mode-locked lasers emitting at a wavelength of 1.6 μm. The references corresponding to the data points are indicated in the figure. (b) Optical bandwidth vs repetition rate for the on-chip optical comb sources listed in Tables III–VI. (c) Average optical output power vs repetition rate for the on-chip optical comb sources listed in Tables III–VI.

Whether on-chip comb sources will find widespread commercial adoption remains an open question and will largely depend on the price and performance metrics chip-scale comb systems will be able to offer compared to other solutions. We would expect the first commercial applications of on-chip, electrically pumped comb sources to be in telecommunication, spectroscopic sensing, and/or LiDAR, rather than in highly demanding metrological applications requiring fully stabilized, octave-spanning frequency combs. In fact, dual-comb spectrometers based on QCL comb sources are already commercially available,[347] and a start-up is developing chip-based comb sources for extreme-bandwidth data transmission.[348]

While there has already been a lot of research on on-chip optical comb sources, we foresee that on-chip comb sources will continue to be a topic of interest, given their vast application space. We believe that hybrid and heterogeneous integration approaches will play an increasingly important role given their ability to combine the best of all worlds. We expect to see more system-level demonstrations in the coming years where the majority of required components are integrated on a chip. These demonstrations may form the basis for future commercial products.

ACKNOWLEDGMENTS

A.H. and K.V.G. were supported by a Fellowship of the Belgian American Educational Foundation. The authors acknowledge

© Author(s) 2022

the support of the European Research Council (ERC starting grant ELECTRIC, Grant Agreement No. 759483).

AUTHOR DECLARATIONS

Conflict of Interest

The authors have no conflicts to disclose.

Author Contributions

Artur Hermans: Conceptualization (lead); Investigation (lead); Visualization (lead); Writing – original draft (lead); Writing – review & editing (lead). **Kasper Van Gasse**: Conceptualization (supporting); Supervision (supporting); Writing – original draft (supporting); Writing – review & editing (supporting). **Bart Kuyken**: Conceptualization (supporting); Supervision (lead); Writing – original draft (supporting); Writing – review & editing (supporting).

DATA AVAILABILITY

Data sharing is not applicable to this article as no new data were created or analyzed in this study.

REFERENCES

[1] N. R. Newbury, "Searching for applications with a fine-tooth comb," Nat. Photonics **5**, 186–188 (2011).
[2] T. Udem, J. Reichert, R. Holzwarth, and T. W. Hänsch, "Absolute optical frequency measurement of the cesium D_1 line with a mode-locked laser," Phys. Rev. Lett. **82**, 3568–3571 (1999).
[3] S. A. Diddams, T. Udem, J. C. Bergquist, E. A. Curtis, R. E. Drullinger, L. Hollberg, W. M. Itano, W. D. Lee, C. W. Oates, K. R. Vogel, and D. J. Wineland, "An optical clock based on a single trapped $^{199}Hg^+$ ion," Science **293**, 825–828 (2001).
[4] I. Coddington, W. C. Swann, L. Nenadovic, and N. R. Newbury, "Rapid and precise absolute distance measurements at long range," Nat. Photonics **3**, 351–356 (2009).
[5] H. Sanjoh, H. Yasaka, Y. Sakai, K. Sato, H. Ishii, and Y. Yoshikuni, "Multiwavelength light source with precise frequency spacing using a mode-locked semiconductor laser and an arrayed waveguide grating filter," IEEE Photonics Technol. Lett. **9**, 818–820 (1997).
[6] F. Keilmann, C. Gohle, and R. Holzwarth, "Time-domain mid-infrared frequency-comb spectrometer," Opt. Lett. **29**, 1542–1544 (2004).
[7] A. L. Gaeta, M. Lipson, and T. J. Kippenberg, "Photonic-chip-based frequency combs," Nat. Photonics **13**, 158–169 (2019).
[8] G. Scalari, J. Faist, and N. Picqué, "On-chip mid-infrared and THz frequency combs for spectroscopy," Appl. Phys. Lett. **114**, 150401 (2019).
[9] W. Wang, L. Wang, and W. Zhang, "Advances in soliton microcomb generation," Adv. Photonics **2**, 034001 (2020).
[10] L. A. Sterczewski, M. Bagheri, C. Frez, C. L. Canedy, I. Vurgaftman, M. Kim, C. S. Kim, C. D. Merritt, W. W. Bewley, and J. R. Meyer, "Interband cascade laser frequency combs," J. Phys.: Photonics **3**, 042003 (2021).
[11] H. Sun, M. Khalil, Z. Wang, and L. R. Chen, "Recent progress in integrated electro-optic frequency comb generation," J. Semicond. **42**, 041301 (2021).
[12] L. Chang, S. Liu, and J. E. Bowers, "Integrated optical frequency comb technologies," Nat. Photonics **16**, 95–108 (2022).
[13] P. Kaur, A. Boes, G. Ren, T. G. Nguyen, G. Roelkens, and A. Mitchell, "Hybrid and heterogeneous photonic integration," APL Photonics **6**, 061102 (2021).
[14] A. Hermans, K. Van Gasse, J. Ø. Kjellman, C. Caër, T. Nakamura, Y. Inada, K. Hisada, T. Hirasawa, S. Cuyvers, S. Kumari, A. Marinins, R. Jansen, G. Roelkens, P. Soussan, X. Rottenberg, and B. Kuyken, "High-pulse-energy III-V-on-silicon-nitride mode-locked laser," APL Photonics **6**, 096102 (2021).
[15] P. M. Anandarajah, S. P. Ó Dúill, R. Zhou, and L. P. Barry, "Enhanced optical comb generation by gain-switching a single-mode semiconductor laser close to its relaxation oscillation frequency," IEEE J. Sel. Top. Quantum Electron. **21**, 1801609 (2015).
[16] M. Pu, L. Ottaviano, E. Semenova, and K. Yvind, "Efficient frequency comb generation in AlGaAs-on-insulator," Optica **3**, 823–826 (2016).
[17] J. Szabados, D. N. Puzyrev, Y. Minet, L. Reis, K. Buse, A. Villois, D. V. Skryabin, and I. Breunig, "Frequency comb generation via cascaded second-order nonlinearities in microresonators," Phys. Rev. Lett. **124**, 203902 (2020).
[18] L. Lundberg, M. Karlsson, A. Lorences-Riesgo, M. Mazur, V. Torres-Company, J. Schröder, and P. Andrekson, "Frequency comb-based WDM transmission systems enabling joint signal processing," Appl. Sci. **8**, 718 (2018).
[19] T. Fortier and E. Baumann, "20 years of developments in optical frequency comb technology and applications," Commun. Phys. **2**, 153 (2019).
[20] S. A. Diddams, K. Vahala, and T. Udem, "Optical frequency combs: Coherently uniting the electromagnetic spectrum," Science **369**, eaay3676 (2020).
[21] J. Hillbrand, D. Auth, M. Piccardo, N. Opačak, E. Gornik, G. Strasser, F. Capasso, S. Breuer, and B. Schwarz, "In-phase and anti-phase synchronization in a laser frequency comb," Phys. Rev. Lett. **124**, 023901 (2020).
[22] K. Sato, "Optical pulse generation using Fabry-Pérot lasers under continuous-wave operation," IEEE J. Sel. Top. Quantum Electron. **9**, 1288–1293 (2003).
[23] D. von der Linde, "Characterization of the noise in continuously operating mode-locked lasers," Appl. Phys. B **39**, 201–217 (1986).
[24] F. Kéfélian, S. O'Donoghue, M. T. Todaro, J. G. McInerney, and G. Huyet, "RF linewidth in monolithic passively mode-locked semiconductor laser," IEEE Photonics Technol. Lett. **20**, 1405–1407 (2008).
[25] M. A. Tran, D. Huang, and J. E. Bowers, "Tutorial on narrow linewidth tunable semiconductor lasers using Si/III-V heterogeneous integration," APL Photonics **4**, 111101 (2019).
[26] Y. Takushima, H. Sotobayashi, M. E. Grein, E. P. Ippen, and H. A. Haus, "Linewidth of mode combs of passively and actively mode-locked semiconductor laser diodes," in *Active and Passive Optical Components for WDM Communications IV*, edited by A. K. Dutta, A. A. S. Awwal, N. K. Dutta, and Y. Ohishi (International Society for Optics and Photonics, SPIE, 2004), Vol. 5595, pp. 213–227.
[27] T. Habruseva, S. O'Donoghue, N. Rebrova, F. Kéfélian, S. P. Hegarty, and G. Huyet, "Optical linewidth of a passively mode-locked semiconductor laser," Opt. Lett. **34**, 3307–3309 (2009).
[28] A. Parriaux, K. Hammani, and G. Millot, "Electro-optic frequency combs," Adv. Opt. Photonics **12**, 223–287 (2020).
[29] K. Y. Lau, I. Ury, and A. Yariv, "Passive and active mode locking of a semiconductor laser without an external cavity," Appl. Phys. Lett. **46**, 1117–1119 (1985).
[30] L. F. Tiemeijer, P. I. Kuindersma, P. J. A. Thijs, and G. L. J. Rikken, "Passive FM locking in InGaAsP semiconductor lasers," IEEE J. Quantum Electron. **25**, 1385–1392 (1989).
[31] R. S. Tucker, U. Koren, G. Raybon, C. A. Burrus, B. I. Miller, T. L. Koch, and G. Eisenstein, "40 GHz active mode-locking in a 1.5 μm monolithic extended-cavity laser," Electron. Lett. **25**, 621–622 (1989).
[32] X. Huang, A. Stintz, H. Li, L. F. Lester, J. Cheng, and K. J. Malloy, "Passive mode-locking in 1.3 μm two-section InAs quantum dot lasers," Appl. Phys. Lett. **78**, 2825–2827 (2001).
[33] P. Del'Haye, A. Schliesser, O. Arcizet, T. Wilken, R. Holzwarth, and T. J. Kippenberg, "Optical frequency comb generation from a monolithic microresonator," Nature **450**, 1214–1217 (2007).
[34] B. R. Koch, A. W. Fang, O. Cohen, and J. E. Bowers, "Mode-locked silicon evanescent lasers," Opt. Express **15**, 11225–11233 (2007).
[35] C. Y. Wang, L. Kuznetsova, V. M. Gkortsas, L. Diehl, F. X. Kärtner, M. A. Belkin, A. Belyanin, X. Li, D. Ham, H. Schneider, P. Grant, C. Y. Song, S. Haffouz, Z. R. Wasilewski, H. C. Liu, and F. Capasso, "Mode-locked pulses from mid-infrared quantum cascade lasers," Opt. Express **17**, 12929–12943 (2009).

© Author(s) 2022

[36]P. M. Anandarajah, K. Shi, J. O'Carroll, A. Kaszubowska, R. Phelan, L. P. Barry, A. D. Ellis, P. Perry, D. Reid, B. Kelly, and J. O'Gorman, "Phase shift keyed systems based on a gain switched laser transmitter," Opt. Express **17**, 12668–12677 (2009).
[37]A. Hugi, G. Villares, S. Blaser, H. C. Liu, and J. Faist, "Mid-infrared frequency comb based on a quantum cascade laser," Nature **492**, 229–233 (2012).
[38]G. Villares, A. Hugi, S. Blaser, and J. Faist, "Dual-comb spectroscopy based on quantum-cascade-laser frequency combs," Nat. Commun. **5**, 5192 (2014).
[39]F. Leo, S.-P. Gorza, S. Coen, B. Kuyken, and G. Roelkens, "Coherent supercontinuum generation in a silicon photonic wire in the telecommunication wavelength range," Opt. Lett. **40**, 123–126 (2015).
[40]B. Kuyken, T. Ideguchi, S. Holzner, M. Yan, T. W. Hänsch, J. Van Campenhout, P. Verheyen, S. Coen, F. Leo, R. Baets, G. Roelkens, and N. Picqué, "An octave-spanning mid-infrared frequency comb generated in a silicon nanophotonic wire waveguide," Nat. Commun. **6**, 6310 (2015).
[41]S. Liu, D. Jung, J. C. Norman, M. J. Kennedy, A. C. Gossard, and J. E. Bowers, "490 fs pulse generation from passively mode-locked single section quantum dot laser directly grown on on-axis GaP/Si," Electron. Lett. **54**, 432–433 (2018).
[42]B. Stern, X. Ji, Y. Okawachi, A. L. Gaeta, and M. Lipson, "Battery-operated integrated frequency comb generator," Nature **562**, 401–405 (2018).
[43]N. Andriolli, T. Cassese, M. Chiesa, C. de Dios, and G. Contestabile, "Photonic integrated fully tunable comb generator cascading optical modulators," J. Lightwave Technol. **36**, 5685–5689 (2018).
[44]R. Ikuta, M. Asano, R. Tani, T. Yamamoto, and N. Imoto, "Frequency comb generation in a quadratic nonlinear waveguide resonator," Opt. Express **26**, 15551–15558 (2018).
[45]L. A. Sterczewski, M. Bagheri, C. Frez, C. L. Canedy, I. Vurgaftman, M. Kim, C. S. Kim, C. D. Merritt, W. W. Bewley, and J. R. Meyer, "Near-infrared frequency comb generation in mid-infrared interband cascade lasers," Opt. Lett. **44**, 5828–5831 (2019).
[46]Q. Lu, F. Wang, D. Wu, S. Slivken, and M. Razeghi, "Room temperature terahertz semiconductor frequency comb," Nat. Commun. **10**, 2403 (2019).
[47]J. Mak, A. van Rees, Y. Fan, E. J. Klein, D. Geskus, P. J. M. van der Slot, and K.-J. Boller, "Linewidth narrowing via low-loss dielectric waveguide feedback circuits in hybrid integrated frequency comb lasers," Opt. Express **27**, 13307–13318 (2019).
[48]J. Hauck, A. Zazzi, A. Garreau, F. Lelarge, A. Moscoso-Mártir, F. Merget, and J. Witzens, "Semiconductor laser mode locking stabilization with optical feedback from a silicon PIC," J. Lightwave Technol. **37**, 3483–3494 (2019).
[49]C. Xiang, J. Liu, J. Guo, L. Chang, R. N. Wang, W. Weng, J. Peters, W. Xie, Z. Zhang, J. Riemensberger, J. Selvidge, T. J. Kippenberg, and J. E. Bowers, "Laser soliton microcombs heterogeneously integrated on silicon," Science **373**, 99–103 (2021).
[50]S. Shao, J. Li, H. Chen, S. Yang, and M. Chen, "Gain-switched optical frequency comb source using a hybrid integrated self-injection locking DFB laser," IEEE Photonics J. **14**, 6613606 (2022).
[51]I. Luntadila Lufungula, A. Shams-Ansari, D. Renaud, C. Op de Beeck, S. Cuyvers, S. Poelman, G. Roelkens, M. Loncar, and B. Kuyken, "On-chip electro-optic frequency comb generation using a heterogeneously integrated laser," in *Conference on Lasers and Electro-Optics* (Optica Publishing Group, 2022), p. JTh6B.7.
[52]P. Trocha, J. N. Kemal, Q. Gaimard, G. Aubin, F. Lelarge, A. Ramdane, W. Freude, S. Randel, and C. Koos, "Ultra-fast optical ranging using quantum-dash mode-locked laser diodes," Sci. Rep. **12**, 1076 (2022).
[53]A. M. Weiner, *Ultrafast Optics* (John Wiley & Sons, Inc., 2009).
[54]D. J. Derickson, R. J. Helkey, A. Mar, J. R. Karin, J. G. Wasserbauer, and J. E. Bowers, "Short pulse generation using multisegment mode-locked semiconductor lasers," IEEE J. Quantum Electron. **28**, 2186–2202 (1992).
[55]M. Dong, S. T. Cundiff, and H. G. Winful, "Physics of frequency-modulated comb generation in quantum-well diode lasers," Phys. Rev. A **97**, 053822 (2018).
[56]D. Kuizenga and A. Siegman, "FM and AM mode locking of the homogeneous laser - Part I: Theory," IEEE J. Quantum Electron. **6**, 694–708 (1970).
[57]U. Keller, K. J. Weingarten, F. X. Kärtner, D. Kopf, B. Braun, I. D. Jung, R. Fluck, C. Hönninger, N. Matuschek, and J. Aus der Au, "Semiconductor saturable absorber mirrors (SESAM's) for femtosecond to nanosecond pulse generation in solid-state lasers," IEEE J. Sel. Top. Quantum Electron. **2**, 435–453 (1996).
[58]J. R. Karin, R. J. Helkey, D. J. Derickson, R. Nagarajan, D. S. Allin, J. E. Bowers, and R. L. Thornton, "Ultrafast dynamics in field-enhanced saturable absorbers," Appl. Phys. Lett. **64**, 676–678 (1994).
[59]K. Shtyrkova, P. T. Callahan, N. Li, E. S. Magden, A. Ruocco, D. Vermeulen, F. X. Kärtner, M. R. Watts, and E. P. Ippen, "Integrated CMOS-compatible Q-switched mode-locked lasers at 1900 nm with an on-chip artificial saturable absorber," Opt. Express **27**, 3542–3556 (2019).
[60]Z. G. Lu, J. R. Liu, S. Raymond, P. J. Poole, P. J. Barrios, and D. Poitras, "312-fs pulse generation from a passive C-band InAs/InP quantum dot mode-locked laser," Opt. Express **16**, 10835–10840 (2008).
[61]J. Liu, Z. Lu, S. Raymond, P. J. Poole, P. J. Barrios, and D. Poitras, "Dual-wavelength 92.5 GHz self-mode-locked InP-based quantum dot laser," Opt. Lett. **33**, 1702–1704 (2008).
[62]W. W. Chow, S. Liu, Z. Zhang, J. E. Bowers, and M. Sargent, "Multimode description of self-mode locking in a single-section quantum-dot laser," Opt. Express **28**, 5317–5330 (2020).
[63]A. J. DeMaria, D. A. Stetser, and H. Heynau, "Self mode-locking of lasers with saturable absorbers," Appl. Phys. Lett. **8**, 174–176 (1966).
[64]D. J. Derickson, R. J. Helkey, A. Mar, P. A. Morton, and J. E. Bowers, "Self-mode-locking of a semiconductor laser using positive feedback," Appl. Phys. Lett. **56**, 7–9 (1990).
[65]C.-P. Huang, H. C. Kapteyn, J. W. Mclntosh, and M. M. Murnane, "Generation of transform-limited 32-fs pulses from a self-mode-locked Ti:sapphire laser," Opt. Lett. **17**, 139–141 (1992).
[66]H. Bao, A. Cooper, M. Rowley, L. Di Lauro, J. S. Totero Gongora, S. T. Chu, B. E. Little, G.-L. Oppo, R. Morandotti, D. J. Moss, B. Wetzel, M. Peccianti, and A. Pasquazi, "Laser cavity-soliton microcombs," Nat. Photonics **13**, 384–389 (2019).
[67]S. Arahira, S. Oshiba, Y. Matsui, T. Kunii, and Y. Ogawa, "Terahertz-rate optical pulse generation from a passively mode-locked semiconductor laser diode," Opt. Lett. **19**, 834–836 (1994).
[68]L. Hou, M. Haji, and J. H. Marsh, "Mode locking at terahertz frequencies using a distributed Bragg reflector laser with a sampled grating," Opt. Lett. **38**, 1113–1115 (2013).
[69]K. Y. Lau, "Gain switching of semiconductor injection lasers," Appl. Phys. Lett. **52**, 257–259 (1988).
[70]A. Rosado, A. Pérez-Serrano, J. M. G. Tijero, Á. Valle, L. Pesquera, and I. Esquivias, "Enhanced optical frequency comb generation by pulsed gain-switching of optically injected semiconductor lasers," Opt. Express **27**, 9155–9163 (2019).
[71]M. D. Gutierrez Pascual, V. Vujicic, J. Braddell, F. Smyth, P. M. Anandarajah, and L. P. Barry, "InP photonic integrated externally injected gain switched optical frequency comb," Opt. Lett. **42**, 555–558 (2017).
[72]U. D. Dave, C. Ciret, S.-P. Gorza, S. Combrie, A. De Rossi, F. Raineri, G. Roelkens, and B. Kuyken, "Dispersive-wave-based octave-spanning supercontinuum generation in InGaP membrane waveguides on a silicon substrate," Opt. Lett. **40**, 3584–3587 (2015).
[73]D. R. Carlson, D. D. Hickstein, A. Lind, S. Droste, D. Westly, N. Nader, I. Coddington, N. R. Newbury, K. Srinivasan, S. A. Diddams, and S. B. Papp, "Self-referenced frequency combs using high-efficiency silicon-nitride waveguides," Opt. Lett. **42**, 2314–2317 (2017).
[74]N. Singh, M. Xin, D. Vermeulen, K. Shtyrkova, N. Li, P. T. Callahan, E. S. Magden, A. Ruocco, N. Fahrenkopf, C. Baiocco, B. P.-P. Kuo, S. Radic, E. Ippen, F. X. Kärtner, and M. R. Watts, "Octave-spanning coherent supercontinuum generation in silicon on insulator from 1.06 μm to beyond 2.4 μm," Light: Sci. Appl. **7**, 17131 (2018).
[75]M. Yu, B. Desiatov, Y. Okawachi, A. L. Gaeta, and M. Lončar, "Coherent two-octave-spanning supercontinuum generation in lithium-niobate waveguides," Opt. Lett. **44**, 1222–1225 (2019).
[76]C. Lafforgue, S. Guerber, J. M. Ramírez, G. Marcaud, C. Alonso-Ramos, X. Le Roux, D. Marris-Morini, E. Cassan, C. Baudot, F. Boeuf, S. Cremer, S. Monfray, and L. Vivien, "Broadband supercontinuum generation in nitrogen-rich silicon nitride waveguides using a 300 mm industrial platform," Photonics Res. **8**, 352–358 (2020).

© Author(s) 2022

[77]B. Kuyken, M. Billet, F. Leo, K. Yvind, and M. Pu, "Octave-spanning coherent supercontinuum generation in an AlGaAs-on-insulator waveguide," Opt. Lett. **45**, 603–606 (2020).
[78]T. J. Kippenberg, R. Holzwarth, and S. A. Diddams, "Microresonator-based optical frequency combs," Science **332**, 555–559 (2011).
[79]B. Shen, L. Chang, J. Liu, H. Wang, Q.-F. Yang, C. Xiang, R. N. Wang, J. He, T. Liu, W. Xie, J. Guo, D. Kinghorn, L. Wu, Q.-X. Ji, T. J. Kippenberg, K. Vahala, and J. E. Bowers, "Integrated turnkey soliton microcombs," Nature **582**, 365–369 (2020).
[80]W. Jin, Q.-F. Yang, L. Chang, B. Shen, H. Wang, M. A. Leal, L. Wu, M. Gao, A. Feshali, M. Paniccia, K. J. Vahala, and J. E. Bowers, "Hertz-linewidth semiconductor lasers using CMOS-ready ultra-high-*Q* microresonators," Nat. Photonics **15**, 346–353 (2021).
[81]T. J. Kippenberg, A. L. Gaeta, M. Lipson, and M. L. Gorodetsky, "Dissipative Kerr solitons in optical microresonators," Science **361**, eaan8083 (2018).
[82]D. C. Cole, E. S. Lamb, P. Del'Haye, S. A. Diddams, and S. B. Papp, "Soliton crystals in Kerr resonators," Nat. Photonics **11**, 671–676 (2017).
[83]J. K. Jang, Y. Okawachi, X. Ji, C. Joshi, M. Lipson, and A. L. Gaeta, "Universal conversion efficiency scaling with free-spectral-range for soliton Kerr combs," in *Conference on Lasers and Electro-Optics* (Optica Publishing Group, 2020), p. JTu2F.32.
[84]G. Lihachev, J. Liu, W. Weng, L. Chang, J. Guo, J. He, R. N. Wang, M. H. Anderson, J. E. Bowers, and T. J. Kippenberg, "Platicon microcomb generation using laser self-injection locking," arXiv:2103.07795v3 [physics.optics] (2021).
[85]X. Xue, X. Zheng, and B. Zhou, "Super-efficient temporal solitons in mutually coupled optical cavities," Nat. Photonics **13**, 616–622 (2019).
[86]Ó. B. Helgason, F. R. Arteaga-Sierra, Z. Ye, K. Twayana, P. A. Andrekson, M. Karlsson, J. Schröder, and V. Victor Torres-Company, "Dissipative solitons in photonic molecules," Nat. Photonics **15**, 305–310 (2021).
[87]Q. Li, T. C. Briles, D. A. Westly, T. E. Drake, J. R. Stone, B. R. Ilic, S. A. Diddams, S. B. Papp, and K. Srinivasan, "Stably accessing octave-spanning microresonator frequency combs in the soliton regime," Optica **4**, 193–203 (2017).
[88]M. H. P. Pfeiffer, C. Herkommer, J. Liu, H. Guo, M. Karpov, E. Lucas, M. Zervas, and T. J. Kippenberg, "Octave-spanning dissipative Kerr soliton frequency combs in Si_3N_4 microresonators," Optica **4**, 684–691 (2017).
[89]E. Obrzud, S. Lecomte, and T. Herr, "Temporal solitons in microresonators driven by optical pulses," Nat. Photonics **11**, 600–607 (2017).
[90]M. H. Anderson, R. Bouchand, J. Liu, W. Weng, E. Obrzud, T. Herr, and T. J. Kippenberg, "Photonic chip-based resonant supercontinuum via pulse-driven Kerr microresonator solitons," Optica **8**, 771–779 (2021).
[91]J. Li, C. Bao, Q.-X. Ji, H. Wang, L. Wu, S. Leifer, C. Beichman, and K. Vahala, "Efficiency of pulse pumped soliton microcombs," Optica **9**, 231–239 (2022).
[92]E. U. Rafailov, M. A. Cataluna, W. Sibbett, N. D. Il'inskaya, Y. M. Zadiranov, A. E. Zhukov, V. M. Ustinov, D. A. Livshits, A. R. Kovsh, and N. N. Ledentsov, "High-power picosecond and femtosecond pulse generation from a two-section mode-locked quantum-dot laser," Appl. Phys. Lett. **87**, 081107 (2005).
[93]S. Latkowski, V. Moskalenko, S. Tahvili, L. Augustin, M. Smit, K. Williams, and E. Bente, "Monolithically integrated 2.5 GHz extended cavity mode-locked ring laser with intracavity phase modulators," Opt. Lett. **40**, 77–80 (2015).
[94]T. C. Briles, S.-P. Yu, L. Chang, C. Xiang, J. Guo, D. Kinghorn, G. Moille, K. Srinivasan, J. E. Bowers, and S. B. Papp, "Hybrid InP and SiN integration of an octave-spanning frequency comb," APL Photonics **6**, 026102 (2021).
[95]Z. Wang, K. Van Gasse, V. Moskalenko, S. Latkowski, E. Bente, B. Kuyken, and G. Roelkens, "A III-V-on-Si ultra-dense comb laser," Light: Sci. Appl. **6**, e16260 (2017).
[96]S. Liu, X. Wu, D. Jung, J. C. Norman, M. J. Kennedy, H. K. Tsang, A. C. Gossard, and J. E. Bowers, "High-channel-count 20 GHz passively mode-locked quantum dot laser directly grown on Si with 4.1 Tbit/s transmission capacity," Optica **6**, 128–134 (2019).
[97]S. Cuyvers, B. Haq, C. Op de Beeck, S. Poelman, A. Hermans, Z. Wang, A. Gocalinska, E. Pelucchi, B. Corbett, G. Roelkens, K. Van Gasse, and B. Kuyken, "Low noise heterogeneous III-V-on-silicon-nitride mode-locked comb laser," Laser Photonics Rev. **15**, 2000485 (2021).
[98]M. Zimmermann, C. Gohle, R. Holzwarth, T. Udem, and T. W. Hänsch, "Optical clockwork with an offset-free difference-frequency comb: Accuracy of sum- and difference-frequency generation," Opt. Lett. **29**, 310–312 (2004).
[99]P. Maddaloni, P. Malara, G. Gagliardi, and P. D. Natale, "Mid-infrared fibre-based optical comb," New J. Phys. **8**, 262 (2006).
[100]H. Jung, R. Stoll, X. Guo, D. Fischer, and H. X. Tang, "Green, red, and IR frequency comb line generation from single IR pump in AlN microring resonator," Optica **1**, 396–399 (2014).
[101]Y. He, Q.-F. Yang, J. Ling, R. Luo, H. Liang, M. Li, B. Shen, H. Wang, K. Vahala, and Q. Lin, "Self-starting bi-chromatic $LiNbO_3$ soliton microcomb," Optica **6**, 1138–1144 (2019).
[102]C. Bao, Z. Yuan, H. Wang, L. Wu, B. Shen, K. Sung, S. Leifer, Q. Lin, and K. Vahala, "Interleaved difference-frequency generation for microcomb spectral densification in the mid-infrared," Optica **7**, 309–315 (2020).
[103]D. J. Wilson, K. Schneider, S. Hönl, M. Anderson, Y. Baumgartner, L. Czornomaz, T. J. Kippenberg, and P. Seidler, "Integrated gallium phosphide nonlinear photonics," Nat. Photonics **14**, 57–62 (2020).
[104]J. H. Sun, B. J. S. Gale, and D. T. Reid, "Composite frequency comb spanning 0.4–2.4 μm from a phase-controlled femtosecond Ti:sapphire laser and synchronously pumped optical parametric oscillator," Opt. Lett. **32**, 1414–1416 (2007).
[105]V. Ulvila, C. R. Phillips, L. Halonen, and M. Vainio, "Frequency comb generation by a continuous-wave-pumped optical parametric oscillator based on cascading quadratic nonlinearities," Opt. Lett. **38**, 4281–4284 (2013).
[106]S. Mosca, I. Ricciardi, M. Parisi, P. Maddaloni, L. Santamaria, P. De Natale, and M. De Rosa, "Direct generation of optical frequency combs in $\chi^{(2)}$ nonlinear cavities," Nanophotonics **5**, 316–331 (2016).
[107]A. W. Bruch, X. Liu, Z. Gong, J. B. Surya, M. Li, C.-L. Zou, and H. X. Tang, "Pockels soliton microcomb," Nat. Photonics **15**, 21–27 (2021).
[108]C. R. Phillips, C. Langrock, J. S. Pelc, M. M. Fejer, J. Jiang, M. E. Fermann, and I. Hartl, "Supercontinuum generation in quasi-phase-matched $LiNbO_3$ waveguide pumped by a Tm-doped fiber laser system," Opt. Lett. **36**, 3912–3914 (2011).
[109]M. Jankowski, C. Langrock, B. Desiatov, A. Marandi, C. Wang, M. Zhang, C. R. Phillips, M. Lončar, and M. M. Fejer, "Ultrabroadband nonlinear optics in nanophotonic periodically poled lithium niobate waveguides," Optica **7**, 40–46 (2020).
[110]R. W. Boyd, *Nonlinear Optics*, 3rd ed. (Academic Press, 2008).
[111]T. Ning, H. Pietarinen, O. Hyvärinen, J. Simonen, G. Genty, and M. Kauranen, "Strong second-harmonic generation in silicon nitride films," Appl. Phys. Lett. **100**, 161902 (2012).
[112]K. Koskinen, R. Czaplicki, A. Slablab, T. Ning, A. Hermans, B. Kuyken, V. Mittal, G. S. Murugan, T. Niemi, R. Baets, and M. Kauranen, "Enhancement of bulk second-harmonic generation from silicon nitride films by material composition," Opt. Lett. **42**, 5030 (2017).
[113]M. A. G. Porcel, J. Mak, C. Taballione, V. K. Schermerhorn, J. P. Epping, P. J. M. van der Slot, and K.-J. Boller, "Photo-induced second-order nonlinearity in stoichiometric silicon nitride waveguides," Opt. Express **25**, 33143–33159 (2017).
[114]X. Lu, G. Moille, A. Rao, D. A. Westly, and K. Srinivasan, "Efficient photoinduced second-harmonic generation in silicon nitride photonics," Nat. Photonics **15**, 131–136 (2021).
[115]E. Nitiss, J. Hu, A. Stroganov, and C.-S. Brès, "Optically reconfigurable quasi-phase-matching in silicon nitride microresonators," Nat. Photonics **16**, 134–141 (2022).
[116]E. Timurdogan, C. V. Poulton, M. J. Byrd, and M. R. Watts, "Electric field-induced second-order nonlinear optical effects in silicon waveguides," Nat. Photonics **11**, 200–206 (2017).
[117]H.-H. Lin, R. Sharma, A. Friedman, B. M. Cromey, F. Vallini, M. W. Puckett, K. Kieu, and Y. Fainman, "On the observation of dispersion in tunable second-order nonlinearities of silicon-rich nitride thin films," APL Photonics **4**, 036101 (2019).
[118]R. A. Myers, N. Mukherjee, and S. R. J. Brueck, "Large second-order nonlinearity in poled fused silica," Opt. Lett. **16**, 1732–1734 (1991).
[119]M. Berciano, G. Marcaud, P. Damas, X. Le Roux, P. Crozat, C. Alonso Ramos, D. Pérez Galacho, D. Benedikovic, D. Marris-Morini, E. Cassan, and L. Vivien, "Fast linear electro-optic effect in a centrosymmetric semiconductor," Commun. Phys. **1**, 64 (2018).
[120]L. Alloatti, C. Kieninger, A. Froelich, M. Lauermann, T. Frenzel, K. Köhnle, W. Freude, J. Leuthold, M. Wegener, and C. Koos, "Second-order nonlinear

© Author(s) 2022

optical metamaterials: ABC-type nanolaminates," Appl. Phys. Lett. **107**, 121903 (2015).
[121] S. Clemmen, A. Hermans, E. Solano, J. Dendooven, K. Koskinen, M. Kauranen, E. Brainis, C. Detavernier, and R. Baets, "Atomic layer deposited second-order nonlinear optical metamaterial for back-end integration with CMOS-compatible nanophotonic circuitry," Opt. Lett. **40**, 5371–5374 (2015).
[122] A. Hermans, C. Kieninger, K. Koskinen, A. Wickberg, E. Solano, J. Dendooven, M. Kauranen, S. Clemmen, M. Wegener, C. Koos, and R. Baets, "On the determination of $\chi^{(2)}$ in thin films: A comparison of one-beam second-harmonic generation measurement methodologies," Sci. Rep. **7**, 44581 (2017).
[123] M. Zhang, C. Wang, R. Cheng, A. Shams-Ansari, and M. Lončar, "Monolithic ultra-high-*Q* lithium niobate microring resonator," Optica **4**, 1536–1537 (2017).
[124] C. Xiong, W. H. P. Pernice, and H. X. Tang, "Low-loss, silicon integrated, aluminum nitride photonic circuits and their use for electro-optic signal processing," Nano Lett. **12**, 3562–3568 (2012).
[125] D. M. Lukin, C. Dory, M. A. Guidry, K. Y. Yang, S. D. Mishra, R. Trivedi, M. Radulaski, S. Sun, D. Vercruysse, G. H. Ahn, and J. Vučković, "4H-silicon-carbide-on-insulator for integrated quantum and nonlinear photonics," Nat. Photonics **14**, 330–334 (2020).
[126] L. Chang, A. Boes, P. Pintus, W. Xie, J. D. Peters, M. J. Kennedy, W. Jin, X.-W. Guo, S.-P. Yu, S. B. Papp, and J. E. Bowers, "Low loss (Al)GaAs on an insulator waveguide platform," Opt. Lett. **44**, 4075–4078 (2019).
[127] T. Cassese, N. Andriolli, M. Chiesa, A. R. Criado, and G. Contestabile, "InP photonic integrated comb generator made by a cascade of optical modulators," in *Optical Fiber Communication Conference* (Optica Publishing Group, 2018), p. Th1I.
[128] F. Bontempi, N. Andriolli, F. Scotti, M. Chiesa, and G. Contestabile, "Comb line multiplication in an InP integrated photonic circuit based on cascaded modulators," IEEE J. Sel. Top. Quantum Electron. **25**, 3500107 (2019).
[129] M. Yu, C. Reimer, D. Barton, P. Kharel, R. Cheng, L. He, L. Shao, D. Zhu, Y. Hu, H. R. Grant, L. Johansson, Y. Okawachi, A. L. Gaeta, M. Zhang, and M. Lončar, "Femtosecond pulse generation via an integrated electro-optic time lens," arXiv:2112.09204v1 [physics.optics] (2021).
[130] P. P. Vasil'ev, A. B. Sergeev, I. V. Smetanin, T. Weig, U. T. Schwarz, L. Sulmoni, J. Dorsaz, J.-M. Lamy, J.-F. Carlin, N. Grandjean, X. Zeng, T. Stadelmann, S. Grossmann, A. C. Hoogerwerf, and D. L. Boiko, "Mode locking in monolithic two-section InGaN blue-violet semiconductor lasers," Appl. Phys. Lett. **102**, 121115 (2013).
[131] L. Kong, H. L. Wang, D. Bajek, S. E. White, A. F. Forrest, X. L. Wang, B. F. Cui, J. Q. Pan, Y. Ding, and M. A. Cataluna, "Deep-red semiconductor monolithic mode-locked lasers," Appl. Phys. Lett. **105**, 221115 (2014).
[132] A. D. Ludlow, M. M. Boyd, J. Ye, E. Peik, and P. O. Schmidt, "Optical atomic clocks," Rev. Mod. Phys. **87**, 637–701 (2015).
[133] M. T. Murphy, T. Udem, R. Holzwarth, A. Sizmann, L. Pasquini, C. Araujo-Hauck, H. Dekker, S. D'Odorico, M. Fischer, T. W. Hänsch, and A. Manescau, "High-precision wavelength calibration of astronomical spectrographs with laser frequency combs," Mon. Not. R. Astron. Soc. **380**, 839–847 (2007).
[134] X. Shu, L. Beckmann, and H. F. Zhang, "Visible-light optical coherence tomography: a review," J. Biomed. Opt. **22**, 121707 (2017).
[135] H. Wang, L. Kong, A. Forrest, D. Bajek, S. E. Haggett, X. Wang, B. Cui, J. Pan, Y. Ding, and M. A. Cataluna, "Ultrashort pulse generation by semiconductor mode-locked lasers at 760 nm," Opt. Express **22**, 25940–25946 (2014).
[136] G. Tandoi, J. Javaloyes, E. Avrutin, C. N. Ironside, and J. H. Marsh, "Subpicosecond colliding pulse mode locking at 126 GHz in monolithic GaAs/AlGaAs quantum well lasers: Experiments and theory," IEEE J. Sel. Top. Quantum Electron. **19**, 1100608 (2013).
[137] J. T. Gopinath, B. Chann, R. K. Huang, C. Harris, J. J. Plant, L. Missaggia, J. P. Donnelly, P. W. Juodawlkis, and D. J. Ripin, "980-nm monolithic passively mode-locked diode lasers with 62 pJ of pulse energy," IEEE Photonics Technol. Lett. **19**, 937–939 (2007).
[138] A. Gubenko, D. Livshits, I. Krestnikov, S. Mikhrin, A. Kozhukhov, A. Kovsh, N. Ledentsov, A. Zhukov, and E. Portnoi, "High-power monolithic passively modelocked quantum-dot laser," Electron. Lett. **41**, 1124–1125 (2005).
[139] D. I. Nikitichev, Y. Ding, M. A. Cataluna, E. U. Rafailov, L. Drzewietzki, S. Breuer, W. Elsaesser, M. Rossetti, P. Bardella, T. Xu, I. Montrosset, I. Krestnikov, D. Livshits, M. Ruiz, M. Tran, Y. Robert, and M. Krakowski, "High peak power and sub-picosecond Fourier-limited pulse generation from passively mode-locked monolithic two-section gain-guided tapered InGaAs quantum-dot lasers," Laser Phys. **22**, 715–724 (2012).
[140] A. R. Rae, M. G. Thompson, R. V. Penty, I. H. White, A. R. Kovsh, S. S. Mikhrin, D. A. Livshits, and I. L. Krestnikov, "Harmonic mode-locking of a quantum-dot laser diode," in *IEEE Lasers and Electro-Optics Society Annual Meeting* (IEEE, 2006), pp. 874–875.
[141] G. Carpintero, M. G. Thompson, K. Yvind, R. V. Penty, and I. H. White, "Comparison of the noise performance of 10 GHz repetition rate quantum-dot and quantum well monolithic mode-locked semiconductor lasers," IET Optoelectron. **5**, 195–201 (2011).
[142] Y. Barbarin, E. A. J. M. Bente, M. J. R. Heck, Y. S. Oei, R. Nötzel, and M. K. Smit, "Characterization of a 15 GHz integrated bulk InGaAsP passively modelocked ring laser at 1.53 μm," Opt. Express **14**, 9716–9727 (2006).
[143] M. J. R. Heck, E. A. J. M. Bente, B. Smalbrugge, Y.-S. Oei, M. K. Smit, S. Anantathanasarn, and R. Nötzel, "Observation of Q-switching and mode-locking in two-section InAs/InP (100) quantum dot lasers around 1.55 μm," Opt. Express **15**, 16292–16301 (2007).
[144] M.-C. Lo, R. Guzmán, M. Ali, R. Santos, L. Augustin, and G. Carpintero, "1.8-THz-wide optical frequency comb emitted from monolithic passively mode-locked semiconductor quantum-well laser," Opt. Lett. **42**, 3872–3875 (2017).
[145] Z. G. Lu, J. R. Liu, C. Y. Song, J. Weber, Y. Mao, S. D. Chang, H. P. Ding, P. J. Poole, P. J. Barrios, D. Poitras, S. Janz, and M. O'Sullivan, "High performance InAs/InP quantum dot 34.462-GHz C-band coherent comb laser module," Opt. Express **26**, 2160–2167 (2018).
[146] Z. G. Lu, J. R. Liu, P. J. Poole, Z. J. Jiao, P. J. Barrios, D. Poitras, J. Caballero, and X. P. Zhang, "Ultra-high repetition rate InAs/InP quantum dot mode-locked lasers," Opt. Commun. **284**, 2323–2326 (2011).
[147] J. J. Plant, J. T. Gopinath, B. Chann, D. J. Ripin, R. K. Huang, and P. W. Juodawlkis, "250 mW, 1.5 μm monolithic passively mode-locked slab-coupled optical waveguide laser," Opt. Lett. **31**, 223–225 (2006).
[148] X. Guo, A. H. Quarterman, A. Wonfor, R. V. Penty, and I. H. White, "Monolithically integrated tunable mode-locked laser diode source with individual pulse selection and post-amplification," Opt. Lett. **41**, 4835–4838 (2016).
[149] M.-C. Lo, R. Guzmán, and G. Carpintero, "InP femtosecond mode-locked laser in a compound feedback cavity with a switchable repetition rate," Opt. Lett. **43**, 507–510 (2018).
[150] M. A. Alloush, M. van Delden, A. Bassal, N. Kleemann, C. Brenner, M.-C. Lo, L. Augustin, R. Guzmán, T. Musch, G. Carpintero, and M. R. Hofmann, "RF analysis of a sub-GHz InP-based 1550 nm monolithic mode-locked laser chip," IEEE Photonics Technol. Lett. **33**, 828–831 (2021).
[151] M. Dong, M. W. Day, H. G. Winful, and S. T. Cundiff, "Quantum-well laser diodes for frequency comb spectroscopy," Opt. Express **28**, 21825–21834 (2020).
[152] R. Rosales, S. G. Murdoch, R. T. Watts, K. Merghem, A. Martinez, F. Lelarge, A. Accard, L. P. Barry, and A. Ramdane, "High performance mode locking characteristics of single section quantum dash lasers," Opt. Express **20**, 8649–8657 (2012).
[153] G. Liu, Z. Lu, J. Liu, Y. Mao, M. Vachon, C. Song, P. Barrios, and P. J. Poole, "Passively mode-locked quantum dash laser with an aggregate 5.376 Tbit/s PAM-4 transmission capacity," Opt. Express **28**, 4587–4593 (2020).
[154] L. Hou, M. Haji, J. H. Marsh, and A. C. Bryce, "10 GHz AlGaInAs/InP 1.55 μm passively mode-locked laser with low divergence angle and timing jitter," Opt. Express **19**, B75–B80 (2011).
[155] R. Rosales, K. Merghem, A. Martinez, A. Akrout, J.-P. Tourrenc, A. Accard, F. Lelarge, and A. Ramdane, "InAs/InP quantum-dot passively mode-locked lasers for 1.55-μm applications," IEEE J. Sel. Top. Quantum Electron. **17**, 1292–1301 (2011).
[156] J. K. Alexander, P. E. Morrissey, L. Caro, M. Dernaika, N. P. Kelly, and F. H. Peters, "On-chip investigation of phase noise in monolithically integrated gain-switched lasers," IEEE Photonics Technol. Lett. **29**, 731–734 (2017).
[157] S. Cheung, J.-H. Baek, R. P. Scott, N. K. Fontaine, F. M. Soares, X. Zhou, D. M. Baney, and S. J. B. Yoo, "1-GHz monolithically integrated hybrid mode-locked InP laser," IEEE Photonics Technol. Lett. **22**, 1793–1795 (2010).

© Author(s) 2022

[158]M. Faugeron, F. Lelarge, M. Tran, Y. Robert, E. Vinet, A. Enard, J. Jacquet, and F. Van Dijk, "High peak power, narrow RF linewidth asymmetrical cladding quantum-dash mode-locked lasers," IEEE J. Sel. Top. Quantum Electron. **19**, 1101008 (2013).
[159]X. Li, J. X. B. Sia, J. Wang, Z. Qiao, W. Wang, X. Guo, H. Wang, and C. Liu, "Optical frequency comb generation from a 1.65 μm single-section quantum well laser," Opt. Express **30**, 4117–4124 (2022).
[160]P. A. Morton, J. E. Bowers, L. A. Koszi, M. Soler, J. Lopata, and D. P. Wilt, "Monolithic hybrid mode-locked 1.3 μm semiconductor lasers," Appl. Phys. Lett. **56**, 111–113 (1990).
[161]S. Sanders, L. Eng, J. Paslaski, and A. Yariv, "108 GHz passive mode locking of a multiple quantum well semiconductor laser with an intracavity absorber," Appl. Phys. Lett. **56**, 310–311 (1990).
[162]Y. K. Chen, M. C. Wu, T. Tanbun-Ek, R. A. Logan, and M. A. Chin, "Subpicosecond monolithic colliding-pulse mode-locked multiple quantum well lasers," Appl. Phys. Lett. **58**, 1253–1255 (1991).
[163]E. A. Avrutin, J. H. Marsh, and E. L. Portnoi, "Monolithic and multi-gigahertz mode-locked semiconductor lasers: Constructions, experiments, models and applications," IEE Proc.-Optoelectron. **147**, 251–278 (2000).
[164]K. A. Williams, M. G. Thompson, and I. H. White, "Long-wavelength monolithic mode-locked diode lasers," New J. Phys. **6**, 179 (2004).
[165]M. G. Thompson, A. R. Rae, M. Xia, R. V. Penty, and I. H. White, "InGaAs quantum-dot mode-locked laser diodes," IEEE J. Sel. Top. Quantum Electron. **15**, 661–672 (2009).
[166]M. L. Davenport, S. Liu, and J. E. Bowers, "Integrated heterogeneous silicon/III-V mode-locked lasers," Photonics Res. **6**, 468–478 (2018).
[167]K. Van Gasse, S. Uvin, V. Moskalenko, S. Latkowski, G. Roelkens, E. Bente, and B. Kuyken, "Recent advances in the photonic integration of mode-locked laser diodes," IEEE Photonics Technol. Lett. **31**, 1870–1873 (2019).
[168]R. G. Hunsperger, *Integrated Optics: Theory and Technology*, 6th ed. (Springer, 2009).
[169]L. Hou, M. Haji, J. H. Marsh, and A. C. Bryce, "490 fs pulse generation from a passive C-band AlGaInAs/InP quantum well mode-locked laser," Opt. Lett. **37**, 773–775 (2012).
[170]J. H. Marsh and L. Hou, "Mode-locked laser diodes and their monolithic integration," IEEE J. Sel. Top. Quantum Electron. **23**, 1100611 (2017).
[171]C. Gosset, K. Merghem, A. Martinez, G. Moreau, G. Patriarche, G. Aubin, A. Ramdane, J. Landreau, and F. Lelarge, "Subpicosecond pulse generation at 134 GHz using a quantum-dash-based Fabry-Perot laser emitting at 1.56 μm," Appl. Phys. Lett. **88**, 241105 (2006).
[172]F. Lelarge, B. Dagens, J. Renaudier, R. Brenot, A. Accard, F. van Dijk, D. Make, O. Le Gouezigou, J.-G. Provost, F. Poingt, J. Landreau, O. Drisse, E. Derouin, B. Rousseau, F. Pommereau, and G.-H. Duan, "Recent advances on InAs/InP quantum dash based semiconductor lasers and optical amplifiers operating at 1.55 μm," IEEE J. Sel. Top. Quantum Electron. **13**, 111–124 (2007).
[173]M. J. R. Heck, A. Renault, E. A. J. M. Bente, Y.-S. Oei, M. K. Smit, K. S. E. Eikema, W. Ubachs, S. Anantathanasarn, and R. Nötzel, "Passively mode-locked 4.6 and 10.5 GHz quantum dot laser diodes around 1.55 μm with large operating regime," IEEE J. Sel. Top. Quantum Electron. **15**, 634–643 (2009).
[174]F. Robert, A. C. Bryce, J. H. Marsh, A. J. SpringThorpe, and J. K. White, "Passive mode locking of InAlGaAs 1.3 μm strained quantum wells extended cavity laser fabricated by quantum-well intermixing," IEEE Photonics Technol. Lett. **16**, 374–376 (2004).
[175]J. K. Mee, M. T. Crowley, N. Patel, D. Murrell, R. Raghunathan, A. Aboketaf, A. Elshaari, S. F. Preble, P. Ampadu, and L. F. Lester, "A passively mode-locked quantum-dot laser operating over a broad temperature range," Appl. Phys. Lett. **101**, 071112 (2012).
[176]S. Pan, J. Huang, Z. Zhou, Z. Liu, L. Ponnampalam, Z. Liu, M. Tang, M.-C. Lo, Z. Cao, K. Nishi, K. Takemasa, M. Sugawara, R. Penty, I. White, A. Seeds, H. Liu, and S. Chen, "Quantum dot mode-locked frequency comb with ultra-stable 25.5 GHz spacing between 20 °C and 120 °C," Photonics Res. **8**, 1937–1942 (2020).
[177]J. F. Martins-Filho, E. A. Avrutin, C. N. Ironside, and J. S. Roberts, "Monolithic multiple colliding pulse mode-locked quantum-well lasers, experiment and theory," IEEE J. Sel. Top. Quantum Electron. **1**, 539–551 (1995).
[178]S. R. Chinn and E. A. Swanson, "Passive FM locking and pulse generation from 980-nm strained-quantum-well Fabry-Perot lasers," IEEE Photonics Technol. Lett. **5**, 969–971 (1993).
[179]C. C. Renaud, M. Pantouvaki, S. Gregoire, I. Lealman, P. Cannard, S. Cole, R. Moore, R. Gwilliam, and A. J. Seeds, "A monolithic MQW InP–InGaAsP-based optical comb generator," IEEE J. Quantum Electron. **43**, 998–1005 (2007).
[180]M. W. Day, M. Dong, B. C. Smith, R. C. Owen, G. C. Kerber, T. Ma, H. G. Winful, and S. T. Cundiff, "Simple single-section diode frequency combs," APL Photonics **5**, 121303 (2020).
[181]R. Rosales, K. Merghem, C. Calo, G. Bouwmans, I. Krestnikov, A. Martinez, and A. Ramdane, "Optical pulse generation in single section InAs/GaAs quantum dot edge emitting lasers under continuous wave operation," Appl. Phys. Lett. **101**, 221113 (2012).
[182]Z. G. Lu, J. R. Liu, P. J. Poole, S. Raymond, P. J. Barrios, D. Poitras, G. Pakulski, P. Grant, and D. Roy-Guay, "An L-band monolithic InAs/InP quantum dot mode-locked laser with femtosecond pulses," Opt. Express **17**, 13609–13614 (2009).
[183]M. Smit, K. Williams, and J. van der Tol, "Past, present, and future of InP-based photonic integration," APL Photonics **4**, 050901 (2019).
[184]R. Guzmán, C. Gordon, L. Orbe, and G. Carpintero, "1 GHz InP on-chip monolithic extended cavity colliding-pulse mode-locked laser," Opt. Lett. **42**, 2318–2321 (2017).
[185]J. S. Parker, R. S. Guzzon, E. J. Norberg, A. Bhardwaj, P. R. A. Binetti, and L. A. Coldren, "Theory and design of THz intracavity gain-flattened filters for monolithically integrated mode-locked lasers," IEEE J. Quantum Electron. **48**, 114–122 (2012).
[186]M. J. R. Heck, P. Munoz, B. W. Tilma, E. A. J. M. Bente, Y. Barbarin, Y.-S. Oei, R. Notzel, and M. K. Smit, "Design, fabrication and characterization of an InP-based tunable integrated optical pulse shaper," IEEE J. Quantum Electron. **44**, 370–377 (2008).
[187]S. Tahvili, S. Latkowski, B. Smalbrugge, X. J. M. Leijtens, P. J. Williams, M. J. Wale, J. Parra-Cetina, R. Maldonado-Basilio, P. Landais, M. K. Smit, and E. A. J. M. Bente, "InP-based integrated optical pulse shaper: Demonstration of chirp compensation," IEEE Photonics Technol. Lett. **25**, 450–453 (2013).
[188]Z. Zhang, J. C. Norman, S. Liu, A. Malik, and J. E. Bowers, "Integrated dispersion compensated mode-locked quantum dot laser," Photonics Res. **8**, 1428–1434 (2020).
[189]E. U. Rafailov, M. A. Cataluna, and W. Sibbett, "Mode-locked quantum-dot lasers," Nat. Photonics **1**, 395–401 (2007).
[190]Z. Zhang, D. Jung, J. C. Norman, W. W. Chow, and J. E. Bowers, "Linewidth enhancement factor in InAs/GaAs quantum dot lasers and its implication in isolator-free and narrow linewidth applications," IEEE J. Sel. Top. Quantum Electron. **25**, 1900509 (2019).
[191]W. W. Chow, Z. Zhang, J. C. Norman, S. Liu, and J. E. Bowers, "On quantum-dot lasing at gain peak with linewidth enhancement factor $\alpha_H = 0$," APL Photonics **5**, 026101 (2020).
[192]M. Asada, Y. Miyamoto, and Y. Suematsu, "Gain and the threshold of three-dimensional quantum-box lasers," IEEE J. Quantum Electron. **22**, 1915–1921 (1986).
[193]Y. Arakawa and H. Sakaki, "Multidimensional quantum well laser and temperature dependence of its threshold current," Appl. Phys. Lett. **40**, 939–941 (1982).
[194]H. Huang, J. Duan, D. Jung, A. Y. Liu, Z. Zhang, J. Norman, J. E. Bowers, and F. Grillot, "Analysis of the optical feedback dynamics in InAs/GaAs quantum dot lasers directly grown on silicon," J. Opt. Soc. Am. B **35**, 2780–2787 (2018).
[195]J. M. Gérard, O. Cabrol, and B. Sermage, "InAs quantum boxes: Highly efficient radiative traps for light emitting devices on Si," Appl. Phys. Lett. **68**, 3123–3125 (1996).

© Author(s) 2022

[196]P. M. Anandarajah, R. Maher, Y. Q. Xu, S. Latkowski, J. O'Carroll, S. G. Murdoch, R. Phelan, J. O'Gorman, and L. P. Barry, "Generation of coherent multicarrier signals by gain switching of discrete mode lasers," IEEE Photonics J. **3**, 112–122 (2011).
[197]J. K. Alexander, P. E. Morrissey, H. Yang, M. Yang, P. J. Marraccini, B. Corbett, and F. H. Peters, "Monolithically integrated low linewidth comb source using gain switched slotted Fabry-Perot lasers," Opt. Express **24**, 7960–7965 (2016).
[198]M. D. Gutierrez Pascual, V. Vujicic, J. Braddell, F. Smyth, P. M. Anandarajah, and L. P. Barry, "Photonic integrated gain switched optical frequency comb for spectrally efficient optical transmission systems," IEEE Photonics J. **9**, 7202008 (2017).
[199]J. K. Alexander, L. Caro, M. Dernaika, S. P. Duggan, H. Yang, S. Chandran, E. P. Martin, A. A. Ruth, P. M. Anandarajah, and F. H. Peters, "Integrated dual optical frequency comb source," Opt. Express **28**, 16900–16906 (2020).
[200]M. N. Hammad, P. D. Lakshmijayasimha, A. Kaszubowska-Anandarajah, and P. M. Anandarajah, "Photonically integrated gain-switched lasers for optical frequency comb generation," Microwave Opt. Technol. Lett. **63**, 2219–2226 (2021).
[201]X. Li, H. Wang, Z. Qiao, X. Guo, G. I. Ng, Y. Zhang, Z. Niu, C. Tong, and C. Liu, "Modal gain characteristics of a 2 μm InGaSb/AlGaAsSb passively mode-locked quantum well laser," Appl. Phys. Lett. **111**, 251105 (2017).
[202]L. A. Sterczewski, C. Frez, S. Forouhar, D. Burghoff, and M. Bagheri, "Frequency-modulated diode laser frequency combs at 2 μm wavelength," APL Photonics **5**, 076111 (2020).
[203]K. Merghem, R. Teissier, G. Aubin, A. M. Monakhov, A. Ramdane, and A. N. Baranov, "Passive mode locking of a GaSb-based quantum well diode laser emitting at 2.1 μm," Appl. Phys. Lett. **107**, 111109 (2015).
[204]S. Becker, J. Scheuermann, R. Weih, K. Rößner, C. Kistner, J. Koeth, J. Hillbrand, B. Schwarz, and M. Kamp, "Picosecond pulses from a monolithic GaSb-based passive mode-locked laser," Appl. Phys. Lett. **116**, 022102 (2020).
[205]T. Feng, L. Shterengas, T. Hosoda, A. Belyanin, and G. Kipshidze, "Passive mode-locking of 3.25 μm GaSb-based cascade diode lasers," ACS Photonics **5**, 4978–4985 (2018).
[206]L. A. Sterczewski, J. Westberg, M. Bagheri, C. Frez, I. Vurgaftman, C. L. Canedy, W. W. Bewley, C. D. Merritt, C. S. Kim, M. Kim, J. R. Meyer, and G. Wysocki, "Mid-infrared dual-comb spectroscopy with interband cascade lasers," Opt. Lett. **44**, 2113–2116 (2019).
[207]J. Hillbrand, M. Beiser, A. M. Andrews, H. Detz, R. Weih, A. Schade, S. Höfling, G. Strasser, and B. Schwarz, "Picosecond pulses from a mid-infrared interband cascade laser," Optica **6**, 1334–1337 (2019).
[208]D. Kazakov, M. Piccardo, Y. Wang, P. Chevalier, T. S. Mansuripur, F. Xie, C.-E. Zah, K. Lascola, A. Belyanin, and F. Capasso, "Self-starting harmonic frequency comb generation in a quantum cascade laser," Nat. Photonics **11**, 789–792 (2017).
[209]F. Cappelli, G. Campo, I. Galli, G. Giusfredi, S. Bartalini, D. Mazzotti, P. Cancio, S. Borri, B. Hinkov, J. Faist, and P. De Natale, "Frequency stability characterization of a quantum cascade laser frequency comb," Laser Photonics Rev. **10**, 623–630 (2016).
[210]Q. Y. Lu, S. Manna, D. H. Wu, S. Slivken, and M. Razeghi, "Shortwave quantum cascade laser frequency comb for multi-heterodyne spectroscopy," Appl. Phys. Lett. **112**, 141104 (2018).
[211]F. Cappelli, G. Villares, S. Riedi, and J. Faist, "Intrinsic linewidth of quantum cascade laser frequency combs," Optica **2**, 836–840 (2015).
[212]B. Meng, M. Singleton, J. Hillbrand, M. Franckié, M. Beck, and J. Faist, "Dissipative Kerr solitons in semiconductor ring lasers," Nat. Photonics **16**, 142–147 (2022).
[213]J. Hillbrand, N. Opačak, M. Piccardo, H. Schneider, G. Strasser, F. Capasso, and B. Schwarz, "Mode-locked short pulses from an 8 μm wavelength semiconductor laser," Nat. Commun. **11**, 5788 (2020).
[214]P. Jouy, J. M. Wolf, Y. Bidaux, P. Allmendinger, M. Mangold, M. Beck, and J. Faist, "Dual comb operation of $\lambda \sim 8.2$ μm quantum cascade laser frequency comb with 1 W optical power," Appl. Phys. Lett. **111**, 141102 (2017).
[215]Q. Y. Lu, M. Razeghi, S. Slivken, N. Bandyopadhyay, Y. Bai, W. J. Zhou, M. Chen, D. Heydari, A. Haddadi, R. McClintock, M. Amanti, and C. Sirtori, "High power frequency comb based on mid-infrared quantum cascade laser at $\lambda \sim 9$ μm," Appl. Phys. Lett. **106**, 051105 (2015).
[216]M. Wienold, B. Röben, L. Schrottke, and H. T. Grahn, "Evidence for frequency comb emission from a Fabry-Pérot terahertz quantum-cascade laser," Opt. Express **22**, 30410–30424 (2014).
[217]Y. Zhao, Z. Li, K. Zhou, X. Liao, W. Guan, W. Wan, S. Yang, J. C. Cao, D. Xu, S. Barbieri, and H. Li, "Active stabilization of terahertz semiconductor dual-comb laser sources employing a phase locking technique," Laser Photonics Rev. **15**, 2000498 (2021).
[218]H. Li, Z. Li, W. Wan, K. Zhou, X. Liao, S. Yang, C. Wang, J. C. Cao, and H. Zeng, "Toward compact and real-time terahertz dual-comb spectroscopy employing a self-detection scheme," ACS Photonics **7**, 49–56 (2020).
[219]M. Jaidl, N. Opačak, M. A. Kainz, S. Schönhuber, D. Theiner, B. Limbacher, M. Beiser, M. Giparakis, A. M. Andrews, G. Strasser, B. Schwarz, J. Darmo, and K. Unterrainer, "Comb operation in terahertz quantum cascade ring lasers," Optica **8**, 780–787 (2021).
[220]D. Burghoff, T.-Y. Kao, N. Han, C. W. I. Chan, X. Cai, Y. Yang, D. J. Hayton, J.-R. Gao, J. L. Reno, and Q. Hu, "Terahertz laser frequency combs," Nat. Photonics **8**, 462 (2014).
[221]D. Burghoff, Y. Yang, D. J. Hayton, J.-R. Gao, J. L. Reno, and Q. Hu, "Evaluating the coherence and time-domain profile of quantum cascade laser frequency combs," Opt. Express **23**, 1190–1202 (2015).
[222]M. Rösch, M. Beck, M. J. Süess, D. Bachmann, K. Unterrainer, J. Faist, and G. Scalari, "Heterogeneous terahertz quantum cascade lasers exceeding 1.9 THz spectral bandwidth and featuring dual comb operation," Nanophotonics **7**, 237–242 (2018).
[223]M. Rösch, G. Scalari, M. Beck, and J. Faist, "Octave-spanning semiconductor laser," Nat. Photonics **9**, 42–47 (2015).
[224]F. Wang, H. Nong, T. Fobbe, V. Pistore, S. Houver, S. Markmann, N. Jukam, M. Amanti, C. Sirtori, S. Moumdji, R. Colombelli, L. Li, E. Linfield, G. Davies, J. Mangeney, J. Tignon, and S. Dhillon, "Short terahertz pulse generation from a dispersion compensated modelocked semiconductor laser," Laser Photonics Rev. **11**, 1700013 (2017).
[225]S. Barbieri, M. Ravaro, P. Gellie, G. Santarelli, C. Manquest, C. Sirtori, S. P. Khanna, E. H. Linfield, and A. G. Davies, "Coherent sampling of active mode-locked terahertz quantum cascade lasers and frequency synthesis," Nat. Photonics **5**, 306 (2011).
[226]X. Li, H. Wang, Z. Qiao, X. Guo, W. Wang, G. I. Ng, Y. Zhang, Y. Xu, Z. Niu, C. Tong, and C. Liu, "Investigation of regime switching from mode locking to Q-switching in a 2 μm InGaSb/AlGaAsSb quantum well laser," Opt. Express **26**, 8289–8295 (2018).
[227]T. Feng, L. Shterengas, T. Hosoda, G. Kipshidze, A. Belyanin, C. C. Teng, J. Westberg, G. Wysocki, and G. Belenky, "Passively mode-locked 2.7 and 3.2 μm GaSb-based cascade diode lasers," J. Lightwave Technol. **38**, 1895–1899 (2020).
[228]L. A. Sterczewski, J. Westberg, C. L. Patrick, C. S. Kim, M. Kim, C. L. Canedy, W. W. Bewley, C. D. Merritt, I. Vurgaftman, J. R. Meyer, and G. Wysocki, "Multiheterodyne spectroscopy using interband cascade lasers," Opt. Eng. **57**, 011014 (2018).
[229]M. Bagheri, C. Frez, L. A. Sterczewski, I. Gruidin, M. Fradet, I. Vurgaftman, C. L. Canedy, W. W. Bewley, C. D. Merritt, C. S. Kim, M. Kim, and J. R. Meyer, "Passively mode-locked interband cascade optical frequency combs," Sci. Rep. **8**, 3322 (2018).
[230]B. Schwarz, J. Hillbrand, M. Beiser, A. M. Andrews, G. Strasser, H. Detz, A. Schade, R. Weih, and S. Höfling, "Monolithic frequency comb platform based on interband cascade lasers and detectors," Optica **6**, 890–895 (2019).
[231]L. A. Sterczewski, M. Bagheri, C. Frez, C. L. Canedy, I. Vurgaftman, and J. R. Meyer, "Mid-infrared dual-comb spectroscopy with room-temperature bi-functional interband cascade lasers and detectors," Appl. Phys. Lett. **116**, 141102 (2020).
[232]G. Villares, J. Wolf, D. Kazakov, M. J. Süess, A. Hugi, M. Beck, and J. Faist, "On-chip dual-comb based on quantum cascade laser frequency combs," Appl. Phys. Lett. **107**, 251104 (2015).
[233]R. Wang, P. Täschler, F. Kapsalidis, M. Shahmohammadi, M. Beck, and J. Faist, "Mid-infrared quantum cascade laser frequency combs based on multi-section waveguides," Opt. Lett. **45**, 6462–6465 (2020).
[234]M. Piccardo, B. Schwarz, D. Kazakov, M. Beiser, N. Opačak, Y. Wang, S. Jha, J. Hillbrand, M. Tamagnone, W. T. Chen, A. Y. Zhu, L. L. Columbo, A. Belyanin,

© Author(s) 2022

and F. Capasso, "Frequency combs induced by phase turbulence," Nature **582**, 360–364 (2020).
[235]F. Kapsalidis, B. Schneider, M. Singleton, M. Bertrand, E. Gini, M. Beck, and J. Faist, "Mid-infrared quantum cascade laser frequency combs with a microstrip-like line waveguide geometry," Appl. Phys. Lett. **118**, 071101 (2021).
[236]B. Meng, M. Singleton, M. Shahmohammadi, F. Kapsalidis, R. Wang, M. Beck, and J. Faist, "Mid-infrared frequency comb from a ring quantum cascade laser," Optica **7**, 162–167 (2020).
[237]M. S. Vitiello, L. Consolino, M. Inguscio, and P. De Natale, "Toward new frontiers for terahertz quantum cascade laser frequency combs," Nanophotonics **10**, 187–194 (2021).
[238]L. Consolino, M. Nafa, F. Cappelli, K. Garrasi, F. P. Mezzapesa, L. Li, A. G. Davies, E. H. Linfield, M. S. Vitiello, P. De Natale, and S. Bartalini, "Fully phase-stabilized quantum cascade laser frequency comb," Nat. Commun. **10**, 2938 (2019).
[239]J. R. Freeman, J. Maysonnave, N. Jukam, P. Cavalié, K. Maussang, H. E. Beere, D. A. Ritchie, J. Mangeney, S. S. Dhillon, and J. Tignon, "Direct intensity sampling of a modelocked terahertz quantum cascade laser," Appl. Phys. Lett. **101**, 181115 (2012).
[240]J. R. Freeman, J. Maysonnave, H. E. Beere, D. A. Ritchie, J. Tignon, and S. S. Dhillon, "Electric field sampling of modelocked pulses from a quantum cascade laser," Opt. Express **21**, 16162–16169 (2013).
[241]F. Wang, K. Maussang, S. Moumdji, R. Colombelli, J. R. Freeman, I. Kundu, L. Li, E. H. Linfield, A. G. Davies, J. Mangeney, J. Tignon, and S. S. Dhillon, "Generating ultrafast pulses of light from quantum cascade lasers," Optica **2**, 944–949 (2015).
[242]A. Mottaghizadeh, D. Gacemi, P. Laffaille, H. Li, M. Amanti, C. Sirtori, G. Santarelli, W. Hänsel, R. Holzwart, L. H. Li, E. H. Linfield, and S. Barbieri, "5-ps-long terahertz pulses from an active-mode-locked quantum cascade laser," Optica **4**, 168–171 (2017).
[243]F. Cappelli, L. Consolino, G. Campo, I. Galli, D. Mazzotti, A. Campa, M. Siciliani de Cumis, P. Cancio Pastor, R. Eramo, M. Rösch, M. Beck, G. Scalari, J. Faist, P. De Natale, and S. Bartalini, "Retrieval of phase relation and emission profile of quantum cascade laser frequency combs," Nat. Photonics **13**, 562–568 (2019).
[244]A. Forrer, Y. Wang, M. Beck, A. Belyanin, J. Faist, and G. Scalari, "Self-starting harmonic comb emission in THz quantum cascade lasers," Appl. Phys. Lett. **118**, 131112 (2021).
[245]J. B. Khurgin, Y. Dikmelik, A. Hugi, and J. Faist, "Coherent frequency combs produced by self frequency modulation in quantum cascade lasers," Appl. Phys. Lett. **104**, 081118 (2014).
[246]H. Li, P. Laffaille, D. Gacemi, M. Apfel, C. Sirtori, J. Leonardon, G. Santarelli, M. Rösch, G. Scalari, M. Beck, J. Faist, W. Hänsel, R. Holzwarth, and S. Barbieri, "Dynamics of ultra-broadband terahertz quantum cascade lasers for comb operation," Opt. Express **23**, 33270–33294 (2015).
[247]P. Tzenov, I. Babushkin, R. Arkhipov, M. Arkhipov, N. Rosanov, U. Morgner, and C. Jirauschek, "Passive and hybrid mode locking in multi-section terahertz quantum cascade lasers," New J. Phys. **20**, 053055 (2018).
[248]H. M. J. Bastiaens, G. Neijts, A. Memon, Y. Fan, J. Mak, D. Geskus, M. Hoekman, V. Moskalenko, E. A. J. M. Bente, and K.-J. Boller, "First demonstration of a hybrid integrated InP-Si_3N_4 diode laser for broadband optical frequency comb generation," in *Novel In-Plane Semiconductor Lasers XX*, edited by A. A. Belyanin and P. M. Smowton (International Society for Optics and Photonics SPIE, 2021), Vol. 11705, pp. 11–18.
[249]Y. Klaver, J. P. Epping, C. G. H. Roeloffzen, and D. A. I. Marpaung, "Self-mode-locking in a high-power hybrid silicon nitride integrated laser," Opt. Lett. **47**, 198–201 (2022).
[250]A. S. Voloshin, N. M. Kondratiev, G. V. Lihachev, J. Liu, V. E. Lobanov, N. Y. Dmitriev, W. Weng, T. J. Kippenberg, and I. A. Bilenko, "Dynamics of soliton self-injection locking in optical microresonators," Nat. Commun. **12**, 235 (2021).
[251]Y. Ibrahimi, S. Boust, Q. Wilmart, J.-F. Paret, A. Garreau, K. Mekhazni, C. Fortin, F. Duport, J.-M. Fedeli, C. Sciancalepore, S. Garcia, and F. van Dijk, "Low FSR mode-locked laser based on InP-Si_3N_4 hybrid integration," J. Lightwave Technol. **39**, 7573–7580 (2021).
[252]N. Y. Dmitriev, S. N. Koptyaev, A. S. Voloshin, N. M. Kondratiev, K. N. Min′kov, V. E. Lobanov, M. V. Ryabko, S. V. Polonsky, and I. A. Bilenko, "Hybrid integrated dual-microcomb source," Phys. Rev. Appl. **18**, 034068 (2022).
[253]E. Vissers, S. Poelman, C. O. de Beeck, K. Van Gasse, and B. Kuyken, "Hybrid integrated mode-locked laser diodes with a silicon nitride extended cavity," Opt. Express **29**, 15013–15022 (2021).
[254]S. Boust, H. E. Dirani, L. Youssef, Y. Robert, A. Larrue, C. Petit-Etienne, E. Vinet, S. Kerdiles, E. Pargon, M. Faugeron, M. Vallet, F. Duport, C. Sciancalepore, and F. van Dijk, "Microcomb source based on InP DFB/Si_3N_4 microring butt-coupling," J. Lightwave Technol. **38**, 5517–5525 (2020).
[255]X. Li, J. X. B. Sia, W. Wang, Z. Qiao, X. Guo, G. I. Ng, Y. Zhang, Z. Niu, C. Tong, H. Wang, and C. Liu, "Phase noise reduction of a 2 μm passively mode-locked laser through hybrid III-V/silicon integration," Optica **8**, 855–860 (2021).
[256]A. S. Raja, A. S. Voloshin, H. Guo, S. E. Agafonova, J. Liu, A. S. Gorodnitskiy, M. Karpov, N. G. Pavlov, E. Lucas, R. R. Galiev, A. E. Shitikov, J. D. Jost, M. L. Gorodetsky, and T. J. Kippenberg, "Electrically pumped photonic integrated soliton microcomb," Nat. Commun. **10**, 680 (2019).
[257]J. Liu, E. Lucas, A. S. Raja, J. He, J. Riemensberger, R. N. Wang, M. Karpov, H. Guo, R. Bouchand, and T. J. Kippenberg, "Photonic microwave generation in the X- and K-band using integrated soliton microcombs," Nat. Photonics **14**, 486–491 (2020).
[258]G. Kurczveil, A. Descos, D. Liang, M. Fiorentino, and R. Beausoleil, "Hybrid silicon quantum dot comb laser with record wide comb width," in *Frontiers in Optics/Laser* (Science Optica Publishing Group, 2020), p. FTu6E.6.
[259]S. Liu, T. Komljenovic, S. Srinivasan, E. Norberg, G. Fish, and J. E. Bowers, "Characterization of a fully integrated heterogeneous silicon/III-V colliding pulse mode-locked laser with on-chip feedback," Opt. Express **26**, 9714–9723 (2018).
[260]D. Auth, S. Liu, J. Norman, J. Edward Bowers, and S. Breuer, "Passively mode-locked semiconductor quantum dot on silicon laser with 400 Hz RF line width," Opt. Express **27**, 27256–27266 (2019).
[261]S. Liu, J. C. Norman, D. Jung, M. J. Kennedy, A. C. Gossard, and J. E. Bowers, "Monolithic 9 GHz passively mode locked quantum dot lasers directly grown on on-axis (001) Si," Appl. Phys. Lett. **113**, 041108 (2018).
[262]G. Kurczveil, C. Zhang, A. Descos, D. Liang, M. Fiorentino, and R. Beausoleil, "On-chip hybrid silicon quantum dot comb laser with 14 error-free channels," in IEEE International Semiconductor Laser Conference, 2018.
[263]M. J. R. Heck, M. L. Davenport, H. Park, D. J. Blumenthal, and J. E. Bowers, "Ultra-long cavity hybrid silicon mode-locked laser diode operating at 930 MHz," in *Optical Fiber Communication Conference* (Optica Publishing Group, 2010), p. OMI5.
[264]S. Liu, M. Davenport, and J. E. Bowers, "Hybrid mode-locked 20 GHz colliding pulse Si/III-V laser with 890 fs pulsewidth," in *Conference on Lasers and Electro-Optics* (Optica Publishing Group, 2020), p. STh3E.4.
[265]K. Van Gasse, Z. Chen, E. Vicentini, J. Huh, S. Poelman, Z. Wang, G. Roelkens, T. W. Hänsch, B. Kuyken, and N. Picqué, "An on-chip III-V-semiconductor-on-silicon laser frequency comb for gas-phase molecular spectroscopy in real-time," arXiv:2006.15113v1 [physics.optics] (2020).
[266]R. Paschotta, "Noise of mode-locked lasers (Part II): Timing jitter and other fluctuations," Appl. Phys. B **79**, 163–173 (2004).
[267]R. Paschotta, A. Schlatter, S. C. Zeller, H. R. Telle, and U. Keller, "Optical phase noise and carrier-envelope offset noise of mode-locked lasers," Appl. Phys. B **82**, 265–273 (2006).
[268]S. Srinivasan, E. Norberg, T. Komljenovic, M. Davenport, G. Fish, and J. E. Bowers, "Hybrid silicon colliding-pulse mode-locked lasers with on-chip stabilization," IEEE J. Sel. Top. Quantum Electron. **21**, 24–29 (2015).
[269]Z. Wang, M. L. Fanto, J. A. Steidle, A. A. Aboketaf, N. A. Rummage, P. M. Thomas, C.-S. Lee, W. Guo, L. F. Lester, and S. F. Preble, "Passively mode-locked InAs quantum dot lasers on a silicon substrate by Pd-GaAs wafer bonding," Appl. Phys. Lett. **110**, 141110 (2017).
[270]G. Kurczveil, M. A. Seyedi, D. Liang, M. Fiorentino, and R. G. Beausoleil, "Error-free operation in a hybrid-silicon quantum dot comb laser," IEEE Photonics Technol. Lett. **30**, 71–74 (2018).
[271]M. L. Davenport, G. Kurczveil, M. J. Heck, and J. E. Bowers, "A hybrid silicon colliding pulse mode-locked laser with integrated passive waveguide section," in *IEEE Photonics Conference* (IEEE, 2012), pp. 816–817.

© Author(s) 2022

[272]S. Keyvaninia, S. Uvin, M. Tassaert, X. Fu, S. Latkowski, J. Mariën, L. Thomassen, F. Lelarge, G. Duan, P. Verheyen, G. Lepage, J. Van Campenhout, E. Bente, and G. Roelkens, "Narrow-linewidth short-pulse III-V-on-silicon mode-locked lasers based on a linear and ring cavity geometry," Opt. Express **23**, 3221–3229 (2015).
[273]S. Srinivasan, A. Arrighi, M. J. R. Heck, J. Hutchinson, E. Norberg, G. Fish, and J. E. Bowers, "Harmonically mode-locked hybrid silicon laser with intra-cavity filter to suppress supermode noise," IEEE J. Sel. Top. Quantum Electron. **20**, 8–15 (2014).
[274]B. Dong, H. Huang, J. Duan, G. Kurczveil, D. Liang, R. G. Beausoleil, and F. Grillot, "Frequency comb dynamics of a 1.3 μm hybrid-silicon quantum dot semiconductor laser with optical injection," Opt. Lett. **44**, 5755–5758 (2019).
[275]A. W. Fang, B. R. Koch, K.-G. Gan, H. Park, R. Jones, O. Cohen, M. J. Paniccia, D. J. Blumenthal, and J. E. Bowers, "A racetrack mode-locked silicon evanescent laser," Opt. Express **16**, 1393–1398 (2008).
[276]Z.-H. Wang, W.-Q. Wei, Q. Feng, T. Wang, and J.-J. Zhang, "InAs/GaAs quantum dot single-section mode-locked lasers on Si (001) with optical self-injection feedback," Opt. Express **29**, 674–683 (2021).
[277]B. Dong, X. C. de Labriolle, S. Liu, M. Dumont, H. Huang, J. Duan, J. C. Norman, J. E. Bowers, and F. Grillot, "1.3-μm passively mode-locked quantum dot lasers epitaxially grown on silicon: Gain properties and optical feedback stabilization," J. Phys.: Photonics **2**, 045006 (2020).
[278]Z. L. Newman, V. Maurice, T. Drake, J. R. Stone, T. C. Briles, D. T. Spencer, C. Fredrick, Q. Li, D. Westly, B. R. Ilic, B. Shen, M.-G. Suh, K. Y. Yang, C. Johnson, D. M. S. Johnson, L. Hollberg, K. J. Vahala, K. Srinivasan, S. A. Diddams, J. Kitching, S. B. Papp, and M. T. Hummon, "Architecture for the photonic integration of an optical atomic clock," Optica **6**, 680–685 (2019).
[279]E. Obrzud, M. Rainer, A. Harutyunyan, M. H. Anderson, J. Liu, M. Geiselmann, B. Chazelas, S. Kundermann, S. Lecomte, M. Cecconi, A. Ghedina, E. Molinari, F. Pepe, F. Wildi, F. Bouchy, T. J. Kippenberg, and T. Herr, "A microphotonic astrocomb," Nat. Photonics **13**, 31–35 (2019).
[280]C. Bao, M.-G. Suh, and K. Vahala, "Microresonator soliton dual-comb imaging," Optica **6**, 1110–1116 (2019).
[281]P. J. Marchand, J. Riemensberger, J. C. Skehan, J.-J. Ho, M. H. P. Pfeiffer, J. Liu, C. Hauger, T. Lasser, and T. J. Kippenberg, "Soliton microcomb based spectral domain optical coherence tomography," Nat. Commun. **12**, 427 (2021).
[282]A. Akrout, A. Shen, R. Brenot, F. Van Dijk, O. Legouezigou, F. Pommereau, F. Lelarge, A. Ramdane, and G.-H. Duan, "Separate error-free transmission of eight channels at 10 Gb/s using comb generation in a quantum-dash-based mode-locked laser," IEEE Photonics Technol. Lett. **21**, 1746–1748 (2009).
[283]Y. Ben M'Sallem, Q. T. Le, L. Bramerie, Q.-T. Nguyen, E. Borgne, P. Besnard, A. Shen, F. Lelarge, S. LaRochelle, L. A. Rusch, and J.-C. Simon, "Quantum-dash mode-locked laser as a source for 56-Gb/s DQPSK modulation in WDM multicast applications," IEEE Photonics Technol. Lett. **23**, 453–455 (2011).
[284]V. Vujicic, P. M. Anandarajah, R. Zhou, C. Browning, and L. P. Barry, "Performance investigation of IM/DD compatible SSB-OFDM systems based on optical multicarrier sources," IEEE Photonics J. **6**, 7903110 (2014).
[285]C. Calò, V. Vujicic, R. Watts, C. Browning, K. Merghem, V. Panapakkam, F. Lelarge, A. Martinez, B.-E. Benkelfat, A. Ramdane, and L. P. Barry, "Single-section quantum well mode-locked laser for 400 Gb/s SSB-OFDM transmission," Opt. Express **23**, 26442–26449 (2015).
[286]C.-H. Chen, M. Ashkan Seyedi, M. Fiorentino, D. Livshits, A. Gubenko, S. Mikhrin, V. Mikhrin, and R. G. Beausoleil, "A comb laser-driven DWDM silicon photonic transmitter based on microring modulators," Opt. Express **23**, 21541–21548 (2015).
[287]V. Vujicic, C. Calò, R. Watts, F. Lelarge, C. Browning, K. Merghem, A. Martinez, A. Ramdane, and L. P. Barry, "Quantum dash mode-locked lasers for data centre applications," IEEE J. Sel. Top. Quantum Electron. **21**, 53–60 (2015).
[288]J. Müller, J. Hauck, B. Shen, S. Romero-García, E. Islamova, S. Sharif Azadeh, S. Joshi, N. Chimot, A. Moscoso-Mártir, F. Merget, F. Lelarge, and J. Witzens, "Silicon photonics WDM transmitter with single section semiconductor mode-locked laser," Adv. Opt. Technol. **4**, 119–145 (2015).
[289]T. N. Huynh, R. Watts, V. Vujicic, M. D. Gutierrez Pascual, C. Calo, K. Merghem, V. Panapakkam, F. Lelarge, A. Martinez, B.-E. Benkelfat, A. Ramdane, and L. P. Barry, "200-Gb/s baudrate-pilot-aided QPSK/direct detection with single-section quantum-well mode-locked laser," IEEE Photonics J. **8**, 7903107 (2016).
[290]A. Moscoso-Mártir, J. Müller, J. Hauck, N. Chimot, R. Setter, A. Badihi, D. E. Rasmussen, A. Garreau, M. Nielsen, E. Islamova, S. Romero-García, B. Shen, A. Sandomirsky, S. Rockman, C. Li, S. Sharif Azadeh, G.-Q. Lo, E. Mentovich, F. Merget, F. Lelarge, and J. Witzens, "Silicon photonics transmitter with SOA and semiconductor mode-locked laser," Sci. Rep. **7**, 13857 (2017).
[291]A. Moscoso-Mártir, A. Tabatabaei-Mashayekh, J. Müller, J. Nojić, R. Setter, M. Nielsen, A. Sandomirsky, S. Rockman, E. Mentovich, F. Merget, A. Garreau, F. Lelarge, and J. Witzens, "8-channel WDM silicon photonics transceiver with SOA and semiconductor mode-locked laser," Opt. Express **26**, 25446–25459 (2018).
[292]J. N. Kemal, P. Marin-Palomo, V. Panapakkam, P. Trocha, S. Wolf, K. Merghem, F. Lelarge, A. Ramdane, S. Randel, W. Freude, and C. Koos, "Coherent WDM transmission using quantum-dash mode-locked laser diodes as multi-wavelength source and local oscillator," Opt. Express **27**, 31164–31175 (2019).
[293]P. Marin-Palomo, J. N. Kemal, P. Trocha, S. Wolf, K. Merghem, F. Lelarge, A. Ramdane, W. Freude, S. Randel, and C. Koos, "Comb-based WDM transmission at 10 Tbit/s using a DC-driven quantum-dash mode-locked laser diode," Opt. Express **27**, 31110–31129 (2019).
[294]S. Pan, H. Zhang, Z. Liu, M. Liao, M. Tang, D. Wu, X. Hu, J. Yan, L. Wang, M. Guo, Z. Wang, T. Wang, P. M. Smowton, A. Seeds, H. Liu, X. Xiao, and S. Chen, "Multi-wavelength 128 Gbit s^{-1} λ^{-1} PAM4 optical transmission enabled by a 100 GHz quantum dot mode-locked optical frequency comb," J. Phys. D: Appl. Phys. **55**, 144001 (2022).
[295]J. Wu, X. Xu, T. G. Nguyen, S. T. Chu, B. E. Little, R. Morandotti, A. Mitchell, and D. J. Moss, "RF photonics: An optical microcombs' perspective," IEEE J. Sel. Top. Quantum Electron. **24**, 6101020 (2018).
[296]K. Hei, G. Shi, A. Hänsel, Z. Deng, S. Latkowski, S. A. Van den Berg, E. Bente, and N. Bhattacharya, "Distance metrology with integrated mode-locked ring laser," IEEE Photonics J. **11**, 1505210 (2019).
[297]J. Riemensberger, A. Lukashchuk, M. Karpov, W. Weng, E. Lucas, J. Liu, and T. J. Kippenberg, "Massively parallel coherent laser ranging using a soliton microcomb," Nature **581**, 164–170 (2020).
[298]A. Lukashchuk, J. Riemensberger, M. Karpov, J. Liu, and T. J. Kippenberg, "Megapixel per second hardware efficient LiDAR based on microcombs," in *Conference on Lasers and Electro-Optics* (Optica Publishing Group, 2021), p. AW3S.2.
[299]J. Feldmann, N. Youngblood, M. Karpov, H. Gehring, X. Li, M. Stappers, M. Le Gallo, X. Fu, A. Lukashchuk, A. S. Raja, J. Liu, C. D. Wright, A. Sebastian, T. J. Kippenberg, W. H. P. Pernice, and H. Bhaskaran, "Parallel convolutional processing using an integrated photonic tensor core," Nature **589**, 52–58 (2021).
[300]X. Xu, M. Tan, B. Corcoran, J. Wu, A. Boes, T. G. Nguyen, S. T. Chu, B. E. Little, D. G. Hicks, R. Morandotti, A. Mitchell, and D. J. Moss, "11 TOPS photonic convolutional accelerator for optical neural networks," Nature **589**, 44–51 (2021).
[301]M.-G. Suh, X. Yi, Y.-H. Lai, S. Leifer, I. S. Grudinin, G. Vasisht, E. C. Martin, M. P. Fitzgerald, G. Doppmann, J. Wang, D. Mawet, S. B. Papp, S. A. Diddams, C. Beichman, and K. Vahala, "Searching for exoplanets using a microresonator astrocomb," Nat. Photonics **13**, 25–30 (2019).
[302]S. Coburn, C. B. Alden, R. Wright, K. Cossel, E. Baumann, G.-W. Truong, F. Giorgetta, C. Sweeney, N. R. Newbury, K. Prasad, I. Coddington, and G. B. Rieker, "Regional trace-gas source attribution using a field-deployed dual frequency comb spectrometer," Optica **5**, 320–327 (2018).
[303]Z. Chen, K. Van Gasse, E. Vicentini, J. Huh, S. Poelman, Z. Wang, G. Roelkens, T. W. Hänsch, B. Kuyken, and N. Picqué, "High-resolution dual-comb gas-phase spectroscopy with a mode-locked laser on a photonic chip," in *Conference on Lasers and Electro-Optics* (Optica Publishing Group, 2020), p. JTh4A.8.
[304]K. Van Gasse, Z. Chen, E. Vincentini, J. Huh, S. Poelman, Z. Wang, G. Roelkens, T. W. Hänsch, B. Kuyken, and N. Picqué, "Dual-comb spectroscopy with two on-chip III-V-on-silicon 1-GHz mode-locked lasers," in *Conference on Lasers and Electro-Optics* (Optica Publishing Group, 2021), p. SM3A.7.

© Author(s) 2022

[305]J. Westberg, L. A. Sterczewski, and G. Wysocki, "Mid-infrared multiheterodyne spectroscopy with phase-locked quantum cascade lasers," Appl. Phys. Lett. **110**, 141108 (2017).
[306]J. Westberg, L. A. Sterczewski, F. Kapsalidis, Y. Bidaux, J. M. Wolf, M. Beck, J. Faist, and G. Wysocki, "Dual-comb spectroscopy using plasmon-enhanced-waveguide dispersion-compensated quantum cascade lasers," Opt. Lett. **43**, 4522–4525 (2018).
[307]J. L. Klocke, M. Mangold, P. Allmendinger, A. Hugi, M. Geiser, P. Jouy, J. Faist, and T. Kottke, "Single-shot sub-microsecond mid-infrared spectroscopy on protein reactions with quantum cascade laser frequency combs," Anal. Chem. **90**, 10494–10500 (2018).
[308]V. Balan, C.-T. Mihai, F.-D. Cojocaru, C.-M. Uritu, G. Dodi, D. Botezat, and I. Gardikiotis, "Vibrational spectroscopy fingerprinting in medicine: From molecular to clinical practice," Materials **12**, 2884 (2019).
[309]Y. Han, S. Ling, Z. Qi, Z. Shao, and X. Chen, "Application of far-infrared spectroscopy to the structural identification of protein materials," Phys. Chem. Chem. Phys. **20**, 11643–11648 (2018).
[310]L. A. Sterczewski, J. Westberg, Y. Yang, D. Burghoff, J. Reno, Q. Hu, and G. Wysocki, "Terahertz hyperspectral imaging with dual chip-scale combs," Optica **6**, 766–771 (2019).
[311]Y. Yang, D. Burghoff, D. J. Hayton, J.-R. Gao, J. L. Reno, and Q. Hu, "Terahertz multiheterodyne spectroscopy using laser frequency combs," Optica **3**, 499–502 (2016).
[312]H. Hu and L. K. Oxenløwe, "Chip-based optical frequency combs for high-capacity optical communications," Nanophotonics **10**, 1367–1385 (2021).
[313]E. Temprana, E. Myslivets, B. P.-P. Kuo, L. Liu, V. Ataie, N. Alic, and S. Radic, "Overcoming Kerr-induced capacity limit in optical fiber transmission," Science **348**, 1445–1448 (2015).
[314]L. Lundberg, M. Mazur, A. Mirani, B. Foo, J. Schröder, V. Torres-Company, M. Karlsson, and P. A. Andrekson, "Phase-coherent lightwave communications with frequency combs," Nat. Commun. **11**, 201 (2019).
[315]Telecommunication Standardization Sector of ITU (ITU-T), "Spectral grids for WDM applications: DWDM frequency grid," Recommendation ITU-T G.694.1, 2020.
[316]I. Coddington, N. Newbury, and W. Swann, "Dual-comb spectroscopy," Optica **3**, 414–426 (2016).
[317]N. Picqué and T. W. Hänsch, "Frequency comb spectroscopy," Nat. Photonics **13**, 146–157 (2019).
[318]R. M. Goody and T. W. Wormell, "The quantitative determination of atmospheric gases by infra-red spectroscopic methods I. Laboratory determination of the absorption of the 7.8 and 8.6μ bands of nitrous oxide with dry air as a foreign gas," Proc. R. Soc. London, Ser. A **209**, 178–196 (1951).
[319]A. Adel, "Absorption line width in the infrared spectrum of atmospheric carbon dioxide," Phys. Rev. **90**, 1024–1025 (1953).
[320]L. S. Rothman, R. L. Hawkins, R. B. Wattson, and R. R. Gamache, "Energy levels, intensities, and linewidths of atmospheric carbon dioxide bands," J. Quant. Spectrosc. Radiat. Transfer **48**, 537–566 (1992).
[321]Y.-D. Hsieh, S. Nakamura, D. G. Abdelsalam, T. Minamikawa, Y. Mizutani, H. Yamamoto, T. Iwata, F. Hindle, and T. Yasui, "Dynamic terahertz spectroscopy of gas molecules mixed with unwanted aerosol under atmospheric pressure using fibre-based asynchronous optical-sampling terahertz time-domain spectroscopy," Sci. Rep. **6**, 28114 (2016).
[322]T.-A. Liu, N. R. Newbury, and I. Coddington, "Sub-micron absolute distance measurements in sub-millisecond times with dual free-running femtosecond Er fiber-lasers," Opt. Express **19**, 18501–18509 (2011).
[323]C. Weimann, F. Hoeller, Y. Schleitzer, C. A. Diez, B. Spruck, W. Freude, Y. Boeck, and C. Koos, "Measurement of length and position with frequency combs," J. Phys.: Conf. Ser. **605**, 012030 (2015).
[324]M.-G. Suh and K. J. Vahala, "Soliton microcomb range measurement," Science **359**, 884–887 (2018).
[325]P. Trocha, M. Karpov, D. Ganin, M. H. P. Pfeiffer, A. Kordts, S. Wolf, J. Krockenberger, P. Marin-Palomo, C. Weimann, S. Randel, W. Freude, T. J. Kippenberg, and C. Koos, "Ultrafast optical ranging using microresonator soliton frequency combs," Science **359**, 887–891 (2018).
[326]D. T. Spencer, T. Drake, T. C. Briles, J. Stone, L. C. Sinclair, C. Fredrick, Q. Li, D. Westly, B. R. Ilic, A. Bluestone, N. Volet, T. Komljenovic, L. Chang, S. H. Lee, D. Y. Oh, M.-G. Suh, K. Y. Yang, M. H. P. Pfeiffer, T. J. Kippenberg, E. Norberg, L. Theogarajan, K. Vahala, N. R. Newbury, K. Srinivasan, J. E. Bowers, S. A. Diddams, and S. B. Papp, "An optical-frequency synthesizer using integrated photonics," Nature **557**, 81–85 (2018).
[327]K. Ohtani, M. Beck, M. J. Süess, J. Faist, A. M. Andrews, T. Zederbauer, H. Detz, W. Schrenk, and G. Strasser, "Far-infrared quantum cascade lasers operating in the AlAs phonon reststrahlen band," ACS Photonics **3**, 2280–2284 (2016).
[328]B. Desiatov, A. Shams-Ansari, M. Zhang, C. Wang, and M. Lončar, "Ultra-low-loss integrated visible photonics using thin-film lithium niobate," Optica **6**, 380–384 (2019).
[329]T. J. Morin, L. Chang, W. Jin, C. Li, J. Guo, H. Park, M. A. Tran, T. Komljenovic, and J. E. Bowers, "CMOS-foundry-based blue and violet photonics," Optica **8**, 755–756 (2021).
[330]M. Corato-Zanarella, A. Gil-Molina, M. C. Shin, X. Ji, A. Mohanty, and M. Lipson, "Narrow linewidth, widely tunable integrated lasers from visible to near-IR," in *Conference on Lasers and Electro-Optics* (Optica Publishing Group, 2021), p. SF1B.6.
[331]A. Spott, J. Peters, M. L. Davenport, E. J. Stanton, C. D. Merritt, W. W. Bewley, I. Vurgaftman, C. S. Kim, J. R. Meyer, J. Kirch, L. J. Mawst, D. Botez, and J. E. Bowers, "Quantum cascade laser on silicon," Optica **3**, 545–551 (2016).
[332]S. Jung, J. Kirch, J. H. Kim, L. J. Mawst, D. Botez, and M. A. Belkin, "Quantum cascade lasers transfer-printed on silicon-on-sapphire," Appl. Phys. Lett. **111**, 211102 (2017).
[333]S. Radosavljevic, A. Radosavljević, C. Schilling, S. Hugger, R. Ostendorf, B. Kuyken, and G. Roelkens, "Thermally tunable quantum cascade laser with an external germanium-on-SOI distributed Bragg reflector," IEEE J. Sel. Top. Quantum Electron. **25**, 1200407 (2019).
[334]E. Akiki, M. Verstuyft, B. Kuyken, B. Walter, M. Faucher, J.-F. Lampin, G. Ducournau, and M. Vanwolleghem, "High-*Q* THz photonic crystal cavity on a low-loss suspended silicon platform," IEEE Trans. Terahertz Sci. Technol. **11**, 42–53 (2021).
[335]J. F. Bauters, M. J. R. Heck, D. D. John, J. S. Barton, C. M. Bruinink, A. Leinse, R. G. Heideman, D. J. Blumenthal, and J. E. Bowers, "Planar waveguides with less than 0.1 dB/m propagation loss fabricated with wafer bonding," Opt. Express **19**, 24090–24101 (2011).
[336]J. Liu, G. Huang, R. N. Wang, J. He, A. S. Raja, T. Liu, N. J. Engelsen, and T. J. Kippenberg, "High-yield, wafer-scale fabrication of ultralow-loss, dispersion-engineered silicon nitride photonic circuits," Nat. Commun. **12**, 2236 (2021).
[337]H. R. Telle, G. Steinmeyer, A. E. Dunlop, J. Stenger, D. H. Sutter, and U. Keller, "Carrier-envelope offset phase control: A novel concept for absolute optical frequency measurement and ultrashort pulse generation," Appl. Phys. B **69**, 327–332 (1999).
[338]S. T. Cundiff and J. Ye, "*Colloquium*: Femtosecond optical frequency combs," Rev. Mod. Phys. **75**, 325–342 (2003).
[339]P. J. Delfyett, A. Klee, K. Bagnell, P. Juodawlkis, J. Plant, and A. Zaman, "Exploring the limits of semiconductor-laser-based optical frequency combs," Appl. Opt. **58**, D39–D49 (2019).
[340]D. Waldburger, A. S. Mayer, C. G. E. Alfieri, J. Nürnberg, A. R. Johnson, X. Ji, A. Klenner, Y. Okawachi, M. Lipson, A. L. Gaeta, and U. Keller, "Tightly locked optical frequency comb from a semiconductor disk laser," Opt. Express **27**, 1786–1797 (2019).
[341]P. Del'Haye, A. Coillet, T. Fortier, K. Beha, D. C. Cole, K. Y. Yang, H. Lee, K. J. Vahala, S. B. Papp, and S. A. Diddams, "Phase-coherent microwave-to-optical link with a self-referenced microcomb," Nat. Photonics **10**, 516–520 (2016).
[342]M. Malinowski, R. Bustos-Ramirez, J.-E. Tremblay, G. F. Camacho-Gonzalez, M. C. Wu, P. J. Delfyett, and S. Fathpour, "Towards on-chip self-referenced frequency-comb sources based on semiconductor mode-locked lasers," Micromachines **10**, 391 (2019).

© Author(s) 2022

[343]Y. Okawachi, M. Yu, J. Cardenas, X. Ji, A. Klenner, M. Lipson, and A. L. Gaeta, "Carrier envelope offset detection via simultaneous supercontinuum and second-harmonic generation in a silicon nitride waveguide," Opt. Lett. **43**, 4627–4630 (2018).
[344]D. Kharas, J. J. Plant, W. Loh, R. B. Swint, S. Bramhavar, C. Heidelberger, S. Yegnanarayanan, and P. W. Juodawlkis, "High-power (>300 mW) on-chip laser with passively aligned silicon-nitride waveguide DBR cavity," IEEE Photonics J. **12**, 1504612 (2020).
[345]R. Loi, J. O'Callaghan, B. Roycroft, Z. Quan, K. Thomas, A. Gocalinska, E. Pelucchi, A. J. Trindade, C. A. Bower, and B. Corbett, "Thermal analysis of InP lasers transfer printed to silicon photonics substrates," J. Lightwave Technol. **36**, 5935–5941 (2018).
[346]J. Juvert, T. Cassese, S. Uvin, A. De Groote, B. Snyder, L. Bogaerts, G. Jamieson, J. Van Campenhout, G. Roelkens, and D. Van Thourhout, "Integration of etched facet, electrically pumped, C-band Fabry-Pérot lasers on a silicon photonic integrated circuit by transfer printing," Opt. Express **26**, 21443–21454 (2018).
[347]IRsweep, "Providing the next generation of fast, broadband and high-resolution dual-comb spectrometers," https://irsweep.com/, 2022.
[348]Enlightra, "Extreme-bandwidth data transmission enabled by light," https://enlightra.com/, 2022.

© Author(s) 2022